ROLE OF MOLECULAR MOTORS AND MAPS IN SPINDLE DYNAMICS AND CHROMOSOME SEGREGATION IN THE FISSION YEAST *SCHIZOSACCHAROMYCES POMBE*

Viktoriya Syrovatkina

A DISSERTATION

in

Cell and Molecular Biology

Presented to the Faculties of the University of Pennsylvania

In Partial Fulfillment of the Requirements for the Degree of Doctor of Philosophy

2015

Supervisor of Dissertation

_____

Phong Tran, PhD, Associate Professor of Cell and Developmental Biology

Graduate Group Chairperson

_____

Daniel S. Kessler, PhD, Associate Professor of Cell and Developmental Biology

Dissertation Committee

Erfei Bi, PhD, Professor of Cell and Developmental Biology

Ekaterina L. Grishchuk, PhD, Assistant Professor of Physiology

Erika L.F. Holzbaur, PhD, Professor of Physiology

Michael Lampson, PhD, Associate Professor of Biology

ROLE OF MOLECULAR MOTORS AND MAPS IN SPINDLE DYNAMICS AND CHROMOSOME SEGREGATION IN THE FISSION YEAST *SCHIZOSACCHAROMYCES POMBE*

DEDICATION

I would like to dedicate my thesis to my dear parents, Irina and Aleksander. They had been extremely courageous to their leave home country and loved ones to come to America 16 year ago, with little knowledge of the English language in the search for a better future for their kids, my brother and me. They have selflessly sacrificed much of themselves to provide for the family and to put my brother and me through college. They always encouraged us to explore possible opportunities and pursue our passions. They have been my source of inspiration throughout my life.

ACKNOWLEDGMENT

First and foremost, I would like to thank my mentor, Phong Tran, for his encouragement and support throughout all these years. I am extremely grateful to him for giving me the opportunity to be part of the lab. I thank him for providing an ideal environment where I could explore my passion for science. He allowed me to find answers on my own and to ask for his help when I needed it. Phong taught me to be an independent scientist, not just a skilled and knowledgeable experimentalist. I am fortunate to be his student.

I owe special thanks to my thesis committee- Drs. Erfei Bi, Ekaterina Grishchuk, Erika Holzbaur and Mike Lampson for their valuable time, input and for having my best interests in mind.

I would especially like thank former post-doc, Dr. Chuanhai Fu, who has been a second mentor for me in the lab. He taught me everything I needed to know when I joined the lab. I have been privileged to work closely with Chuanhai on studying spindle length control discussed in Chapter 2. Also, I would like to acknowledge some past and current members of Tran lab: Guilhem Velve Casquillas, Judite Costa, Refael Minnes and Mohini Khare for making the lab fun and collaborative place to work.

I would also like to thank the Cell Biology, Physiology and Metabolism sub-group and the Cell & Molecular Biology body for their strong student support and the fantastic scientific opportunities available.

Finally, I would especially like to thank my friends and family for their love and support. My parents and brother have always supported me on my endeavors. Thank you to my friends, for being there and making me laugh when times were tough. I am so fortunate to be surrounded by these incredible people who have inspired me through the years.

ABSTRACT

ROLE OF MOLECULAR MOTORS AND MAPS IN SPINDLE DYNAMICS AND CHROMOSOME SEGREGATION IN THE FISSION YEAST *SCHIZOSACCHAROMYCES POMBE*

Viktoriya Syrvatkina

Dr. Phong Tran

Mitosis is a key event in the life of a cell, where duplicated chromosomes are separated into the daughter cells. Defects associated with chromosome segregation can lead to aneuploidy, a hallmark of cancer. Chromosome segregation is achieved by the mitotic spindle, which is composed of microtubules (MTs), motors and microtubule associated protein (MAPs). Motors such as kinesins generate forces within the spindle while MAPs perform functions such as organize the spindle pole and maintain the bipolar spindle. Both motors and MAPs contribute to spindle mechanics. Here I used the relatively simple fission yeast to address how defects in spindle mechanics affect chromosome segregation. The metaphase spindle is maintained at a constant length by an antagonistic force-balance model yet how the regulation of metaphase spindle length contribute to subsequent chromosome segregation remains unexplored. To test the force-balance model, I applied gene deletion and fast microfluidic temperature-control with live-cell imaging to monitor the effect of deleting or switching off different combinations of antagonistic forces in the fission yeast metaphase spindle. I show that kinesin-5 cut7p and MT bundler ase1p contribute to outward pushing forces, and kinesin-8 klp5/6p and dam1p contribute to inward pulling forces. Removing these proteins individually led to aberrant metaphase spindle length and chromosome segregation defects. Removing these proteins in antagonistic combination rescued the defective spindle length and, in some combinations, also partially rescued chromosome segregation defects.

Motors and MAPs cooperate to focus MTs at the spindle pole. Defects in MT focusing lead to defects in chromosome segregation, resulting in aneuploidy. The mechanism behind these observations is not well understood. Here I identified a new mechanism for aneuploidy in fission

yeast. Kinesin-14 pkl1p and MAP msd1p localize to the spindle poles and focus the MT minus ends. Their absence leads to pole and MT defocusing, resulting in protrusion of MT minus ends due to cut7p-dependent pushing forces at the spindle midzone. Infrequent long MT minus end protrusions can push the already separated chromosome mass back to the cell center, where cytokinesis will 'cut' the chromosome mass, creating two daughter cells with unequal chromosome content.

TABLE OF CONTENTS

LIST OF FIGURES

LIST OF ABBREVIATIONS

Abbreviations	Full Name
CDK	cyclin-dependant kinase
ChIP	chromatin immunoprecipitation
cs	cold sensitive
γ-TuC	gamma-tubulin complex
MAP	microtubule-associated protein
MT	microtubule
MTOC	microtubule organizing center
NE	nuclear envelope
SPB	spindle pole body
PAA	post-anapahse array
ts	temperature sensitive

CHAPTER 1: INTRODUCTION

1.1 Summary

Mitosis is a process that results in the division of duplicated sets of chromosomes into two genetically identical daughter cells. Chromosome segregation errors in human cells can cause birth defects and contribute to cancer (Weaver and Cleveland, 2006). In all eukaryotes, chromosome segregation is accomplished by the mitotic spindle, a macromolecular machine composed of dynamically interacting proteins such as microtubules (MTs), molecular motors and microtubule-associated proteins (MAPs). The dynamic spindle was first observed by Shinya Inoue and Hidemi Sato in 1967 . Our current understanding of the mitotic spindle has exponentially increased through the use of wide-field epi-fluorescence imaging of MTs, made possible by fusions of green fluorescent protein to tubulin, and allowed for observation and manipulation of mitotic spindle in living cells. After decades of research and contribution from many researchers, the spindle is now viewed as a macromolecular machine that generates forces to assemble itself (Karsenti and Vernos, 2001; McIntosh et al., 2012) to segregate sister chromatids (Inoue and Salmon, 1995). Forces within the spindle are generated by kinesin and dynein, which are MT-based molecular motor proteins that generate directional movement along MTs and perform work. There are 45 kinesins spanning the fourteen kinesin families in human cells (Wordeman, 2010). Complimentarily, there are 16 dyneins spanning the nine families (two cytoplasmic and seven axonemal) in human cells (Roberts et al., 2013; Wickstead and Gull, 2007). To date nine kinesin families and one cytoplasmic dynein are implicated in mitosis (Wordeman, 2010).

In addition to molecular motors, a plethora of MAPs contributes to mitotic spindle mechanics (Maiato et al., 2004). Various MAPs function to 1) organize spindle pole, 2) organize and maintain the bipolar spindle, 3) attach MTs to kinetochores, and 4) help to move chromosomes. This large number of motors and MAPs creates complexity in dissecting core mechanisms of spindle

dynamics. Spindle dynamics is apparent through all phases of mitosis. At prophase, the spindle is formed into a bipolar structure of defined length. At metaphase, spindle length remains relatively constant. The spindle structure contains 3 types of microtubules: astral, interpolar and kinetochore. At anaphase, kinetochore microtubules segregate chromosomes to the poles and then interpolar microtubules slide apart to extend the spindle length to further separate chromosomes (Figure 1.1).

The fission yeast *Schizosaccharomyces pombe* has similar spindle organization and dynamics to mammalian cells (Figure 1.1). However, fission yeast only uses 4 kinesin families and a single dynein during mitosis. In addition, abundant MAPs are highly conserved in eukaryotes from yeasts to humans (Maiato et al., 2004). Therefore, fission yeast mitosis may represent core mechanism underlying spindle dynamics throughout evolution. Furthermore, fission yeast is an ideal model system for molecular dissection of spindle mechanics because of its simple microtubule network, genetic tractability and relative amenability to microscopic analysis.

Historically, fission yeast has proven to be a powerful genetic tool. In fact, *S.pombe* was originally used for groundbreaking work on cell cycle regulation by Paul Nurse (Nurse et al., 1976). The discovery of essential genes in cell division was feasible through the use temperature-sensitive (*ts*) mutants. For example, kinesin-5 cut7p, essential motor for the formation of bipolar spindle, was first discovered through a screen that isolated genes with a shared phenotype of “cut” cells or untimely torn (Hagan and Yanagida, 1990; Hirano et al., 1986). Cut7^{ts} mutants failed to build proper bipolar spindle to segregate chromosomes but proceed through the cell cycle into cytokinesis and septation. As a consequence, an asymmetric separation of chromosomes resulted in either aneuploidy or aploidy and cell death (Hagan and Yanagida, 1990; Hirano et al., 1986). Temperature-sensitive mutants had been extensively used because they offer an effective technique to conditionally inactivate genes to dissect the role of essential proteins in a time-fashion manner.

Figure 1.1

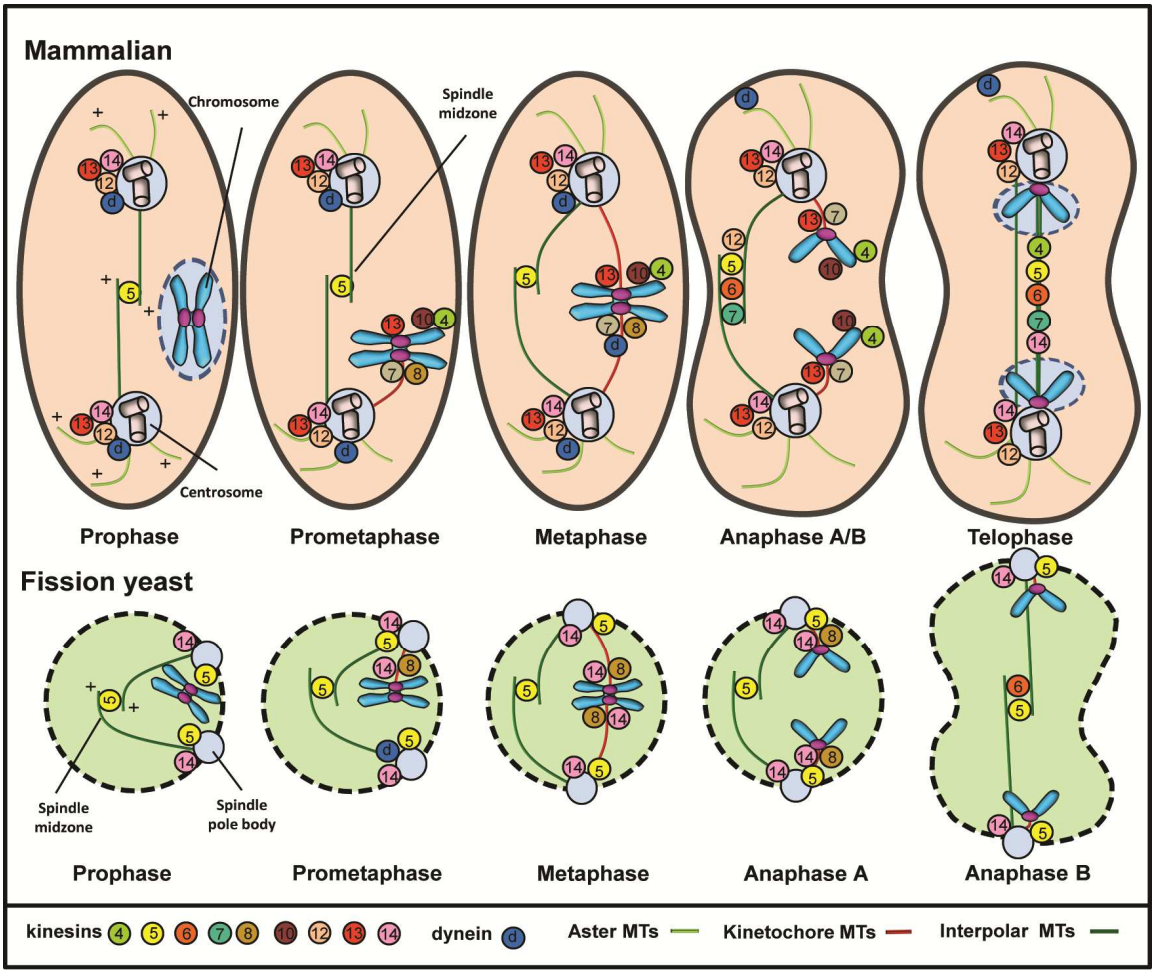

Figure 1.1. Comparison of Motors Localization during Mitosis in Mammalian and Fission Yeast Cells.

In mammalian cells, during prophase chromosomes condense and the duplicated centrosomes are separated by kinesin-5 to form the bipolar spindle. Kinesin-12, kinesin-13, kinesin-14 and dynein localize to the poles where they function in spindle assembly and organization. Nuclear envelope breaks down at prometaphase, and kinesin-5 separates spindle poles apart and maintains bipolarity. In prometaphase, kinesin-4 and kinesin-10 localize to the chromosome arms and kinesin-7, kinesin-8, kinesin-13 and dynein to the kinetochore to facilitate microtubule capture and chromosome congression to the metaphase plate. Kinesin-8 also localizes to the kinetochore

at metaphase to aid in chromosome congression and oscillation. During anaphase, sister chromatid separation and movement toward the poles are driven by kinesin-7 and kinesin-13 localized at the kinetochore and kinesin-12, kinesin-13, kinesin-14 localized at the poles. The spindle midzone, or central spindle, contains residual kinesin-5, kinesin-6 and kinesin-7. Dynein localizes to the cell cortex and pulls on astral microtubules to further separate the poles. During telophase, multiple kinesin families organize the spindle midzone. Mitosis in mammalian cells requires 9 kinesin families and a single dynein. Cartoon representation is modeled after (Roberts et al., 2013; Verhey and Hammond, 2009; Yount et al., 2015).

In contrast to mammalian cells, fission yeast utilizes fewer motors to perform mitosis. Only 4 kinesin families are involved: kinesin-5, kinesin-6, kinesin-8, and kinesin-14 and one dynein. Note that the nuclear envelope does not break down during mitosis in fission yeast. Similarly to mammalian cells, the duplicated spindle pole bodies (analogous to the centrosome) are separated by kinesin-5 to form the bipolar spindle in prophase (Hagan and Yanagida, 1990; Hagan and Yanagida, 1992). In prometaphase and metaphase, kinesin-5 maintains the bipolarity (Syrovatkina et al., 2013). Kinesin-14 and dynein localize to spindle pole bodies where they function in spindle pole organization (Grishchuk et al., 2007; Troxell et al., 2001). In addition, kinesin-14 and kinesin-8 localize to the kinetochores and facilitates chromosome-microtubule attachment (Garcia et al., 2002; Sanchez-Perez et al., 2005; Troxell et al., 2001; Unsworth et al., 2008; West et al., 2002). Finally, during anaphase B, kinesin-6 and kinesin-5 localize to the spindle midzone to slide microtubule apart (Fu et al., 2009; Hagan and Yanagida, 1992).

This thesis addresses the mechanics of the mitotic spindle in fission yeast with particular focus on kinesins and MAPs through use of live-cell imaging, microfluidics temperature-control device to inactivate temperature-sensitive mutants and powerful genetics. In this section, I will first provide a short description of the major components that are essential for proper spindle mechanics in fission yeast (Figure 1.2). I will then focus on the role of various fission yeast motors and MAPs in mitotic spindle mechanics (Figure 1.3).

1.2 Function of Spindle Pole Body in Mitosis

Spindle Pole Body Duplication

In *S. pombe,* the spindle pole body (SPB), analogous to the centrosome in higher eukaryotes, is the principal microtubule organizing center (MTOC) during mitosis. SPBs are sites of MT nucleation and are essential for the formation of the mitotic spindle. The morphology of the SPB at different cell cycle stages and its mechanisms of duplication have been studied using static, fixed cells (Ding et al., 1997; Uzawa et al., 2004). Initially, the timing of SPB duplication has been judged by electron microscopy of cells synchronized with respect to cell cycle progression to be in G2 (Ding et al., 1997). However, a recent study observed unduplicated SPBs in a number of wild-type G2 cells using electron tomography (Hoog et al., 2013). In contrast, a report by Cande and colleagues has proposed that SPB duplication is initiated in G1/S by monitoring the morphology of SPBs in cells during cell cycle arrest/release experiments of fixed cells (Uzawa et al., 2004). Therefore, the timing of SPB duplication in the fission yeast cell cycle is controversial, partially because extensive studies using live cells are lacking. A recent report illustrates the power of using live-cell imaging in combination with electron microscopy to investigate SPB duplication and proposes that it initiates before G1/S phase and continues in G2 phase (Lee et al., 2014). The daughter SPB assembles at the tip of a mother SPB appendage called the bridge that maintains the duplicated SPBs associated until mitosis onset. The SPB bridge contains two major evolutionary conserved proteins, sfi1p and cdc31p/Centrin (Bouhlel et al., 2015). Mutation in sfi1p

or cdc31p leads to monopolar spindle validating that proper SPB duplication is essential for the formation of mitotic spindle.

SPB Insertion into Nuclear Envelope

As the fission yeast cells enter “closed” mitosis, where the nuclear envelope (NE) does not breakdown, cytoplasmic microtubules depolymerize and the nuclear envelop opens to form fenestrae to allow for the insertion of the mother and daughter SPBs (Ding et al., 1997). Disruption in SPBs insertions into the NE leads to the inability of the cell to form a spindle within the nucleus, illustrating the importance of this process for building the bipolar spindle in fission yeast. In cells carrying mutations in an essential gene, *brr6a+*, the SPBs fail to properly anchor within the NE and results in the formation of monopolar spindle instead of normal bipolar spindle (Tamm et al., 2011). Brr6p encodes a member of the transmembrane nuclear envelope protein family restricted to the organisms that undergo “close” mitosis (Tamm et al., 2011). Brr6p also appears to promote nuclear membrane remodeling during SPB extrusion at a later stage of mitosis. Brr6p is not required for spindle formation after SPBs insertion suggesting that brr6p plays exclusive role in generation of the hole within the envelope for SPBs insertion and extrusion (Tamm et al., 2011).

The failure to integrate the SPBs and thus to form a bipolar spindle in brr6p mutants appears to be similar to the consequences of mutating cut11p (West et al., 1998) and cut12p (Bridge et al., 1998). The effect of cut11p deficiency is due to a physical failure in anchoring the SPB within a fenestra (West et al., 1998), while defect in the mitotic regulator cut12p results from compromised commitment to mitosis (Bridge et al., 1998). Cut12p promotes mitosis through boosting the mitotic cyclin-dependant kinase (CDK) activity by amplification of the Polo kinase driving positive feedback loop (Hagan, 2008). In cells carrying conditional loss-of-function alleles of *cut12+*, the NE breaks down in the vicinity of the old, mother SPB but remains intact underneath the daughter SPB born in the previous interphase. The daughter SPB fails to nucleate MTs and thus cut12^{ts}

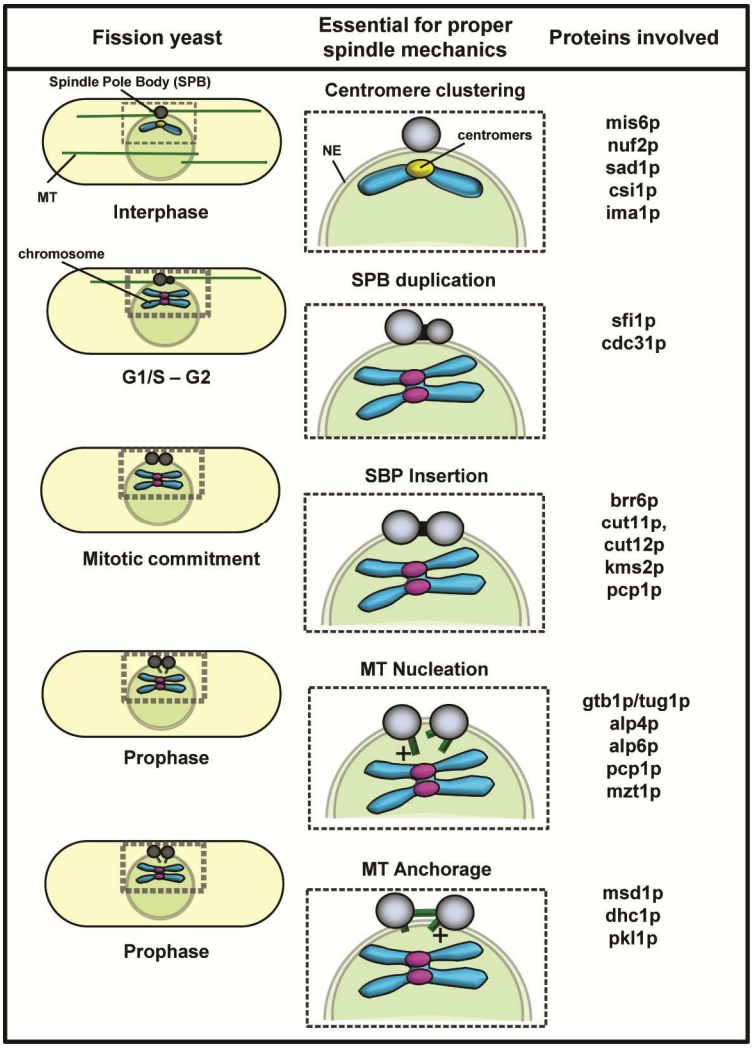

Figure 1.2. List of Essential Processes for Proper Spindle Dynamics

In *S. pombe,* the spindle pole body (SPB) is the principal microtubule organizing center (MTOC) during mitosis. Because fission yeast enters “close” mitosis, where the nuclear envelope (NE) does not breakdown, duplicated SPBs must insert into the NE to begin to nucleate intranuclear microtubules (MTs) to initiate bipolar spindle assembly. Moreover, spindle MTs are anchored at the SPBs which is essential for proper bipolar spindle formation and chromosome segregation. Proteins are listed that contribute to corresponding processes (see text for details).

mutant cells failed to form a bipolar spindle at the restrictive temperature (Bridge et al., 1998). Similar phenotype is observed in conditional mutations in the fission yeast pericentrin pcp1p and the KASH domain protein kms2p, with both leading to delocalization of Polo kinase from the SPBs and a failure of the SPB to insert into NE to form proper bipolar spindle (Fong et al., 2010; Walde and King, 2014). Polo kinase and CDK associate with the mitotic SPBs suggesting that the local activation of these kinases could promote localized NE fenestration and SPB insertion (Zhang and Oliferenko, 2013) and thus linking mitotic commitment and formation of proper bipolar spindle in fission yeast.

Microtubules Nucleation at SPBs

After insertion into NE, duplicated SPBs begin to nucleate spindle MTs. Microtubules are tubular polymers composed of α- and β-tubulin heterodimers. These heterodimers assemble into linear protofilaments in a GTP-dependent manner, and 13 protofilaments in turn associate laterally to form a 24-nm-wide hollow cylinder (Desai and Mitchison, 1997). The longitudinal orientation and distinct biophysical properties of α- and β-tubulins give rise to an intrinsic polarity of microtubules, with β-tubulin facing the fast-growing yet dynamic plus end and α-tubulin the less dynamic minus end (Jiang and Akhmanova, 2011; Nogales, 2000). Microtubules undergo dynamic structural alterations in fission yeast from interphase cytoplasmic MTs to formation of spindle MTs in the nucleus (Hagan, 1998), thus MTs need to be precisely regulated in a spatiotemporal manner during the cell cycle.

The key event in microtubule assembly is an initial nucleation. γ-tubulin nucleates the polymerization of microtubules from α- and β-tubulin subunits, but is not itself incorporated into that polymer (Luders and Stearns, 2007). γ-tubulin forms a complex called gamma-tubulin complex (γ-TuC), which is the core player in MT nucleation at the SPBs where the microtubules minus ends are embedded. γ-TuC contains 6 proteins: gtb1p/tug1p, alp4p, alp6p, gfh1p, mod21p,

alp16p, where gtb1p/tug1p, alp4p, and alp6p are essential for cell viability, while the other three proteins are dispensable (Anders et al., 2006; Fujita et al., 2002; Horio et al., 1991; Stearns et al., 1991; Vardy and Toda, 2000; Venkatram et al., 2004). γ-TuC plays a pivotal role in the formation of the mitotic bipolar spindle. The mutant defective in *alp4+* displays bipolar spindle defects due to a failure in the recruitment of the γ-TuC to the spindle pole body (Vardy et al., 2002; Vardy and Toda, 2000). Cells deleted for *alp16+ or gfh1+* show some defects in mitotic spindle and aster MTs (Fujita et al., 2002; Venkatram et al., 2004), suggesting that they are not required for MT nucleation per se, but rather modulate the function of γ-TuC.

γ-TuC is recruited to the SPBs by the so called γ-TuC binding proteins such as pericentrin pcp1p and mzt1p and thereby promote nucleation and assembly of spindle. For instance, the conditional loss-of-function pcp1-15^{ts} mutant fails to recruit alp4p-GFP to the SPB and consequently unable to build proper bipolar spindle (Fong et al., 2010). Pcp1p interacts directly with γ-tubulin and thus recruits MT nucleation to the SPBs. Mzt1p also interacts directly with γ-tubulin and alp4p, however, it is partially required for the γ-TuC localization to the SPBs (Masuda et al., 2013). It is proposed that mzt1p play a crucial role in the recruitment and/or retention of γ-TuC at the SPBs. A high percentage (47%) of mzt1^{ts} mutant cells display inability to form the stable bipolar spindle at the restrictive temperature due to deficient recruitment alp4p to the SPBs. However, some mzt1^{ts} cells (20%) were able to form apparently normal spindles that display chromosome segregation defect such as chromosome lagging (Masuda et al., 2013). Limited MT nucleation from the SPBs due to deficient γ-TuC recruitment in mzt1^{ts} cells could explain this observation since reduce number of MT plus ends may result in failure to maintain proper attachment of the kinetochores to spindle microtubules. Alternatively, γ-TuC and mzt1p may also play indirect role in regulating MT dynamics at the plus ends possibly through facilitating proper microtubule lattice structure. However, this issue remains an active field of investigation in fission yeast (Anders and Sawin, 2011; Bouissou et al., 2009; Tanaka et al., 2012; Zimmerman and Chang, 2005).

The aster MTs arise from the completely different nucleating sites to those that generate the intranuclear spindle (Ding et al., 1997; Tanaka and Kanbe, 1986). Mto1p mediates γ-TuC recruitment specifically to cytoplasmic site of the SPB, as deletion of mto1p leads to spindles without the aster MTs (Sawin et al., 2004; Venkatram et al., 2004; Zimmerman and Chang, 2005). In addition, mto1p mediates the assembly of other cytoplasmic MTs during spindle disassembly (Sawin et al., 2004) (see below).

Anchoring MTs to the SPBs

MTs are nucleated and stabilized at SPBs in fission yeast, which is essential for proper formation of mitotic spindle. MAP msd1p, which anchors spindle microtubules to the SPBs during mitosis, is not an essential protein (Toya et al., 2007), suggesting that there are other proteins that function to focus the spindle pole body. Cells that lack *msd1+* gene (*msd1Δ* cells) assemble a spindle during mitosis but display defects in chromosome segregation. In addition, the mitotic spindle displays striking structural defects — for example, in addition to the normally anchored spindle MTs emanating from the two SPBs, there are frequent additional spindle MTs that are not attached to the SPBs. Instead, these microtubules abnormally extend beyond the SPB, protruding outward and deforming the nuclear envelope. The outward protruding tips of these MTs were shown to have alp4-GFP, a γ-TuC component, and thus represent microtubule minus ends that are not anchored to the SPB (Toya et al., 2007). Msd1p binds directly to alp4p, and its anchoring ability relies on this interaction as a strain expressing a truncated form of alp4p missing the msd1p-binding domain exhibit spindle defects similar to those observed in *msd1Δ* cells. In addition to msd1p, the molecular motor, dynein, has been proposed to aid in anchoring of MTs at the pole (Grishchuk et al., 2007). Subtle abnormalities in spindle organization in dhc1p deletion (*dhc1Δ)* cells were observed by electron microscopy, suggesting that dynein promote MT bundling by anchoring MT minus ends. Another molecular motor, kinesin-14 pkl1p localizes to the SPBs during mitosis (Troxell et al., 2001). Abnormal pole structure is observed in absence of

pkl1p by electron microscopy (Grishchuk et al., 2007). In addition, pkl1Δ cells display abnormal MT protrusions from the poles (Syrovatkina et al., 2013), suggesting that pkl1p organizes and focus the SPBs. I will describe in Chapter 3, a novel mechanism of how pkl1p and msd1p cooperate to focus minus ends of MTs at the SPBs.

Centromeres Clustering at SPB

The SPB remains close to the cytoplasmic side of the nuclear envelope during interphase (Adams and Kilmartin, 2000). γ-tubulin, which is required for MT nucleation (Horio et al., 1991; Masuda and Shibata, 1996), is found on osmiophilic material that lies near the inner surface of the NE, immediately adjacent to the SPB, even though there are no MTs inside the interphase nucleus . This observation suggests that MTs nucleation is cell-cycle specific. Indeed, *in vitro* experiments have shown that the nuclear complex is inactive for MT nucleation during interphase and is activated at the onset of mitosis (Masuda et al., 1992; Masuda and Shibata, 1996). In addition to its essential role in spindle formation, the nuclear γ-tubulin region may be important for anchoring centromeres close to the SPB during interphase. In *S. pombe* centromeres which are specialized regions of DNA within chromosomes, cluster close to the SPB (Funabiki et al., 1993; Kniola et al., 2001). Centromeres direct the assembly of the kinetochores, which are essential for the attachment of spindle to MTs to drive chromosome segregation during mitosis (Cheeseman and Desai, 2008). Several kinetochore proteins have been reported to affect interphase centromere clustering, for example, mutations in mis6p (inner kinetochore component) and nuf2p (outer kinetochore component) result in centromeres declustering (Appelgren et al., 2003; Asakawa et al., 2005). It is proposed that SUN domain protein sad1p and KASH domain proteins kms1p/kms2p may link the kinetochores to the NE near the SPBs as these are nuclear envelope proteins that concentrate in the vicinity of the SPB, at the site of centromere clustering (Mekhail and Moazed, 2010; Starr, 2009). In fact, sad1^{ts} mutant display centromeres declustering at the restrictive temperature (Hou et al., 2013). It was proposed that an integral inner nuclear

membrane protein, ima1p, couples centromeric heterochromatin to the NE (King et al., 2008). The absence of ima1p leads to defects with centromere clustering at the SPBs, changes in nuclear shape and partial dissociation of SUN-KASH complexes. In contrast, a recent report by Hiraoka and colleagues shown that ima1p is dispensable for centromere clustering at the SPBs. The Hiraoka et al. paper concluded that ima1p collaborates with two other integral inner nuclear membrane proteins, lem2p and man1p to maintain nuclear membrane organization (Hiraoka et al., 2011). Therefore, the role of ima1p in SPB–centromeres interactions at interphase is controversial at this time. Interestingly, a recent report by Hou and colleagues identify a novel protein, csi1p (chromosome segregation impaired protein 1), that directly interacts with sad1p and spc7p, an outer kinetochore component (Hou et al., 2013). A high percentage (70%) of csi1Δ cells display defective centromere clustering at the SPBs. Moreover, the loss of csi1p greatly reduces the association of sad1p to centromeric DNA as assayed by chromatin immunoprecipitation (ChIP) analysis, suggesting that csi1p recruits sad1p to the centromeres (Hou et al., 2013). It is possible that csi1p might serve as a link between the NE and centromeres.

The close proximity of centromeres to SPBs is important for mitosis progression. It has been suggested that in fission yeast the clustering of centromeres during interphase allows for the rapid capture of kinetochores by intranuclear microtubules at the onset of mitosis (Grishchuk et al., 2007). Indeed, in addition to centromere clustering defects, csi1p mutant also exhibits prominent defects in chromosome segregation during mitosis (Hou et al., 2013). Alternatively, csi1p also is reported to organize the bipolar spindle, which is required for proper chromosome segregation (Zheng et al., 2014). To determine the relative contribution of the two phenotypes to chromosome segregation defects in the csi1Δ mutant, it is important to uncoupled spindle assembly defects from centrosome declustering. Csi2p, which recruits csi1p to the SPBs during mitosis, is proven to be useful mutant to address this question (Costa et al., 2014). csi2p deletion (csi2Δ) cells display lack of csi1p-GFP on the SPBs during early mitosis and exhibit similar chromosome segregation defects as reported for csi1Δ cells (Hou et al., 2013). However, csi2Δ

cells do not display the centromere-positioning defects of csi1Δ (Costa et al., 2014), implying that centromere declustering only partially contributes to chromosome segregation defects. Additional experiments such as mutants that lack spindle assembly defects but have declustered centromeres at interphase are needed to directly test contribution of csi1p- dependent centromere clustering at the SPBs to chromosome capture by the spindle MTs at the start of mitosis. In addition, it is reported that lost kinetochores can be retrieved, that is, they re-established an association with SPBs, and then bi-oriented successfully (Grishchuk and McIntosh, 2006). When cold-sensitive (*cs*) mutant of β-tubulin, nda3-KM311^{cs} is grown at 18ºC, MTs are reversibly disrupted, and the kinetochores frequently lose their attachment to SPBs (Hiraoka et al., 1984; Kanbe et al., 1990). When nda3-KM311^{cs} cells are returned to the permissive temperature, their MTs polymerize within minutes to re-establish proper bipolar spindle and the cells proceed through mitosis. In this condition, detached kinetochores are retrieved and then bi-oriented so that sister kinetochores bind to MTs growing from opposite SPBs (Grishchuk and McIntosh, 2006), indicating that there is a mechanism in fission yeast that can potentially aid to chromosome declustering during mitosis. However, it is possible that this mechanism might not be sufficient or accurate to retrieve kinetochores that scattered very far away from the SPBs. Therefore, the combination of both positioning the centromeres at the SPB during interphase and chromosome retrieval in mitosis might be necessary to ensure that inherently stochastic process such as kinetochore capture is properly achieved and chromosomes are segregated with high fidelity.

1.3. Mitotic Spindle Dynamics

Bipolar Spindle Assembly

Spindle assembly takes place in prophase where MTs nucleate at the SPBs and grow with their dynamic plus ends to form overlapping antiparallel region called spindle midzone (Figure 1.3).

Figure 1.3

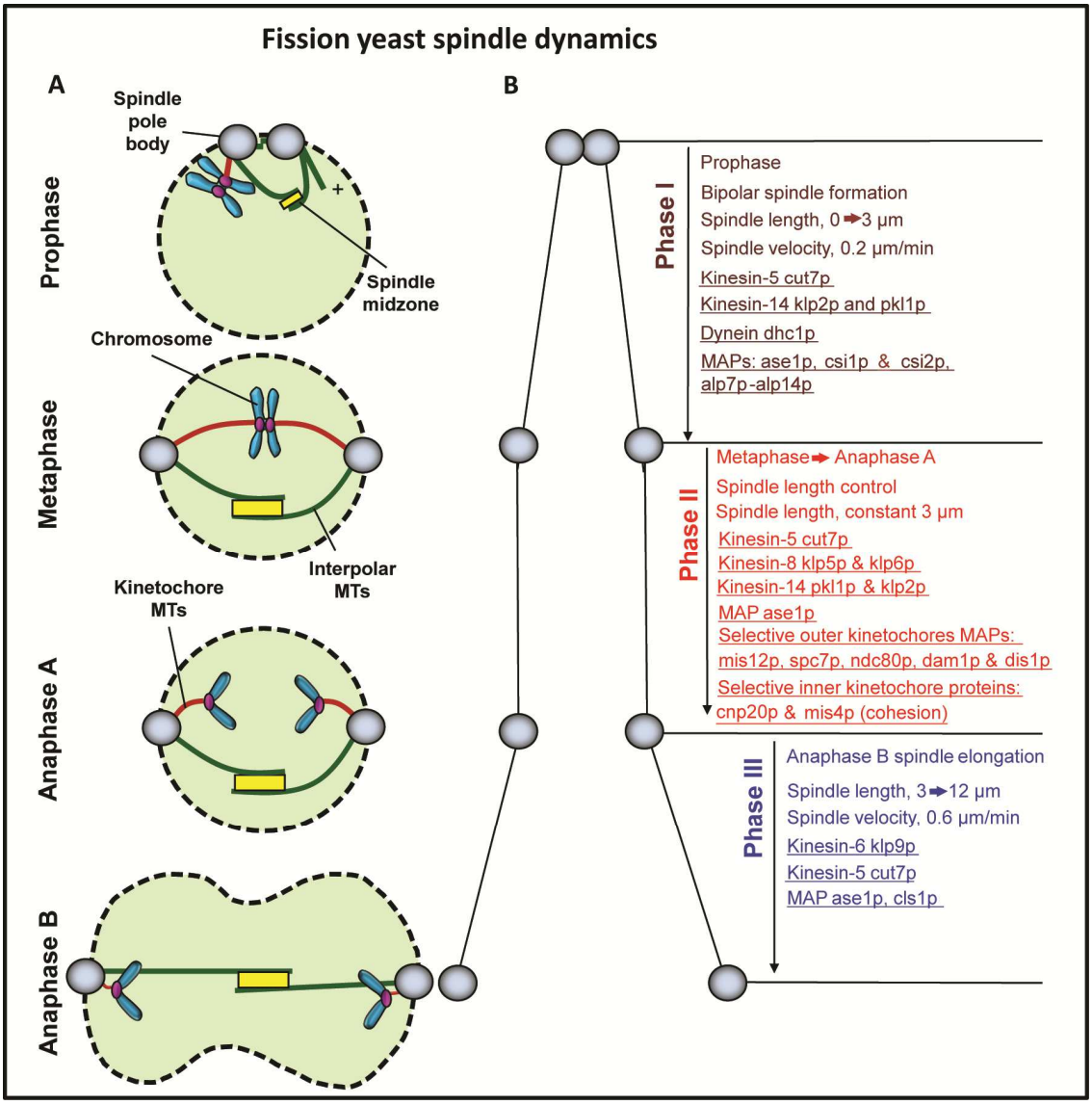

Figure 1.3. Fission Yeast Spindle Dynamics.

(A) The different phases of mitosis in fission yeast correspond to specific stereotypical spindle lengths. Phase I is equivalent to prophase during which the spindle elongates till the two spindle pole bodies (SPBs) have separated to opposite side of the nucleus. Phase II corresponds to metaphase to anaphase A during which the spindle length remains constant. Phase III is

anaphase B, during which the length pole-to-pole spindles elongates rapidly. **(B)** Different phases of mitosis correspond to changes in spindle lengths, which can be characterized by three distinct length scales. Phase I, 0 to 3 μm; Phase II, a relatively constant spindle length of ~ 3 μm; and Phase III, 3 to 12 μm. Motors and selective MAPs are listed that contribute to corresponding Phases (see text for details).

The MAP ase1p, an antiparallel MTs bundler, stabilizes the spindle midzone (Loiodice et al., 2005; Yamashita et al., 2005; Janson et al., 2007). The Kinesin-5 cut7p, a presumably plus-end directed motor, localizes to the spindle midzone and is required for the formation of bipolar spindle (Hagan and Yanagida, 1990; Hagan and Yanagida, 1992). The cut7^{ts} mutants displayed an abnormal V-shaped spindle at the restrictive temperature representing a monopolar spindle, suggesting that cut7p generates force to push two spindle poles apart (Hagan and Yanagida, 1990; Hagan and Yanagida, 1992). Moreover, in *in vitro* experiments Eg5, a human homologue of cut7p, generates pushing forces to slide antiparallel microtubules apart (Kapitein et al., 2005). Surprisingly, recent *in vitro* experiments show that cut7p is a minus-end-directed motor which also exhibits plus-end directionality (Edamatsu, 2014). In addition to the spindle midzone, cut7p localizes to the SPBs during mitosis (Hagan and Yanagida, 1992) but its function near the SPBs has not been reported thus far. It is also not clear how the directionality of cut7p is regulated during mitosis.

The spindle midzone is required to maintain the integrity of the mitotic spindle (Loiodice et al., 2005; Yamashita et al., 2005). However, it is unknown how cut7p and ase1p collaborate to organize the spindle midzone and spindle dynamics in early prophase. Ase1p preferentially binds to antiparallel MTs (Janson et al., 2007) while cut7p is proposed to slide antiparallel MTs (Hagan and Yanagida, 1990; Hagan and Yanagida, 1992). How do MTs become organize into antiparallel initially in early prophase when SPBs are located closer to each other? A recent report proposes a mechanism that promotes the formation of antiparallel MTs between two SPBs in early prophase (Zheng et al., 2014). The proposed mechanism involves the SPB protein csi1p that recruits the transforming acidic coiled-coil (TACC) family protein, alp7p and its adaptor protein alp14p, a TOG family member protein, to the SPBs. Once at the SPB, alp7p-alp14p complex may facilitate the lateral binding of adjacent MTs and MTs that are coming from the opposite pole for promoting bipolar spindle formation. Both csi1p and alp7p are required for bipolar spindle assembly and organization, and their deletions result in delay and compromised spindle formation

(Sato et al., 2004; Zheng et al., 2014). Further, alp14p that acts as a microtubule stabilizer/polymerase (Al-Bassam et al., 2012; Garcia et al., 2001) only when it is targeted to the mitotic SPB via alp7p (Sato and Toda, 2007; Sato et al., 2004), resulting in localization of this complex to the plus end of spindle microtubules including the kinetochore (Sato and Toda, 2007; Sato et al., 2004; Tang et al., 2013). In addition to csi1p, pcp1p is reported to be involved in the recruitment of alp7p to the SPBs (Tang et al., 2014).

Pkl1p, a minus-end- directed kinesin-14 family member, has clearly been implicated in bipolar spindle formation. The first indication that pkl1p provides the inward –directed pulling force to oppose the outward –directed pushing force of the cut7p shown by cell growth assays (Pidoux et al., 1996; Troxell et al., 2001). The cut7^{ts} mutants die at 37ºC due to inability to form bipolar spindle. However, deletion of the *pkl1*+ gene is able to suppress the temperature-sensitivity of growth in cut7^{ts} cells at 37ºC. In addition, a recent report shows that deletion of *cut7*+ in background of pkl1Δ cells results in viable cells, suggesting that cut7p is dispensable in the absence of pkl1p (Olmsted et al., 2014).

How can cells build a bipolar spindle in the absence of essential cut7p? Possibly kinesin-6 klp9p might substitute for the function of cut7p. Klp9p is another plus-directed motor that localizes to the spindle midzone to elongate the spindle (Fu et al, 2009). Alternatively, MT pushing forces may contribute to SPBs separation in prophase. MT dynamics such as assembly and disassembly can generate forces which are coupled to the GTPase activity of tubulin (Inoue and Salmon, 1995). Assembling MTs can generate pushing forces, while disassembling MTs can generate pulling forces (Dogterom et al., 2005). It has been proposed in *Drosophila* embryos that MT pushing forces may contribute to centrosome separation in prophase (Cytrynbaum et al., 2003; Tanenbaum and Medema, 2010). During the process of centrosome separation, MTs growing from one centrosome will encounter the other centrosome and can exert a pushing force on it

Figure 1.4

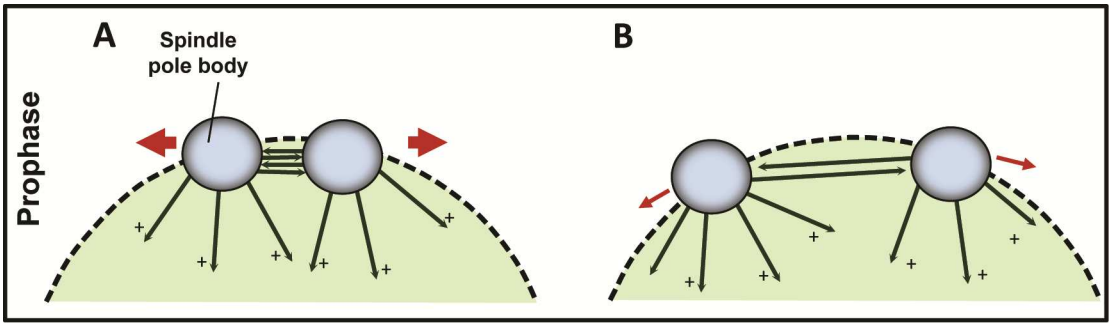

Figure 1.4. Role of Microtubule Pushing Forces in Prophase Spindle Pole Body Separation

View of SPBs imbedded into the nuclear envelope. MTs are growing from each SPB in all directions. **(A)** When SPBs are positioned close together, many short MTs will collide with the opposing SPB, generating a pushing force that propels SPB apart. **(B)** When SPBs are further apart, fewer MTs will collide with the opposing SPB and the outward pushing force is much smaller. Size of the red arrows indicates the magnitude of the outward pushing force. Cartoon representation is modeled after (Tanenbaum and Medema, 2010).

(Figure 1.4). In fission yeast, interphase MT generate pushing forces to position the nucleus in the middle of the cell (Tran et al., 2001), suggesting that MT can generate substantial forces to move SPBs apart in prophase when SPBs are close to each other.

Metaphase Spindle Length Control

Kinesin-5 Cut7p drives spindle pole separation and spindle bipolarity during prometaphase while kinetochore MTs undergo "search and capture" process where dynamically unstable microtubules begin to make associations with kinetochores, a large protein structures organized on centromeres that act as an interface for MT-chromosome attachments (Kirschner and Mitchison, 1986; Cheeseman and Desai, 2008). The search and capture of kinetochores by microtubules is a common feature of mitosis in eukaryotes including fission yeast (Franco et al.,

2007; Gachet et al., 2008). After capture, chromosomes oscillate between the poles while the metaphase spindle is kept at relatively constant length of ~ 3 μm (Mallavarapu et al., 1999; Nabeshima et al., 1998). The force-balance model is proposed to maintain the spindle length at metaphase (Goshima and Scholey, 2010; Pidoux et al., 1996; Saunders et al., 1997). It is based on observations that the interpolar MTs and their interaction with motors and MAPs produce outward pushing forces that tend to lengthen the spindle and the kinetochore MTs and their interaction with the chromosomes produce inward pulling forces that tend to shorten the spindle. These antagonistic forces produced at different spindle MT components balance each other to maintain the constant metaphase spindle length. In a simplified model in which there are two pairs of MTs, one connected by motors and MAPs and the other by sister kinetochores in metaphase (Figure 1.5), the outward pushing force generated by motors sliding apart are balanced by an inward pulling force due to sister kinetochore tension.

One important spindle MT component for the spindle length control model is the spindle midzone. Kinesin-5 cut7p and MAP ase1p localize to the spindle midzone and contribute to outward pushing forces (Hagan and Yanagida, 1992; Loiodice et al., 2005; Yamashita et al., 2005). As shown in Chapter 2, cut7p is essential for metaphase spindle maintenance in fission yeast as oppose to mammalian somatic cells. Ase1p also contribution to metaphase length control as discussed in Chapter 2. Briefly, if the spindle midzone is perturbed due to cut7p inactivation or deletion of ase1p, the inward pulling forces becomes more dominant and pole-to-pole distance decreases.

Another important spindle MT component for the spindle length control model is MT-to-kinetochore connection and therefore whole chromosome. If kinetochore-to-MT interactions are perturbed or if sister chromatid cohesion, which binds sister chromatids together is defective, the outward pushing forces becomes more dominant and pole-to-pole distance increases. Our knowledge of the molecules involved in establishing a proper MT- kinetochore attachment has grown tremendously in last several years. We now know of more than 80 proteins that make up

Figure 1.5

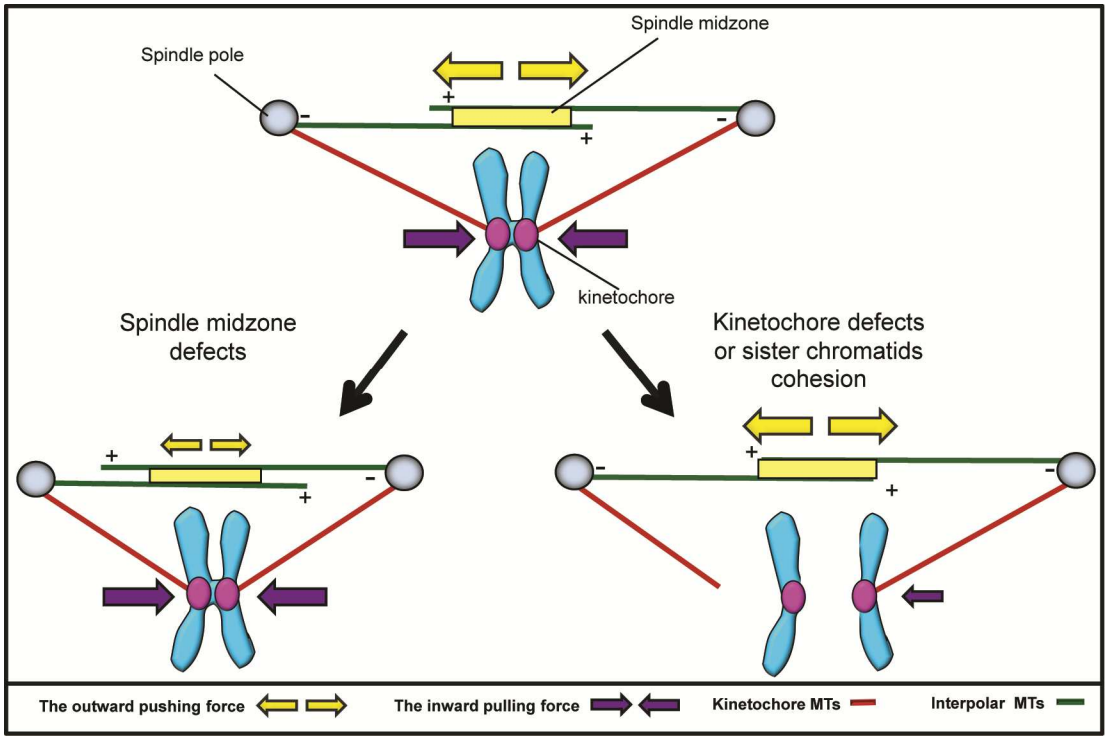

Figure 1.5. Simplified Force-Balance Model

Motors and MAPs that localize to the kinetochore regulate MT dynamics to generate the inward pulling forces on spindle poles whereas motors that localize to the spindle midzone generate the outward pushing forces on spindle poles. These antagonistic forces regulate steady-state constant spindle length at metaphase. If the spindle midzone is perturbed, the inward pulling forces becomes more dominant and pole-to-pole distance decreases. If kinetochore-to-MT interactions are perturbed or if sister chromatid cohesion is defective, the outward pushing forces becomes more dominant and pole-to-pole distance increases.

the kinetochore (Cheeseman and Desai, 2008; Westermann and Schleiffer, 2013; Yamagishi et al., 2014).The kinetochore is roughly divided into two parts, the inner kinetochore and the outer kinetochore. Proteins that form the inner kinetochore interact with centromeric chromatin while the outer kinetochore proteins contribute to the microtubule-binding interface. I will focus here on several important kinetochore proteins that contribute to metaphase spindle length control in fission yeast. More details concerning the composition of kinetochore factors and their conservation can be found by referring to the following excellent reviews (Cheeseman and Desai, 2008; Roy et al., 2013; Westermann and Schleiffer, 2013). Mutations in kinetochore components generally lead to metaphase spindle expansion. For example, in cells carrying conditional lose-of-function alleles of *cnp20+*, an inner kinetochore protein, kinetochores are detached from MTs which results in longer mitotic spindle and subsequent chromosome segregation defects (Tanaka et al., 2009). Furthermore, the disruption of kinetochore attachment caused by mutation in ndc80p, mis12p or spc7p, outer kinetochore proteins, also increases the metaphase spindle length (Goshima et al., 1999; Kerres et al., 2007; Tang et al., 2013). Ndc80p is a part of the ndc80 complex that consist of other 3 conserved subunits nuf2p, spc24p and spc25p while mis12p is a part of the mis12 complex that consist of other 3 subunits mis13p, mis14p and nnf1p (Yamagishi et al., 2014). Metaphase spindle lengths were not measured in many of other subunits of ndc80 or mis12 complexes using live-cell imaging however, it is likely that mutations that disrupt function of many of these subunits in MT-to-kinetochore connection would lead to increase in metaphase spindle length. Moreover, mutations in proteins that are required for sister chromatid cohesion generally lead to metaphase spindle expansion. For example, the loss of sister chromatid cohesin caused by the mutation in mis4p, doubles the metaphase spindle length (Goshima et al., 1999). Investigating contribution of kinetochore components to metaphase spindle length control has been challenging because many proteins are essential and therefore difficult to manipulate. However, as I will discuss in Chapter 2, temperature-sensitive mutants in combination with newly developed live-cell imaging approaches can be extremely useful to

examine relative contribution of many essential proteins to metaphase length regulation and chromosome segregation (Syrovatkina et al., 2013).

The elasticity of kinetochores can also influence spindle size. Bouck & Bloom (2007) showed that histone repression in budding yeast leads to the stretching of pericentric chromatin, which in turn produces an increase in sister centromere spacing and an equivalent increase in metaphase spindle length (Bouck and Bloom, 2007). In fission yeast similar experimental studies have not been performed yet. However, computational model showed fission yeast chromosome behavior at metaphase is the same as budding yeast (Gay et al., 2012), when it is assumed that cohesion associated with centromeres is a spring, representing the elasticity of the kinetochore. It is possible that there are factors that influence the kinetochores elasticity in this model system and those factors may also contribute to the spindle length control.

Chromosome provides passive resistance in the scenario where kinetochore-to-MT interactions and sister chromatid cohesion serves to connect chromosome to the mitotic spindle (Figure 1.5). In addition to passive role, chromosome can also play a dominant role in the control of metaphase spindle length. The interface between MTs and a kinetochore provides a firm attachment where forces can be generated by MT dynamics (McIntosh et al., 2010). MT depolymerization can generate forces because tubulin dynamics are associated with GTP hydrolysis. Tubulin-bound GTP is hydrolyzed shortly after polymerization, so that most of the MT wall is GDP-tubulin. This unfavorable conformation strains the assembled GDP-tubulin (Wang and Nogales, 2005) from interactions with its neighbors in the MT wall. MT depolymerization relieves this strain when strands of tubulin dimers, called protofilaments, become flared at the MT end (Akhmanova and Steinmetz, 2008). Indeed, curved protofilaments during MT depolynerization are observed in many organisms including fission yeast (McIntosh et al., 2013). Protofilament bending during MT shortening has been proposed to do mechanical work (Koshland et al., 1988). Moreover, microbeads coupled to MTs by static links such as a biotin-streptavidin bond, experience a brief tug during protofilament bending (Grishchuk et al., 2005).

Thus, when kinetochores are coupled to MTs, the energy from tubulin depolymerization can drive chromosome movement. The MAP dam1p, a part of DASH complex in fission yeast, functions to couple kinetochores with microtubules and converts MT depolymerization into the inward pulling forces (Buttrick and Millar, 2011). In fact, deletion of dam1p, results in longer metaphase spindle length (Syrovatkina et al., 2013). Dam1p complex, budding homologue, has been studied more extensively *in vitro*. Dam1p complex forms a ring around MTs *in vitro* (Westermann et al., 2005) and when beads loaded with the dam1 complex attached to MTs tips, the beads follow growing or shrinking microtubule ends even under a small and a large loads (Asbury et al., 2006; Franck et al., 2007; Volkov et al., 2013).

Another way by which chromosome can play a dominant role in the control of metaphase spindle length is through motors and MAPs. Kinesin-8 heterodimer klp5p/klp6p and MAP dis1p localize to the kinetochores to regulate MT dynamics and influence spindle length. For example, depletion of klp5p and klp6p proteins results in the formation of longer spindles (Garcia et al., 2002; West et al., 2002). Heterodimer klp5p/klp6p is a MT plus end depolymerase which converts MT depolymerization to cargo movement *in vitro* (Erent et al., 2012; Grissom et al., 2009). On the other hand, dis1p, a TOG family protein, is a MT stabilizer/polymerase that interacts directly with ndc80p to establish proper kinetochore-to-MT attachments and influence MT dynamics at the kinetochores (Hsu and Toda, 2011). Live-cell imaging analysis reveals that mitotic spindles in $dis1^{cs}$ mutant continue to increase and do not establish relatively constant metaphase length of ~ 3 μm (Nabeshima et al., 1998). This phenotype suggests that the outward pushing forces become more dominant to continuously elongate mitotic spindle when kinetochore-to-MT interactions are perturbed in absence of dis1p.

Many studies described above that gave support for the force-balance model were often performed by inhibiting one component of the spindle by, for example, deletion or inhibition of one type of motors or MAPs. In rare studies antagonistic forces have been removed by deletion of two antagonistic motors, the metaphase spindle length appeared rescued based on cell growth

assays (Pidoux et al., 1996; Troxell et al., 2001). It has been technically difficult to monitor a dynamic spindle and its chromosomes while simultaneously inhibiting the function of antagonistic motors and MAPs. Therefore, whether metaphase spindle length regulation is important for chromosome segregation fidelity remains uncertain. We show that removing proteins in antagonistic combination rescued the defective spindle length and, in only some combinations, partially rescued chromosome segregation defects (Chapter 2). This suggests that metaphase spindle length regulation may partially benefit chromosome segregation fidelity.

Spindle mechanics during anaphase A

At anaphase A onset, the spindle reorganizes dramatically. The distance between the spindle poles remains constant while the separated chromosomes move towards opposite poles via shortening of kinetochore microtubules (Hagan, 1998). Chromosome segregation begins with abrupt transition that is initiated by proteolytic severing of cohesion link between sister chromatids (Musacchio and Salmon, 2007). Chromatids separation is synchronous so that most of the chromosomes begin to move within seconds of one another and reach their respective poles within approximately 1 minute (Nabeshima et al., 1995; Saitoh et al., 1997). This precision is important for accurate chromosome segregation, since a lack of synchrony would produce lagging chromosomes that might lead to chromosome mis-segregation (Sanchez-Perez et al., 2005; West et al., 2001). What is responsible for such a fast poleward motion? It is reported that chromosome movement to the spindle pole does not require conventional minus end- directed MT-dependent motors (Grishchuk and McIntosh, 2006), suggesting that MT depolymerization at the kinetochores can generate force to move chromosomes. In fact, defects with DASH complex, MT-to-kinetochore coupler, leads to slower poleward movement of kinetochores and some kinetochores frequently lag behind the rest (Saitoh et al., 2008; Sanchez-Perez et al., 2005). Severing the spindle by laser ablation reveals that these lagging kinetochores are due to a slower rate of anaphase A, and not due to merotelic attachments (Gao et al., 2010). Merotelic

attachments, in which one sister kinetochore is simultaneously attached by MTs emanating from opposite spindle poles, cannot be sensed by the spindle assembly checkpoint because the requirements for both attachment and tension at kinetochores are satisfied (Cimini, 2007). Thus, cells with merotelically attached chromosomes proceed into anaphase but develop lagging chromosomes, which often do not segregate properly.

Furthermore, ndc80p is reported to be important to maintain end-on kinetochore-to-MT attachment during anaphase A (Tang et al., 2013). It is proposed that in addition to its role in establishment of kinetochore-to-MT attachment in metaphase, ndc80p regulates spindle MTs at the kinetochore-MT interface through recruitment of alp7p-alp14p complex. Tang and colleague identified ndc80 mutant (ncd80-NH12^{ts}) that contains a point mutation within internal loop that perturbs the recruitment of alp7p-alp14p complex to the kinetochores. Three-fourths of ncd80-NH12^{ts} mutant cells do not display mitotic delay as evident by similar to normal anaphase spindle dynamics, and yet exhibit chromatids segregation defects during anaphase A (Tang et al., 2013). Live-cell imaging shows that in this mutant, sister chromatids do not move toward their respective spindle pole resulting in chromosome mis-segregation. Alp14p belongs to the conserved TOG, which is thought to stabilize/polymerise MTs (Al-Bassam et al., 2012), therefore it is unclear how recruitment of this alp7p-alp14p complex to the kinetochores can promote microtubule depolymerization. It is possible that recruitment of alp7p-alp14p complex may in turn recruit the third molecule that is responsible for microtubule depolymerization during anaphase. A recent report proposes that alp7p recruits klp5p/6p to kinetochores which promotes chromosome movement at anaphase A (Tang and Toda, 2015). Live-cell imaging shows that localization of klp5p/6p is reduced in ncd80-NH12^{ts} mutant possibly through alp7p interaction. Further, alp7p and klp5/6p are shown to interact directly *in vitro*. A specific mutation in alp7p (alp7-LA6) has been identified that disturbs interaction between alp7p and klp5/6p *in vitro*. The alp7-LA6 mutant leads to slower poleward movement of kinetochores, which prompted the authors to speculate that klp5p/6p promotes chromosome movement at anaphase A. However, alternative

possibilities, such as incorrect kinetochore-to-MT attachments that might also explain lagging chromosomes in the alp7-LA6 mutant, have not been tested. Therefore, precise role of klp5/6p during chromosome movement at anaphase A is not well-defined.

Anaphase B Spindle elongation

The spindle begins to elongate during anaphase B to ensure that separated chromosomes are further away from the cleavage site (Goshima and Scholey, 2010). Considering the importance of this spindle phase, relatively little is known about mechanism that regulate the spindle elongation during anaphase B. It was originally observed by electron microscope that the number of MTs in the spindle midzone decreases while their average length increases as anaphase B progresses (Ding et al, 1997). In photobleaching experiments, bleach marks on spindles did not recover fluorescence at all and instead moved outward at the same rate as spindle elongation (Mallavarapu et al., 1999). These experiments indicate that antiparallel interpolar MTs slide relative to one another to elongate the anaphase B spindle in fission yeast. It was later reported that kinesin-6 klp9p is required to elongate the spindle at anaphase B (Fu et al., 2009). The absence of klp9p results in a ~60% decrease of spindle elongation velocity in comparison to spindle elongation in wild-type cells. Klp9p forms a homo-tetramer that localizes to the spindle midzone by physical binding to ase1p. Failure of klp9p-ase1p interaction leads to decreased spindle elongation velocity. In addition, the interaction between klp9p and ase1p depends on the phosphorylation states of each protein, which provides the spatial temporal control over rapid spindle elongation, restricting it only to anaphase B.

The astral microtubules are known to contribute to anaphase B spindle elongation in other organisms (Fink et al., 2006; Nguyen-Ngoc et al., 2007). In general, dynein at the plus tips of astral microtubules generates pulling forces to mediate spindle elongation. In fission yeast, however, dynein is reported to contribute to chromosome bi-orientation in early mitosis before aster MTs appear (Grishchuk et al., 2007). Kinesin-3 klp8p localizes to the medial cell cortex

(Moseley et al., 2009) but its function in spindle elongation has not been reported. It is possible that klp8p may play similar role to dynein by interacting with aster MTs to generate outward forces to elongate the spindle.

Furthermore, the stability of the spindle midzone and interpolar MT plus end dynamics are additional important factors that contribute to anaphase B spindle elongation. Live-cell imaging analysis shows that MT plus ends at the spindle midzone experience sequential catastrophe and rescue events, however, those interpolar MTs do not generally shrink past the midzone region until late anaphase when the spindle begins to disassemble (Sagolla et al., 2003). This observation suggests that the interpolar MTs are stabilized at the spindle midzone and the dynamics of their plus ends is regulated. Conserved MT-bundler, ase1p is an important factor that stabilizes overlapping MT arrays. Ase1p deletion cells are viable but exhibit spindles that collapse frequently (Loiodice et al., 2005; Yamashita et al., 2005). In addition, it is reported that ase1p recruits cls1p, a CLASP family member protein, to the spindle midzone where cls1p mediates the stabilization of overlapping MTs (Bratman and Chang, 2007). Inactivation of the $cls1^{ts}$ mutant in anaphase leads to rapid loss of spindle MTs by MT depolymerization. Furthermore, *in vitro* experiments indicated that cls1p forms a homodimer that binds αβ -tubulin heterodimers and influence MT dynamics (Al-Bassam et al., 2010). It is proposed that cls1p promotes MT rescue by recruiting tubulin dimers to the MTs plus ends. Overall, the spindle midzone stability and therefore spindle elongation depends on proteins that bundle interpolar MTs and stabilize the dynamics of their plus ends.

In rare occasions, anaphase B spindle elongation can to be influenced by merotelically attached chromosomes that manifest themselves as lagging chromosome (Pidoux et al., 2000). In fission yeast, mutants that affect chromosome segregation display frequent lagging chromosomes and exhibit significant reduction in the rate of anaphase B spindle elongation (Pidoux et al., 2000). Kinetochores of lagging chromosome are thought to interact simultaneously with MTs emanating from both poles creating merotelic attachments. This mode of attachment acts to pull the poles

towards each other, counteracting the outward pushing forces generated in the spindle midzone, thereby slowing spindle elongation. In addition, single merotelic attached sister chromatid is shown to stretch significantly due to the outward pushing force generated at the spinde midzone (Courtheoux et al., 2009). It is thought that anaphase elongation forces can help resolve some merotelically attached kinetochores to prevent chromosome mis-segregation and cell death. However, lagging chromosomes also frequently observed to not segregate properly (Choi and McCollum, 2012), suggesting that this mechanism is not very efficient. Nevertheless, anaphase B spindle elongation can be influenced by merotelically attached kinetochores in rare occasions that mostly observed in mutants and not in wild-type cells. This suggests that this mechanism is a consequence of erroneous kinetochore-to-MTs attachments and not a general principal that normally affect spindle elongation in anaphase B.

1.4. Mitotic Spindle Disassembles in Telophase

Spindle continues to elongate in Anaphase B till the nuclei reach the cell tips. The spindle then breaks down and the post-anaphase array MTs are nucleated at novel MT organization centers that form at the cell equator (Hagan, 1998). The mechanism of spindle disassembly in telophase remains poorly understood. Spindle collapse occurs through microtubules depolymerization from their plus ends towards the SPBs (Sagolla et al., 2003). A striking pattern of alternating single microtubule depolymerization is observed from one half of the spindle and then the other. High temporal live-cell imaging shows that as each microtubule leaves the bipolar array, overall intensity of the spindle fluorescence decreases. Furthermore, MT depolymerization occurs independently at each SPB as the next microtubule begins to depolymerize before the previous one has completely disappeared. The pattern is repeated until the spindle has completely disassembled and the post-anaphase array has formed. These observations suggest spindle collapse occurs gradually where stabilizing proteins at the spindle midzone steadily decrease. It is possible that MT cross-linker klp9p and ase1p are inactivated gradually at the spindle midzone

leading to weakening of spindle midzone integrity and subsequent gradual MT plus ends depolymerizaton.

The post-anaphase array (PAA) MT nucleation is important for proper spindle disassembly. Mto1p recruits γ-TuC to non-spindle pole body MTOCs to initiate MT nucleation (Sawin et al., 2004). Mto1p-deletion cells fail to nucleate the PAA MTs and exhibit defective spindle disassembly (Samejima et al., 2008; Sawin et al., 2004). However, precise role of mto1p or the PAA MTs to spindle disassembly is not understood.

1.5. Summary of Main Results

Chapter 2: Antagonistic Spindle Motors and MAPs Regulate Spindle Length and Chromosome Segregation

- The force-balance model, which proposes that inward and outward forces maintains metaphase constant spindle length, is tested herein
- Microfluidic temperature control enables studies of antagonistic motors and MAPs
- Kinesin-5 cut7p and MT bundler ase1p contribute to outward-pushing forces
- Kinetochore proteins kinesin-8 klp5/6p and dam1p contribute to inward-pulling forces
- Removing inward forces (klp5/6 or dam1p) causes spindle to be longer; removing outward forces (cut7p or ase1p) causes spindle to be shorter
- Removing both forces rescues spindle length defects
- There is a positive correlation between spindle length rescue and proper chromosome segregation
- Some proteins which regulate spindle length also regulate kinetochore-to-MT attachment (dam1p).
- Kinetochore-to-MT attachment is more important than spindle length for chromosome segregation.

Chapter 3: Loss of kinesin-14 results in aneuploidy via kinesin-5-dependent microtubule protrusions leading to chromosome cut

- Kinesin-14 pkl1p focuses the spindle pole
- Pkl1p and MAP msd1p depend on each other to localize to SPBs
- pkl1Δ and msd1Δ lead to SPB fragmentation and unstable spindle poles resulting in MT spindle protrusions
- MT protrusions are due to kinesin-5 cut7p sliding forces
- Long MT protrusions can push the spindle to the cell center
- Cytokinesis ring contraction can “cut” the off-set nucleus causing chromosome segregation defects
- Cell length negatively correlates with protrusion-dependent chromosome loss
- 4% of the aneuploid pkl1Δ cells survive and proliferate

CHAPTER 2: ANTAGONISTIC SPINDLE MOTORS AND MAPS REGULATE METAPHASE SPINDLE LENGTH AND CHROMOSOME SEGREGATION[1,2]

2.1 Summary

Metaphase describes a phase of mitosis where chromosomes are attached and oriented on the bipolar spindle for subsequent segregation at anaphase. In diverse cell types, the metaphase spindle is maintained at characteristic constant length (Dumont and Mitchison, 2009; Goshima and Scholey, 2010; Mogilner and Craig). Metaphase spindle length is proposed to be regulated by a balance of pushing and pulling forces generated by distinct sets of spindle microtubules and their interactions with motors and MAPs. Spindle length is further proposed to be important for chromosome segregation fidelity, as cells with shorter or longer than normal metaphase spindles, generated through deletion or inhibition of individual mitotic motors or MAPs, showed chromosome segregation defects. To test the force balance model of spindle length control and its effect on chromosome segregation, we applied fast microfluidic temperature-control with live-cell imaging to monitor the effect of switching off different combinations of antagonistic forces in the fission yeast metaphase spindle. We show that spindle midzone proteins kinesin-5 cut7p and microtubule bundler ase1p contribute to outward pushing forces, and spindle kinetochore proteins kinesin-8 klp5/6p and dam1p contribute to inward pulling forces. Removing these proteins individually led to aberrant metaphase spindle length and chromosome segregation defects. Removing these proteins in antagonistic combination rescued the defective spindle length and, in some combinations, also partially rescued chromosome segregation defects. Our results highlight

[1] Part of this chapter has been published as:
Syrovatkina V*, Fu C* and Tran PT
Antagonistic Spindle Motors and MAPs Regulate Spindle Length and Chromosome Segregation. Current Biology, December 2, 2013; Volume 23, pp. 2423-9
* These authors contributed equally to this work.

[2] V.S. and C.F. designed and performed experiments and analyzed data. V.S.and P.T.T. wrote the manuscript.

the importance of proper chromosome-to-microtubule attachment over spindle length regulation for proper chromosome segregation.

2.2 Introduction

The metaphase spindle maintains a characteristic steady-state constant length (Dumont and Mitchison, 2009; Goshima and Scholey, 2010; Mogilner and Craig), which is thought to be important for ensuring correct chromosome-to-microtubule attachment prior to anaphase. It is proposed that a balance of antagonistic forces produced by motors and MAPs located at the spindle midzone, the kinetochores, and/or aster MTs is required to maintain constant metaphase spindle length (Dumont and Mitchison, 2009; Goshima and Scholey, 2010; Mogilner and Craig). However, the force-balance model has never been tested in an integrated manner. Studies which gave support for the force-balance model were often performed by inhibiting one component of the spindle, i.e., deletion or inhibition of one type of motors or MAPs. In rare occasions of removal of antagonistic forces, i.e., double-deletion of antagonistic motors, metaphase spindle length appeared rescued (Saunders and Hoyt, 1992; Tanenbaum et al., 2009; Troxell et al., 2001), but its subsequent effect on chromosome segregation was not known.

We present here an integrated study using the simple fission yeast *Schizosaccharomyces pombe*, combined with live-cell imaging, fast microfluidic temperature-control for inactivating thermo-sensitive genes, to directly test the force-balance model and determine its consequences on chromosome segregation. Fission yeast exhibits all the phases of mitosis identical to that of mammalian cells (Nabeshima et al., 1998). However, unlike mammalian cells, the number of motors and MAPs implicated in spindle dynamics in fission yeast are fewer (Fu et al., 2009), e.g., there are 9 kinesins in *S. pombe* compared to ~50 in mammalian. Thus, mechanisms of fission yeast spindle length regulation may be viewed as “core” conserved mechanisms through evolution.

2.3 Results

Motors and MAPs Control the Steady-State Constant Metaphase Spindle Length

We reasoned that forces contributing to the metaphase spindle length maintenance would come from motors and MAPs (Dumont and Mitchison, 2009; Goshima and Scholey, 2010; Mogilner and Craig). To define a set of antagonistic motors and MAPs regulating spindle length, we performed a targeted deletion or inactivation screen of the fission yeast motors and selective MAPs known to have spindle length defects. We used the degradation of cyclin B (cdc13p-GFP) as a proxy for metaphase to anaphase transition (Figure 2.1A) (Decottignies et al., 2001; Tatebe et al., 2001), and defined the final metaphase spindle length as the length immediately before the disappearance of cdc13p-GFP from the spindle. Our screen identified the kinetochore proteins heterodimer kinesin-8 klp5/6p and the MT dam1p as the major contributors to the inward-pulling force on the spindle, as their individual deletion resulted in longer metaphase spindles compared to wild-type (Figure 2.1B), consistent with previous findings (Garcia et al., 2002; West et al., 2002). Kinesin-8 klp5/6p is a MT plus-end polymerase that converts MT depolymerization to cargo movement (Erent et al., 2012; Grissom et al., 2009). Similarly, dam1p is a MAP that binds to processively to MT and converts MT depolymerization to cargo movement (Grishchuk et al., 2008a; Grishchuk et al., 2008b). Thus, klp5/6 can be viewed as an active force transducer and dam1p can be viewed as a passive force transducer, both converting MT depolymerization into the inward-pulling forces experienced by the spindle. We also identified the spindle midzone MAP ase1p as the major contributor to the outward-pushing force on the spindle, as its deletion resulted in shorter metaphase spindles compared to wild-type (Figure 2.1B), consistent with previous findings (Loiodice et al., 2005; Yamashita et al., 2005). As a MT bundler of defined angular polarity (Subramanian et al., 2010), Ase1p can be viewed as a force resistor, resisting the inward force due to klp5/6p and dam1p. Finally, kinesin-14 pkl1p also appeared to play a major role in spindle length control, as its deletion resulted in shorter metaphase spindle compared to wild-type (Figure 2.1B). However, its reported localization at the spindle pole body (Troxell et al.,

2001) and its role in focusing MTs at the spindle poles (Grishchuk et al., 2007) suggest that it does not directly contribute to the pulling or pushing forces for spindle length control but instead plays a role in spindle formation itself. Indeed, we observed a high frequency of MT protrusions from the spindle poles in pkl1Δ cells: ~50% of spindles have protrusion in pkl1Δ cells, compared to zero in wild-type cells (Figure 2.S1A and 2.S1B), indicative of spindle malformation. We thus exclude pkl1p from the current analysis. Although numerous motors and MAPs have been reported to play a role in metaphase spindle length regulation (Goshima et al., 2005; Tanenbaum et al., 2009), for clarity, we focus on the motors and MAPs which have the strongest measureable defects in spindle lengths and localize only to the kinetochores or the spindle midzone.

Kinesin-5 cut7p is reported to play a role in bipolar spindle formation, by organizing and sliding apart antiparallel MTs from opposite poles (Hagan and Yanagida, 1990; Hagan and Yanagida, 1992). Cut7p is essential and a conditional temperature-sensitive strain was isolated previously (Hagan and Yanagida, 1992). We thus used a microfluidic fast temperature-control device created in our lab (Velve Casquillas et al., 2011), to inactivate the temperature-sensitive cut7.24^{ts} strain precisely at metaphase (Figure 2.1C). Upon inactivation of cut7p at the nonpermissive 35°C, the metaphase spindle immediately shortened until the spindle become a focused monopolar structure (Figure 2.1C). Thus, cut7p can be viewed as an active force producer, sliding interpolar MTs apart as the outward-pushing force experienced by the spindle.

Interestingly, in C. elegans and mammalian somatic cells, kinesin-5 Eg5 is not needed for the maintenance of metaphase spindle length (Blangy et al., 1995; Kapoor et al., 2000; Saunders et al., 2007). In mammals, highly dynamic interpolar MTs can compensate for the absence of Eg5 (Kollu et al., 2009), and in C. elegans, the relatively more robust astral MTs, compared to the smaller interpolar MTs, can produce pulling force on the spindle and compensate for the absence of Eg5 (Saunders et al., 2007). In comparison, fission yeast has no astral MTs during metaphase and does not have highly dynamic and robust interpolar MTs. Therefore, cut7p becomes indispensable for spindle length maintenance in fission yeast.

Figure 2.1

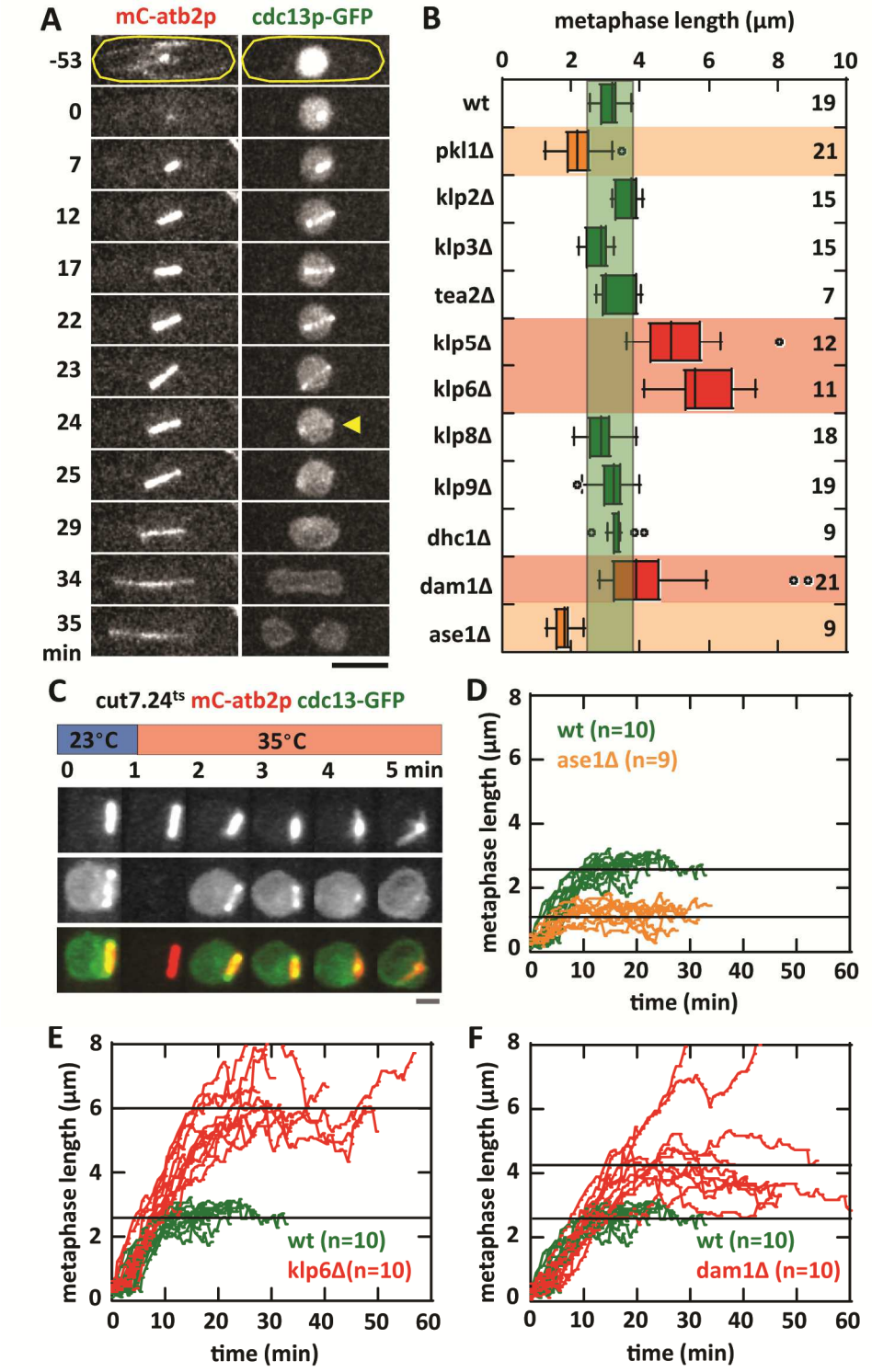
A
mC-atb2p
cdc13p-GFP
-53
0
7
12
17
22
23
24
25
29
34
35 min
B
metaphase length (µm)
0 2 4 6 8 10
wt 19
pkl1Δ 21
klp2Δ 15
klp3Δ 15
tea2Δ 7
klp5Δ 12
klp6Δ 11
klp8Δ 18
klp9Δ 19
dhc1Δ 9
dam1Δ 21
ase1Δ 9
C
cut7.24ts mC-atb2p cdc13-GFP
23°C
35°C
0 1 2 3 4 5 min
D
wt (n=10)
ase1Δ (n=9)
metaphase length (µm)
time (min)
E
metaphase length (µm)
wt (n=10)
klp6Δ(n=10)
time (min)
F
metaphase length (µm)
wt (n=10)
dam1Δ (n=10)
time (min)

Figure 2.1. Motors and MAPs Contribute to Metaphase Spindle Length Force-Balance Mechanism

(A) Time-lapse images of a wildtype cell expressing mCherry-atb2p (tubulin) and cdc13p-GFP (cyclin) through mitosis. cdc13p is degraded from the spindle at the metaphase to anaphase transition (yellow arrow), marking precisely the final metaphase spindle length. The cdc13p-GFP marker is used in the screen for motors and MAPs affecting metaphase spindle length (see Figure 1B). Bar, 5 μm.

(B) Targeted screen of fission yeast motors and selective MAPs for defects in metaphase spindle length at room temperature (23°C). Box plot shows spindle lengths - wildtype (3.1 ± 0.3 μm), pkl1Δ (2.0 ± 0.4 μm, $p<10^{-4}$), klp2Δ (3.6 ± 0.3 μm, $p<10^{-4}$), klp3Δ (2.8 ± 0.4 μm, p=0.1), tea2Δ (3.3 ± 0.5 μm, p=0.3), klp5Δ (5.3 ± 1.2 μm, $p<10^{-4}$), klp6Δ (6.3 ± 1.6 μm, $p<10^{-4}$), klp8Δ (2.9 ± 0.5 μm, p=0.4), klp9Δ (3.4 ± 0.4 μm, p=0.6), dhcΔ (3.4 ± 0.4 μm, p=0.1), dam1Δ (4.4 ± 1.6 μm, $p<10^{-2}$), and ase1Δ (1.8 ± 0.3 μm, $p<10^{-7}$).

(C) Temperature-shift experiment of kinesin-5 $cut7.24^{ts}$ cells expressing mCherry-atb2p and cdc13p-GFP. Within 1 min of shifting to the non-permissive temperature of 35°C, the metaphase spindle exhibits spindle shortening and collapse, ultimately becoming a monopolar spindle. Note: The blank image at time 1-min in the cdc13p-GFP channel was due to thermal expansion of the coverslip causing an out-of-focus image, which was corrected in subsequent frames. Bar, 1 μm.

(D) Comparative plot of spindle length versus time of wild-type (green) and ase1Δ (organe) cells. Shown are pole-to-pole distances measured from prophase to the metaphase-anaphase transition. Wild-type metaphase spindles plateau at ~3 μm length. In contrast, ase1Δ metaphase spindles plateau at ~2 μm length.

(E) Comparative plot of spindle length versus time of wild-type (green) and klp6Δ (red) cells. In contrast to wild-type, klp6Δ metaphase spindles plateau at ~6 μm length. **(F)** Comparative plot of spindle length versus time of wild-type (green) and dam1Δ (red) cells. In contrast to wild-type, dam1Δ metaphase spindles plateau at ~4 μm length.

Figure 2.S1

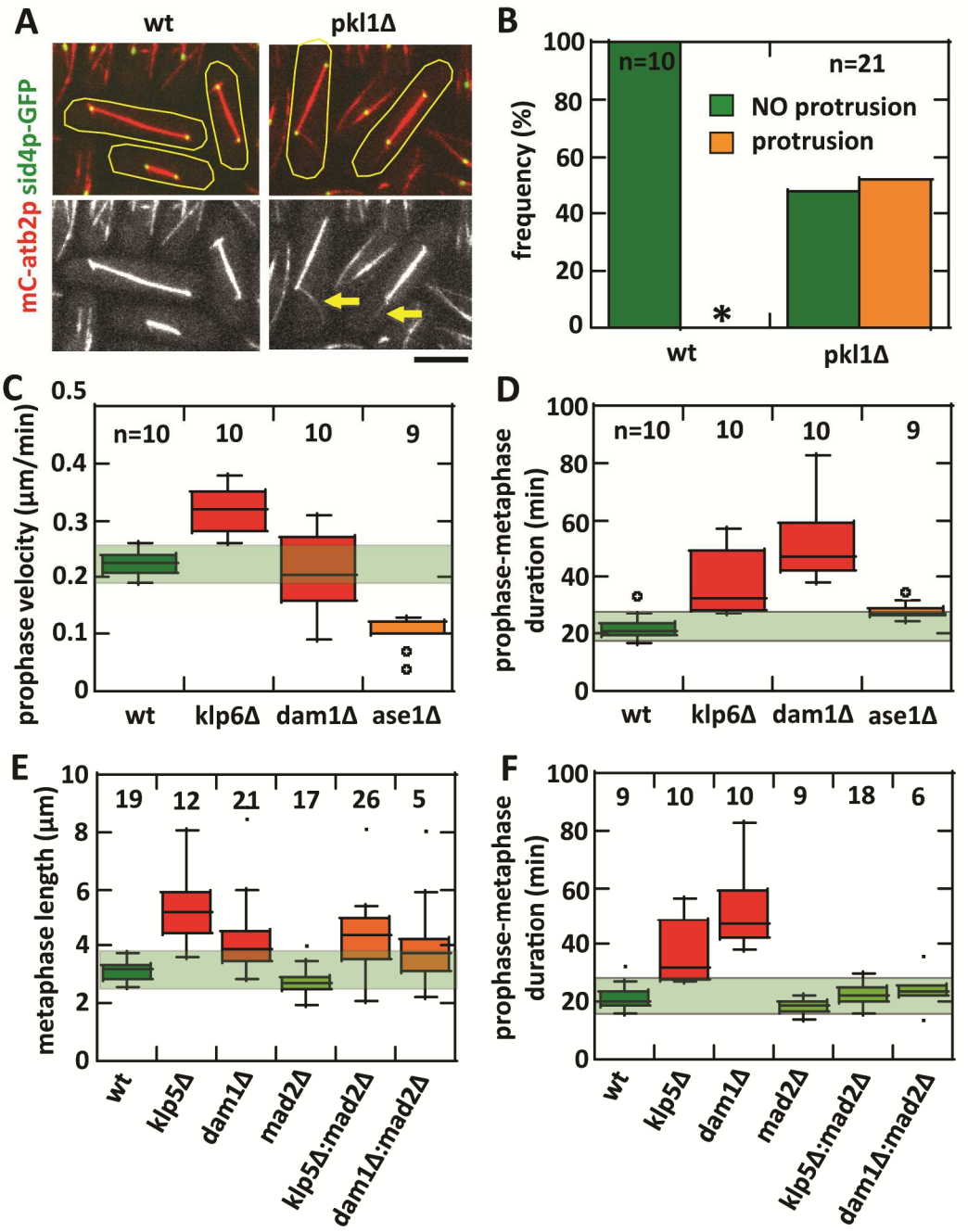
A
wt
pkl1Δ
mC-atb2p sid4p-GFP
B
frequency (%)
n=10
n=21
NO protrusion
protrusion
wt
pkl1Δ
C
prophase velocity (µm/min)
n=10 10 10 9
wt klp6Δ dam1Δ ase1Δ
D
prophase-metaphase duration (min)
n=10 10 10 9
wt klp6Δ dam1Δ ase1Δ
E
metaphase length (µm)
19 12 21 17 26 5
wt klp5Δ dam1Δ mad2Δ klp5Δ:mad2Δ dam1Δ:mad2Δ
F
prophase-metaphase duration (min)
9 10 10 9 18 6
wt klp5Δ dam1Δ mad2Δ klp5Δ:mad2Δ dam1Δ:mad2Δ

Figure 2.S1.

(A) Images of mitotic wildtype and pkl1Δ cells expressing mCherry-atb2p (tubulin) and sid4p-GFP (SPB marker). Wild-type mitotic cells show different spindles at different stages/lengths. Astral MTs are relatively short. In contrast, pkl1Δ cells have long astral MTs which protrude (yellow arrow) from the SPBs. Bar, 5 μm.

(B) Comparative plot of astral MT protrusion in wildtype and pkl1Δ cells. Whereas wild-type cells show no astral MT protrusion, ~50% of pkl1Δ cells have astral MT protrusion, indicating spindle mal-formation (Troxell et al., 2001).

(C) Box plot of prophase velocities. Individual deletion klp6Δ and ase1Δ show different durations than wild-type. dam1Δ is similar to wild-type.

(D) Box plot of prophase-metaphase durations. Individual deletion klp6Δ, dam1Δ, and ase1Δ all show different durations than wild-type.

(E) Box plot of metaphase spindle lengths in response to the absence of the spindle assembly checkpoint proteins mad2p. Individual deletion mad2Δ resulted in similar metaphase spindle length compared to wild-type. In contrast, double-deletion klp5Δ:mad2Δ and dam1Δ:mad2Δ resulted in longer metaphase spindle lengths similar to klp5Δ and dam1Δ, respectively.

We next monitored spindle elongation dynamics to determine how new steady-state spindle lengths is achieved. As inactivation of cut7p shortened completely the metaphase spindle (Fig. 1C, 2A), we examined the ase1Δ, klp6Δ, and dam1Δ mutants. The spindle of wild-type cells typically elongates at 0.23 ± 0.02 μm/min during prophase to reach a steady-state metaphase length of 3.10 ± 0.34 μm, with duration of prophase-metaphase of 22 ± 5 min (Figures 2.1D-F; Figure 2.S1C and 2.S1D). In contrast, ase1Δ elongates at 0.10 ± 0.03 μm/min ($p<10^{-7}$), has metaphase length of 1.82 ± 0.33 μm ($p<10^{-7}$), and prophase-metaphase duration of 28 ± 3 min ($p<10^{-2}$); klp6Δ elongates at 0.32 ± 0.04 μm/min ($p<10^{-4}$), has metaphase length of 6.33 ± 1.60 μm ($p<10^{-4}$), and prophase-metaphase duration of 38 ± 11 min ($p<10^{-2}$); and dam1Δ elongates at 0.21 ± 0.07 μm/min ($p=0.4$), has metaphase length of 4.41 ± 1.62 μm ($p<10^{-2}$), and prophase-metaphase duration of 52 ± 13 min ($p<10^{-4}$) (Figures 2.1D-F; Figure 2.S1B and 2.S1C).

We stress that changes in spindle length is likely due primarily to the force contributors, and not to the activation of the spindle assembly checkpoint (SAC) (Lara-Gonzalez et al., 2012; Musacchio, 2011; Musacchio and Salmon, 2007; Vleugel et al., 2012), which would be expected to prolong the prophase-metaphase duration and lead to changes in spindle length. In the absence of mad2p, a major SAC protein monitoring kinetochore-to-microtubule attachment (Lara-Gonzalez et al., 2012; Musacchio, 2011; Musacchio and Salmon, 2007; Vleugel et al., 2012), metaphase spindle lengths in double deletions klp5Δmad2Δ and dam1Δmad2Δ remained similar to that of klp5Δ and dam1Δ alone, respectively (Figure 2.S1E), while the prophase-metaphase duration of the double-mutants is similar to that of wild-type (Figure 2.S1F). We conclude that, consistent with the force balance model, removing individual contributors of force results in enhanced antagonistic effect from the remaining force contributors, which leads to a new steady-state metaphase spindle length.

Removal of Antagonistic Spindle Forces Can Rescue Metaphase Spindle Length Defects

Pushing and pulling can be viewed as antagonistic forces controlling the steady-state metaphase spindle length. To test if removal of antagonist forces can restore the metaphase spindle length to that of wild-type, we observed metaphase spindle length upon deletion and/or inactivation of antagonistic force contributors. As shown, inactivation of cut7p at 35°C with the fast microfluidic temperature-control device led to an immediate decrease in metaphase spindle length (Figure 2.1C and 2.2A). The decrease was relatively quick, occurring over durations of ~ 3–4 min (Figure 2.2A). The quick spindle shrinkage was the result of the inactivation of cut7.24^{ts} while both klp5/6p and dam1p were still present. In klp6Δ cells, where metaphase spindles were longer than wild-type due to the removal of the inward-pulling force contributor klp6p (Figure 2.1B and 2.2B), inactivation of cut7p did not immediately lead to spindle shrinkage (Figure 2.2B). Instead, the majority of the cut7.24^{ts}:klp6Δ spindles slowly decreased in length over the 10 min observation duration, and some even maintained the same length or slightly increased in length (Figure 2.2B). Our interpretation is that in the absence of klp6Δ, dam1p is still at the kinetochores to capture MTs. Further, dam1p is passive, waiting for a MT depolymerization event to manifest the pulling forces (Grishchuk et al., 2008a; Grishchuk et al., 2008b). If no MT depolymerization occurs, no pulling force would be possible, resulting in no spindle length decrease or even in an increase in spindle length in the short term (~5 min duration). In the long-term, all MTs will tend to depolymerize, and dam1p would then act to pull the spindle inward slowly (Grishchuk et al., 2008a; Grishchuk et al., 2008b). A similar slow spindle length decrease is also observed in the dam1Δ when cut7p is inactivated (Figure 2.2C). However, all cut7.24^{ts}:dam1Δ spindles showed persistent slow spindle length decrease. Our interpretation is that in the absence of dam1Δ, klp6p at the kinetochore can still capture MTs and persistently promote MT depolymerization, resulting in sustained slow spindle shrinkage (Erent et al., 2012; Grissom et al., 2009). Thus, force balance is a tug-of-war between cut7p and ase1p against klp5/6p and dam1p. This model predicts that the triple removal of cut7p, klp5/6p, and dam1p would remove both inward and outward forces,

leading to a static constant-length metaphase spindle. The double deletion dam1Δ: klp5Δ is lethal (Griffiths et al., 2008). Nevertheless, the dam1-A8:klp5Δ double mutant exhibits longer metaphase spindles compared to the individual mutants dam1Δ and klp5Δ or to the wild-type cells (Figure 2.S2B and 2.S2C), consistent with the tug-of-war analogy. In the course of this study, we also discovered that temperature sensitivity is tenuous. It is known that different temperature-sensitive alleles of *cut7+* have different inactivation penetration, e.g., cut7.24^{ts} is lethal but cut7.21^{ts} and cut7.23^{ts} are not lethal (but are very sick) at the nonpermissive temperature (Troxell et al., 2001). Furthermore, we find that the allele cut7.24^{ts}, when tagged with GFP, is no longer lethal at 37°C (Figure 2.S2A), presumably because GFP confers added stability to the cut7.24^{ts} gene product. This implies that creating a fast-acting, strongly penetrant, temperature-sensitive mutant allele requires some serendipity.

We next measured the metaphase spindle lengths of different combinations of antagonist forces. We found that for all combinations of double-deletion, the removal of antagonist forces lead to metaphase spindle lengths which are similar to wild-type and different from individual deletion (Figure 2.2D). Indeed, klp5Δ:ase1Δ has a metaphase length of 3.17± 0.78 μm and dam1Δ:ase1Δ has a metaphase length of 2.65 ± 0.31 μm, values significantly different from individual deletions ($p<10^{-4}$) (Figure 2.2D). Interesting, only the double-deletion dam1Δ:ase1Δ appeared to rescue the prophase-metaphase duration ($p<10^{-4}$) (Figure 2.2F), but klp5Δ:ase1Δ showed similar prophase-metaphase delay as individual klp5Δ deletion (p=0.8). Furthermore, while metaphase spindle length and some prophase-metaphase durations appeared rescued in the double-deletion, the prophase velocities are only partially rescued for dam1Δ:ase1Δ (Figure 2.S2B and 2.S2C), and not rescued at all for klp5Δ:ase1Δ (Figure 2.S2A and 2.S2C). At the restrictive temperature of 35°C, cut7.24^{ts}:klp6Δ has a metaphase length of 2.88 ± 1.04 μm and cut7.24^{ts}:dam1Δ has a metaphase length of 2.65 ± 0.68 μm, values closer to the wildtype 2.16 ± 0.50 μm than the individual deletion or inhibition (Figure 2.2E).These results are consistent with the role of cut7p as an active pushing-force producer, klp5/6p as an active pulling-force transducer, dam1p as a

Figure 2.2

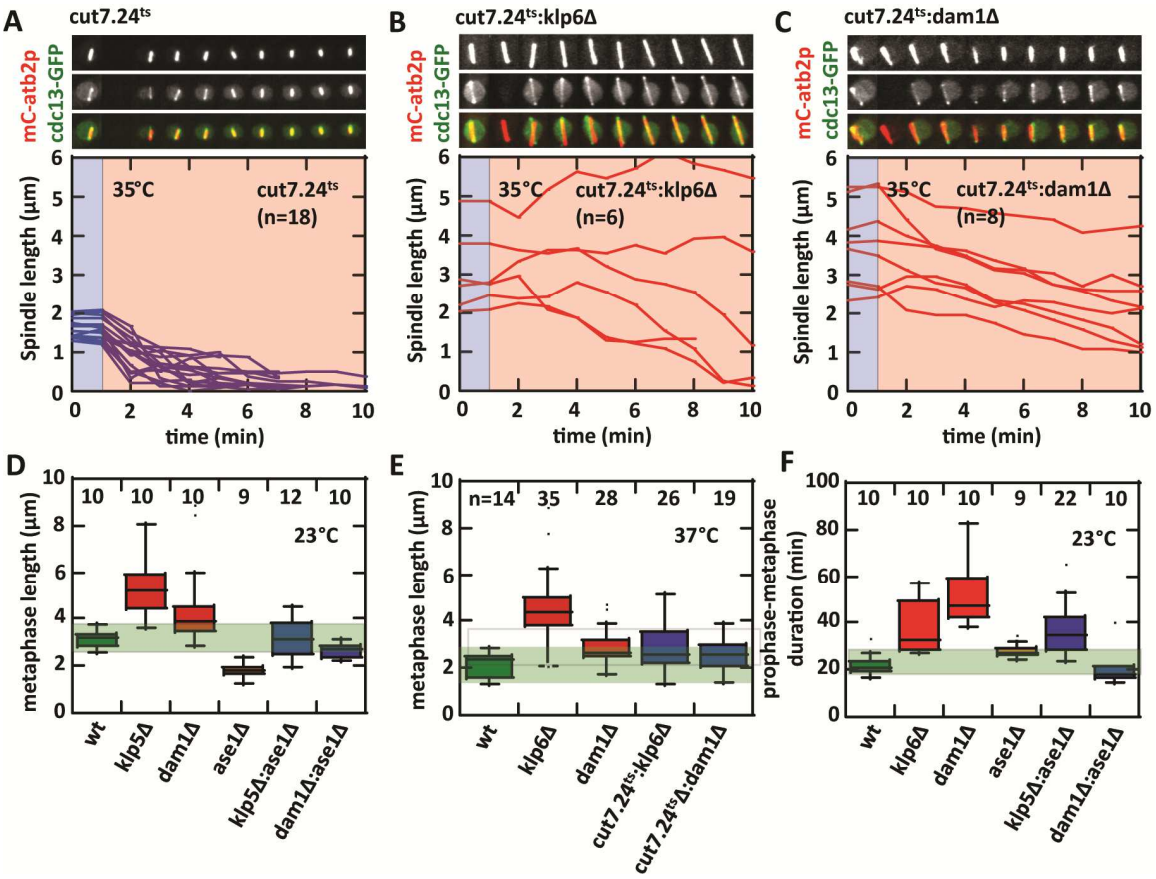

Figure 2.2. Removing Antagonistic Spindle Forces Rescues Metaphase Spindle Length Defects

(A) Temperature-shift experiment of cut7.24^{ts} cells expressing mCherry-atb2p and cdc13p-GFP. The accompanying plot of spindle length versus time shows that all cut7.24^{ts} metaphase spindles shorten and collapse within ~3-4 min at the non-permissive temperature of 35°C.

(B) Temperature-shift experiment of cut7.24^{ts}:klp6Δ double-mutant cells. The double-mutant cells do not exhibit the fast spindle collapse as seen in cut7.24^{ts} alone (see Figure 2.2A). The metaphase spindles maintain transiently stable lengths during the 10 min of observation at the nonpermissive temperature.

(C) Temperature-shift experiment of cut7.24^{ts}:dam1Δ double-mutant cells. The double-mutant cells do not exhibit the fast spindle collapse as seen in cut7.24^{ts} alone. The metaphase spindles slowly shorten during the 10 min of observation at the nonpermissive temperature.

(D) Box plot shows metaphase spindle lengths measured at 23°C. Individual mutants have defective spindle length. Metaphase spindle lengths for wild-type, klp5Δ, dam1Δ, and ase1Δ are reported in Figure 2.1B. In contrast, antagonistic double-mutants rescue the spindle length defects of the single mutants. Metaphase spindle length of klp5Δ:ase1Δ (3.2 ± 0.8 μm) is similar to wild-type ($p=0.8$), and dam1Δ:ase1Δ (2.6 ± 0.3 μm) is between dam1Δ ($p<10^{-4}$) and ase1Δ ($p<10^{-4}$).

(E) Box plot shows metaphase spindle lengths measured at 37°C. Individual mutants have defective spindle length. Metaphase spindle lengths for wild-type (2.2 ± 0.5 μm), cut7.24^{ts} (1.5 ± 0.4 μm, $p<0.004$), klp6Δ (4.6 ± 1.6 μm, $p<10^{-10}$), and dam1Δ (2.9 ± 0.7 μm, $p<10^{-3}$) as shown. In contrast, antagonistic double-mutants rescue the spindle length defects of the single mutants. Metaphase spindle length of cut7.24^{ts}:klp6Δ (2.9 ± 1.0 μm) is between cut7.24^{ts} ($p<10^{-5}$) (and klp6Δ ($p<10^{-5}$), and cut7.24^{ts}:dam1Δ (2.7 ± 0.7 μm) is between cut7.24^{ts} ($p<10^{-4}$) and dam1Δ ($p=0.2$).

(F) Box plot shows prophase-metaphase duration measured at 23°C. Individual mutants have prolonged prophase-metaphase durations. Durations are as follows: wild-type (22 ± 5 min), klp6Δ (38 ± 11 min, $p<0.002$), dam1Δ (52 ± 13 min, $p<10^{-4}$), and ase1Δ (28 ± 3 min, $p<0.007$). In contrast, some antagonistic double-mutants rescue prophase-metaphase duration defects of the single mutants. Durations of dam1Δ:ase1Δ (21 ± 7 min) is similar to wildtype ($p=0.5$), and klp5Δ:ase1Δ (37 ± 11 min) is similar to klp6Δ ($p=0.8$).

Figure 2.S2

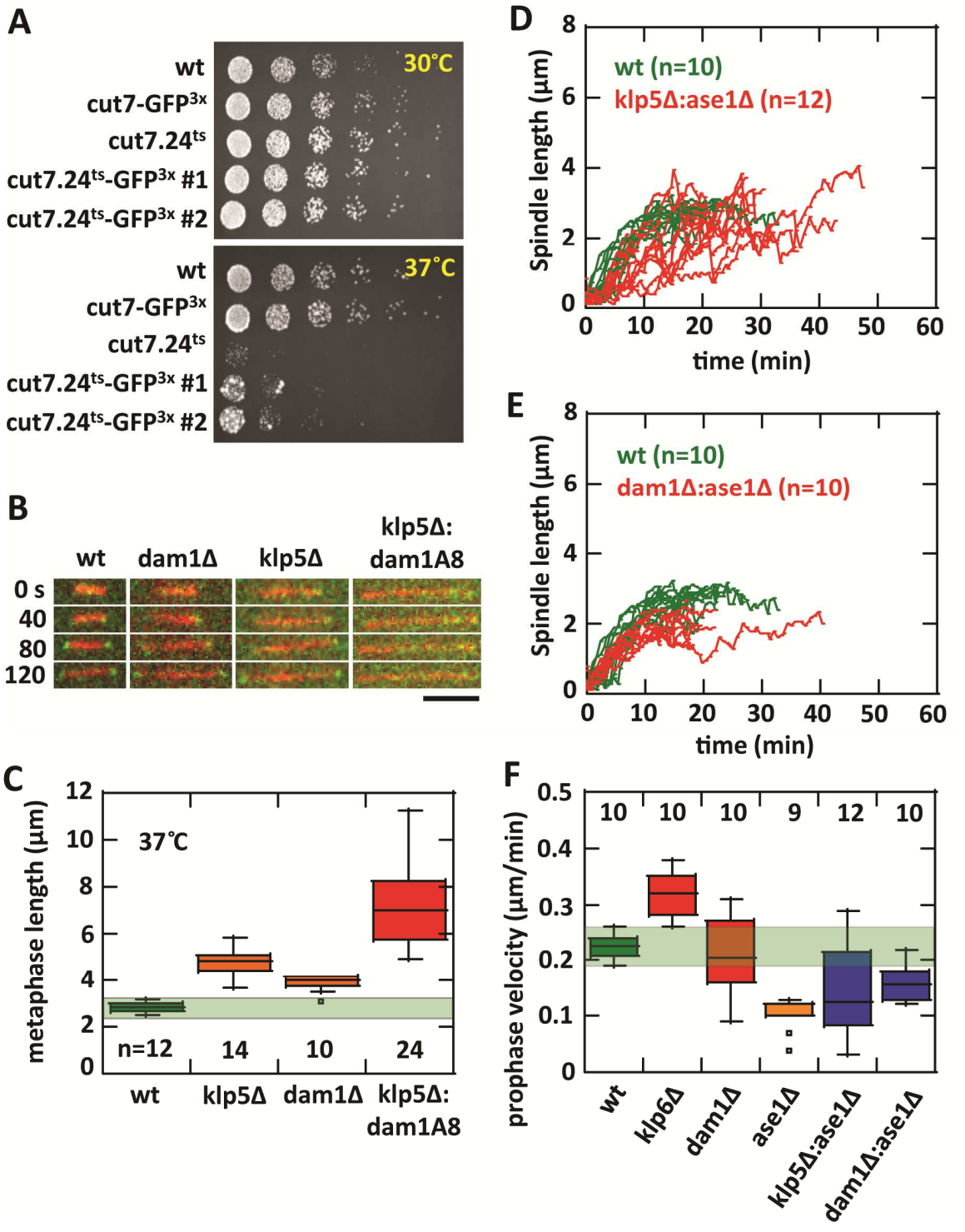
A
wt
cut7-GFP3x
cut7.24ts
cut7.24ts-GFP3x #1
cut7.24ts-GFP3x #2
30°C
37°C
B
wt
dam1Δ
klp5Δ
klp5Δ: dam1A8
0 s
40
80
120
C
37°C
metaphase length (μm)
n=12
14
10
24
wt
klp5Δ
dam1Δ
klp5Δ: dam1A8
D
wt (n=10)
klp5Δ:ase1Δ (n=12)
Spindle length (μm)
time (min)
E
wt (n=10)
dam1Δ:ase1Δ (n=10)
Spindle length (μm)
time (min)
F
prophase velocity (μm/min)
10
10
10
9
12
10
wt
klp6Δ
dam1Δ
ase1Δ
klp5Δ:ase1Δ
dam1Δ:ase1Δ

Figure 2.S2.

(A) Spot assay for temperature sensitivity of fission yeast strains: wild-type, cut7-GFP^{3x}, cut7.24^{ts}, cut7.24ts-GFP^{3x} (1), and cut7.24ts-GFP^{3x} (2). At permissive temperature 30°C, all strains survive well. In contrast, at the non-permissive temperature 37°C, cut7.24^{ts} is lethal (Hagan and Yanagida, 1990; Hagan and Yanagida, 1992). However, when cut7.24^{ts} is tagged with GFP, the new strains survive slightly better than cut7.24^{ts} alone, suggesting that temperature-sensitivity is tenuous.

(B) Time-lapse images of wild-type, dam1Δ, klp5Δ and dam1-A8:klp5Δ mitotic cells expressing mCherry-atb2p (tubulin) and mis12p-GFP (kinetochore marker) at 37°C. Time 0 represents the transition from metaphase to anaphase A and anaphase B, where sister kinetochores (yellow arrow heads) are observed to separate to opposite poles, and the spindle elongates further. Note that the dam1-A8:klp5Δ failed to separate their kinetochores. Bar, 5 μm.

(C) Box plot of metaphase spindle lengths wild-type, dam1Δ, klp5Δ and dam1-A8:klp5Δ. Consistent with the force-balance or tug-of-war model, removal of individual dam1p or klp5p, which are passive and active inward force transducer, respectively, result in longer metaphase spindle lengths compared to wild-type. Further, inactivation of both dam1p and klp5p results in even longer metaphase spindle lengths compared to individual deletion.

(D) Comparative plot of spindle length versus time of wild-type (green) and klp5Δ:ase1Δ (red) cells. Similar to wild-type, klp5Δ:ase1Δ metaphase spindles plateau at ~3 μm length. However, the spindle elongation is unstable, varying from cell to cell.

(E) Comparative plot of spindle length versus time of wild-type (green) and dam1Δ:ase1Δ (red) cells. Similar to wild-type, dam1Δ:ase1Δ metaphase spindles plateau at ~3 μm length.**(F)** Box plot of spindle prophase elongation velocities. Individual deletion klp6Δ, dam1Δ, and ase1Δ, as well as double-deletion klp5Δ:ase1Δ and dam1Δ:ase1Δ all show different velocities than wild-type.

passive pulling-force transducer, and ase1p as a passive pulling force resistor. Antagonism between cut7p and ase1p against klp5/6p and dam1p results in a steady-state spindle length. Removal of any single or combination of force contributors will result in a new steady-state length. The transition from one length to a new length can be smooth (stable) or not smooth (unstable), depending on the state of antagonism. In general, active-active antagonism, such as found in dam1Δ:ase1Δ, tends to produce a stable transition, represented by the smooth length-versus time trace (Figure 2.S2E). In contrast, an active-passive antagonism, such as found in klp5Δ:ase1Δ, tends to produce an unstable transition, represented by strong variations in the length-versus-time trace (Figure 2.S2D). Furthermore, stable spindle transition, such as found in dam1Δ:ase1Δ (Figure 2.S2E), may enable efficient kinetochore-to-MT attachment, which will result in seemingly normal (or rescued) prophase-metaphase duration (Figure 2.2F). In contrast, unstable spindle transition, such as found in klp5Δ:ase1Δ (Figure 2.S2D), will be inefficient at kinetochore-to-MT attachment, which will result in a higher prophase-metaphase duration (Figure 2.2F), likely due to the activation of the SAC.

Rescuing Metaphase Spindle Length Rescues Chromosome Segregation Defects Only When Kinetochore-to-Microtubule Attachment Is Not Severely Compromised

The fidelity of chromosome segregation critically depends on the proper kinetochore-to-microtubule attachment occurring at metaphase (Lara-Gonzalez et al., 2012; Musacchio, 2011; Musacchio and Salmon, 2007; Vleugel et al., 2012). There is a correlation between mutations which change the metaphase steady-state spindle length and chromosome segregation defects (Sanchez-Perez et al., 2005; West et al., 2001; Yamashita et al., 2005). We asked if the apparent rescue of metaphase spindle length seen in the removal of antagonist forces would also rescue chromosome segregation defects. In an artificial mini-chromosome loss assay (Niwa et al., 1989), where cells which lose the artificial chromosome turn pink, we observed apparent rescue of chromosome segregation defects in double-deleted cells. Whereas wildtype has 0.07% of pink colonies, mutant ase1Δ has 0.88%, klp5Δ has 2.98%, dam1Δ has 28.43% pink colonies (Figure

2.S3A), consistent with previous studies (Sanchez-Perez et al., 2005; West et al., 2002; Yamashita et al., 2005). In contrast, klp5Δ:ase1Δ has 0.92% and dam1Δ:ase1Δ has 8.36% pink colonies, an apparent improvement in chromosome segregation (Figure 2.S3A). However, further analysis revealed that the mini-chromosome loss assay biases the results toward living cells, as dead cells cannot form colonies. Indeed, cell survival analysis revealed that wildtype and klp5Δ have similar ~100% survival rates, and mutant ase1Δ and dam1Δ have ~50% survival rate (Figure 2.S3B). Interestingly, while klp5Δ:ase1Δ has 86% survival rate, an improvement over ase1Δ alone, dam1Δ:ase1Δ has 37% survival rate, a significant decrease from dam1Δ alone (Figure 2.S3B). We thus conclude that rescuing spindle length by removing antagonistic forces can, in some cases, rescue chromosome segregation defects.

To understand the differential effect of the inward forces producers klp5/6p and dam1p on chromosome segregation, we performed live-cell imaging on strains expressing mCherry-atb2p and CEN1-GFP (marker for the centromere/kinetochore of chromosome 1) (Yamamoto and Hiraoka, 2003). We observed three distinct kinetochore behaviors: “normal”, where the sister kinetochores separate to opposite poles at anaphase; “lagging”, where the sister kinetochores are mis-segregated to one pole, but ultimately are corrected and separated to opposite poles; and “mis-segregation”, where sister kinetochores stayed at one pole and never separate to opposite poles (Figure 2.3A). Compared to individual klp5Δ (or klp6Δ), both klp5Δ:ase1Δ and klp6Δ:cut7.24^{ts} showed significant increase in normal kinetochore separation and decrease in lagging or mis-segregation of chromosome (Figure 2.3B and 2.3C). In contrast, compared to individual dam1Δ, dam1Δ:ase1Δ showed no significant change in kinetochore behavior (Figure 2.3D), while dam1Δ:cut7.24^{ts} showed a decrease in normal kinetochore separation and an increase in kinetochore mis-segregation (Figure 2.3E). We conclude that while the rescue of metaphase spindle length by removal of antagonist forces may also rescue chromosome segregation defects associated with individual removal of the force producers, this is not a generality. The results highlight the higher importance of proper kinetochore-to-microtubule attachment for proper chromosome segregation over actual spindle length regulation per se.

Figure 2.3

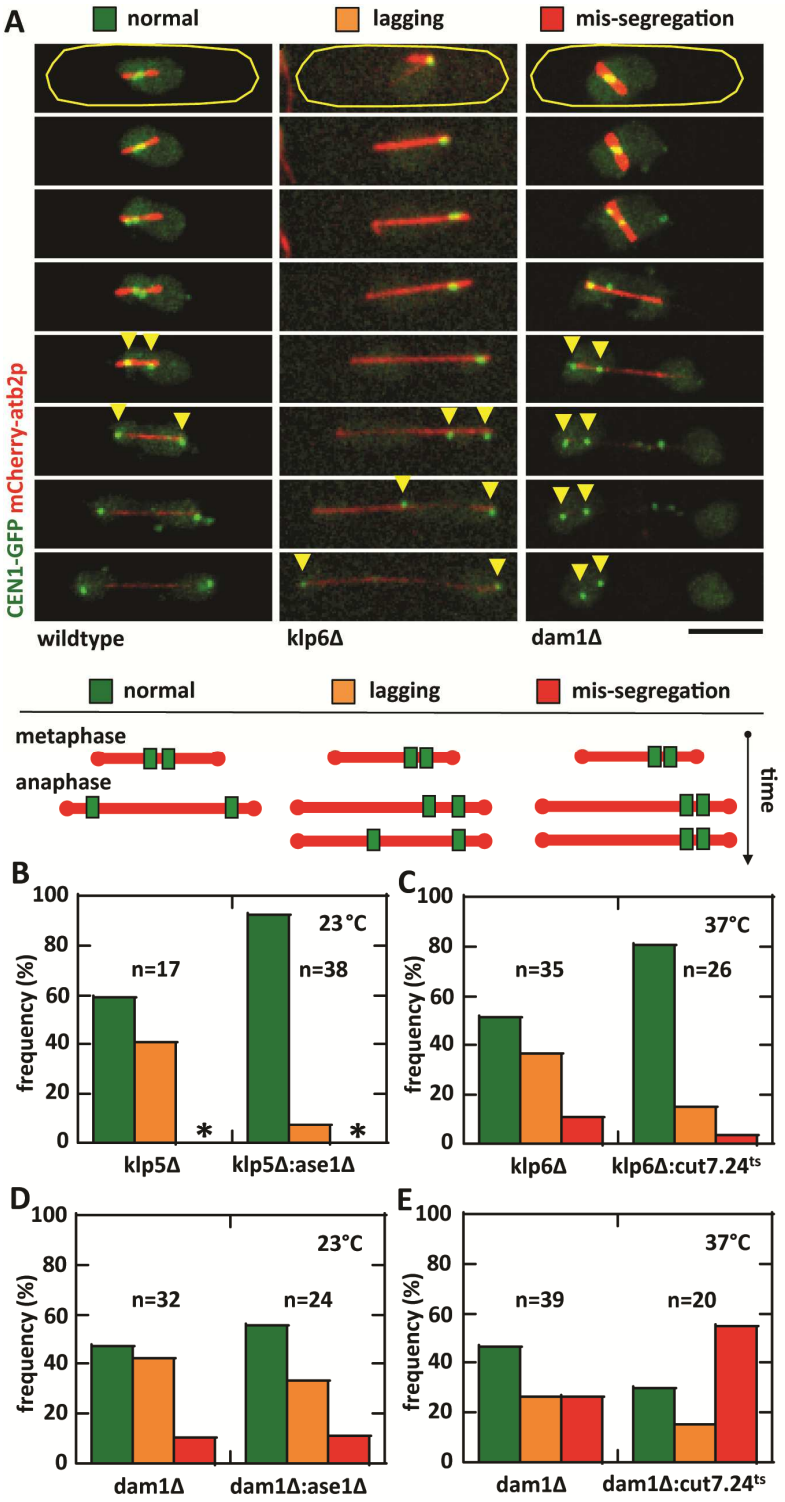
A
normal
lagging
mis-segregation
CEN1-GFP mCherry-atb2p
wildtype
klp6Δ
dam1Δ
normal
lagging
mis-segregation
metaphase
anaphase
time
B
frequency (%)
23°C
n=17
n=38
klp5Δ
klp5Δ:ase1Δ
C
37°C
n=35
n=26
klp6Δ
klp6Δ:cut7.24ts
D
23°C
n=32
n=24
dam1Δ
dam1Δ:ase1Δ
E
37°C
n=39
n=20
dam1Δ
dam1Δ:cut7.24ts

Figure 2.3. Rescuing Metaphase Spindle Length Defects Partially Rescues Chromosome Segregation Defects

(A) Time-lapse images of mitotic cells expressing mCherry-atb2p (tubulin) and CEN1-GFP (centromere of chromosome 1). We defined the behavior of chromosomes as: normal, sister centromeres separate equally to daughter cells at anaphase; lagging, sister centromeres show delayed separation to daughter cells at anaphase (yellow arrow heads); mis-segregation, sister centromeres stay in one daughter cell at the completion of mitosis (orange arrow heads).

(B) Plot shows frequency comparison of chromosome behavior between klp5Δ and klp5Δ:ase1Δ at 23°C. No chromosome mis-segregation is observed for these strains (asterisk). The klp5Δ:ase1Δ strain shows ~90% normal chromosome segregation compared to ~60% for klp5Δ alone ($p<10^{-34}$). Note: wild-type cells have 100% normal chromosome segregation.

(C) Plot shows frequency comparison of chromosome behavior between klp6Δ and cut7.24ts:klp6Δ at 37°C. The cut7.24^{ts}:klp6Δ strain shows ~80% normal chromosome segregation compared to ~50% for klp6Δ alone ($p<10^{-9}$).

(D) Plot shows frequency comparison of chromosome behavior between dam1Δ and dam1Δ:ase1Δ cells at 23°C. No significant changes in the behavior of chromosomes was observed in the double-mutant compared to single-mutant (p=0.2). **(E)** Plot shows frequency comparison of chromosome behavior between dam1Δ and dam1Δ:cut7.24^{ts} at 37°C. Indeed, the dam1Δ:cut7.24^{ts} strain shows ~55% of mis-segregation compared to ~25% for dam1Δ alone ($p<10^{-9}$).

Figure 2.S3

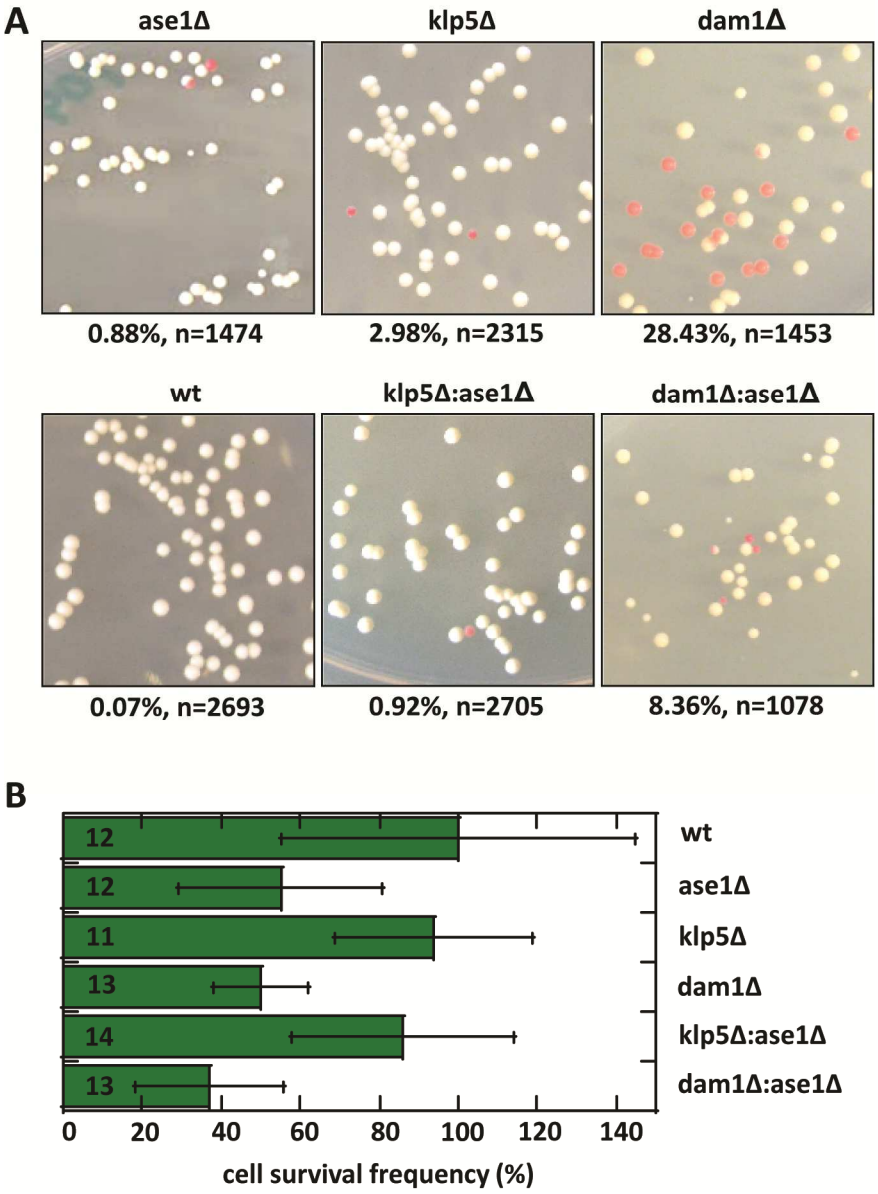

Figure 2.S3.

(A) Artificial mini-chromosome loss assays for wild-type and mutant cells. The double deletion klp5Δ:ase1Δ and dam1Δ:ase1Δ appeared to have less chromosome loss than their respective single deletion. However, this assay does not account for cell death on plates.

(B) Plot comparing cell survival on plates for the artificial mini-chromosome loss assays from Figure 2.S3A. Normalized wild-type cell survival is 100%. Individual deletion ase1Δ and dam1Δ have ~50% survival rate, while klp5Δ has similar survival rate as wild-type. Interestingly, the double deletion klp5Δ:ase1Δ appeared to have better survival rate than ase1Δ, but dam1Δ:ase1Δ has worse survival rate than either ase1Δ or dam1Δ.

Abrupt transient Spindle Shrinkage Precedes Proper Chromosome Segregation in the klp5Δ:ase1Δ and klp6Δ:cut7.24^{ts} Mutants

How do the klp5Δ:ase1Δ and klp6Δ:cut7.24^{ts} double-mutants, which have metaphase spindle lengths similar to wildtype cells, rescue chromosome segregation defects? In live-cell imaging of spindle and kinetochore dynamics, we observed that in all instances where the sister kinetochores are properly separated, approximately 2 min prior to kinetochore separation at anaphase the spindle length exhibited an abrupt length decrease before resuming elongation (Figures 2.4A-D). The start of resumed elongation coincided with kinetochore separation to opposite poles (Figures 2.4A-D). This spindle length decrease only occurs in the double-mutants klp5Δ:ase1Δ and klp6Δ:cut7.24^{ts}, but not the individual mutant klp5Δ or klp6Δ. We conclude that there is a correlation between abrupt transient spindle shrinkage and proper chromosome segregation in the klp5Δ:ase1Δ and klp6Δ:cut7.24^{ts} double-mutants.

Interestingly, the abrupt transient spindle shrinkage prior to kinetochore separation was not observed in dam1Δ, dam1Δ:ase1Δ, nor dam1Δ:cut7.24^{ts} mutants (Figures 2.S4A-S4D). This result suggests that the abrupt spindle length decrease is not a general mechanism for rescuing chromosome segregation defects. Abrupt spindle shrinkage, due to instability in the balance of forces, may be an inadvertent mechanism enabling microtubules to capture the kinetochores because microtubule plus ends are now closer to the kinetochores.

Figure 2.4

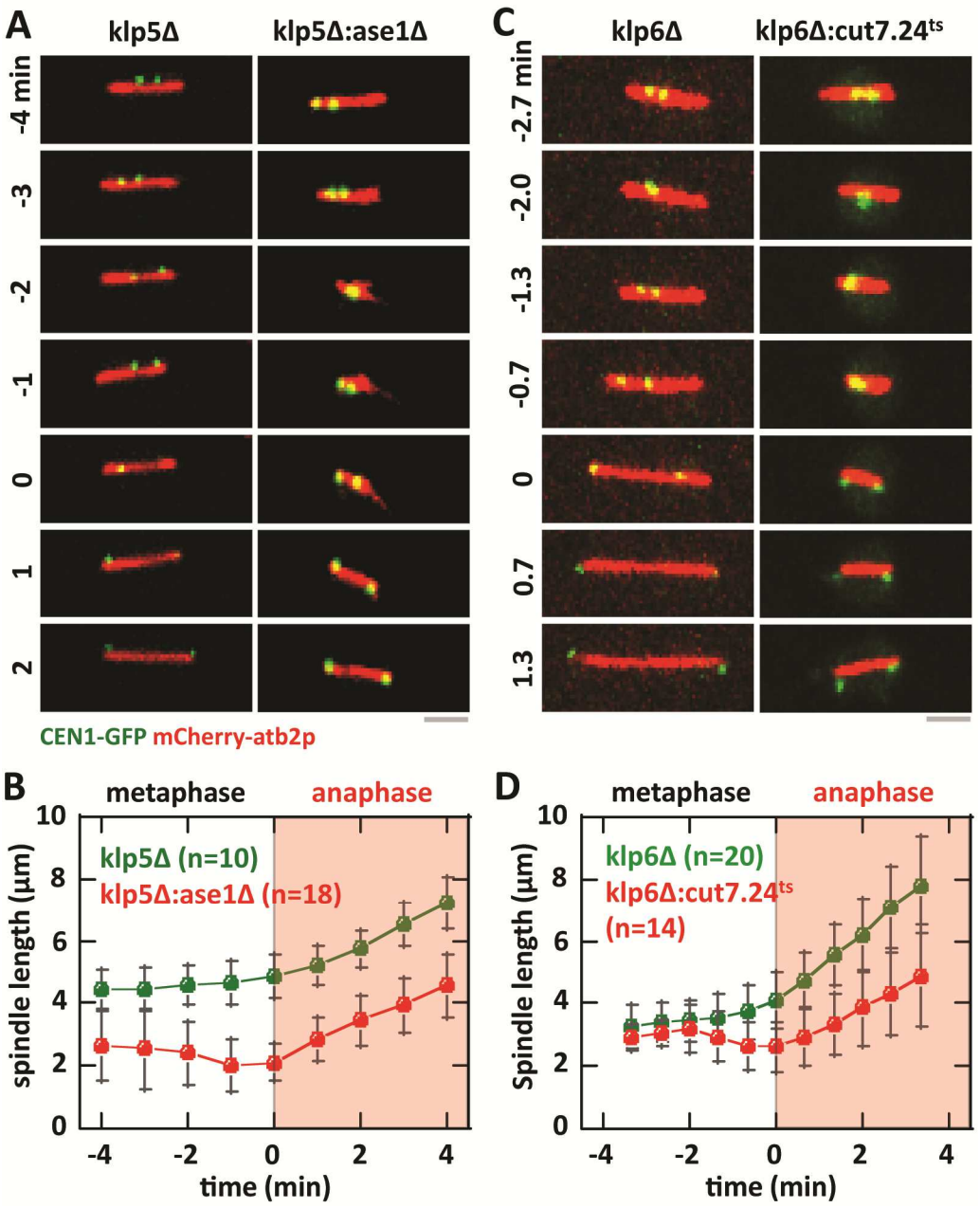
A
klp5Δ
klp5Δ:ase1Δ
-4 min
-3
-2
-1
0
1
2
CEN1-GFP mCherry-atb2p
C
klp6Δ
klp6Δ:cut7.24ts
-2.7 min
-2.0
-1.3
-0.7
0
0.7
1.3
B
metaphase
anaphase
klp5Δ (n=10)
klp5Δ:ase1Δ (n=18)
spindle length (μm)
time (min)
D
metaphase
anaphase
klp6Δ (n=20)
klp6Δ:cut7.24ts
(n=14)
Spindle length (μm)
time (min)

Figure 2.4. Transient Abrupt Metaphase Spindle Length Decrease Precedes Proper Chromosome Segregation

(A) Time-lapse images of klp5Δ and klp5Δ:ase1Δ mitotic cells expressing mCherry-atb2p and CEN1-GFP at 23°C. Time 0 represents the transition from metaphase to anaphase A where sister kinetochores are observed to separate to opposite poles. Whereas the metaphase spindle exhibits sustained elongation during the metaphase/anaphase transition in klp5Δ cells, klp5Δ:ase1Δ cells show transient spindle shrinkage prior to the metaphase/anaphase transition. Bar, 1 μm.

(B) Comparative spindle length versus time plot of klp5Δ (green) and klp5Δ:ase1Δ (red) cells. Pole-to-pole distance was measured 4 minute before and 4 minutes after cells exhibit kinetochore separation to opposite poles. At -2 min, the spindle length of the double mutant exhibits a transient shrinkage.

(C) Time-lapse images of klp6Δ and klp6Δ:cut7.24^{ts} mitotic cells expressing mCherry-atb2p and CEN1-GFP at 37°C. Time 0 represents the transition from metaphase to anaphase A where sister kinetochores are observed to separate to opposite poles. Whereas the metaphase spindle exhibits sustained elongation during the metaphase/ anaphase transition in klp6Δ cells, klp6Δ:cut7.24^{ts} cells show transient spindle shrinkage prior to the metaphase/anaphase transition. Bar, 1 μm.

(D) Comparative spindle length versus time plot of klp6Δ (green) and klp6Δ:cut7.24^{ts} (red) cells. Pole-to-pole distance was measured 3.5 minute before and 3.5 minutes after cells exhibit kinetochore separation to opposite poles. At -2 min, the spindle length of the double mutant exhibits a transient shrinkage.

Figure 2.S4

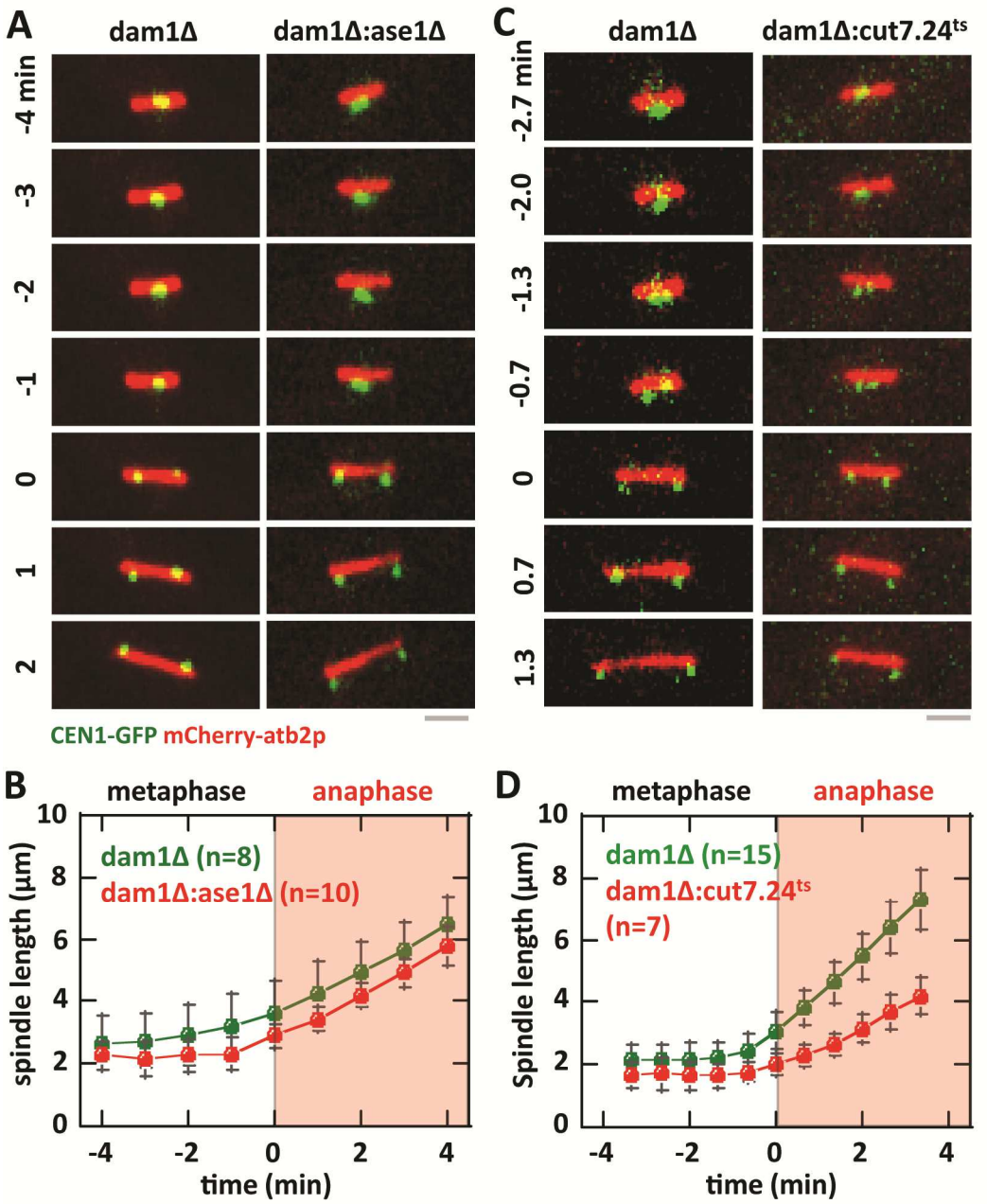
A
dam1Δ
dam1Δ:ase1Δ
-4 min
-3
-2
-1
0
1
2
CEN1-GFP mCherry-atb2p
C
dam1Δ
dam1Δ:cut7.24ts
-2.7 min
-2.0
-1.3
-0.7
0
0.7
1.3
B
metaphase
anaphase
dam1Δ (n=8)
dam1Δ:ase1Δ (n=10)
spindle length (μm)
time (min)
D
metaphase
anaphase
dam1Δ (n=15)
dam1Δ:cut7.24ts
(n=7)
Spindle length (μm)
time (min)

Figure 2.S4.

(A) Time-lapse images of dam1Δ and dam1Δ:ase1Δ mitotic cells expressing mCherry-atb2p and CEN1-GFP at 23°C. Time 0 represents the transition from metaphase to anaphase A where sister kinetochores are observed to separate to opposite poles. No spindle shrinkage prior to the metaphase to anaphase transition was observed. Bar, 1 μm.

(B) Comparative spindle length versus time plot of dam1Δ (green) and dam1Δ:ase1Δ (red) cells. Pole-to pole distance was measured 4 minute before and 4 minutes after cells exhibit kinetochore separation to opposite poles. No spindle shrinkage prior to the metaphase to anaphase transition was observed.

(C) Time-lapse images of dam1Δ and dam1Δ:cut7.24ts mitotic cells expressing mCherry-atb2p and CEN1-GFP at 37°C. Time 0 represents the transition from metaphase to anaphase A where sister kinetochores are observed to separate to opposite poles. No spindle shrinkage prior to the metaphase to anaphase transition was observed. Bar, 1 μm.

(D) Comparative spindle length versus time plot of dam1Δ (green) and dam1Δ:cut7.24ts (red) cells. Pole to-pole distance was measured 3.5 minute before and 3.5 minutes after cells exhibit kinetochore separation to opposite poles. No spindle shrinkage prior to the metaphase to anaphase transition was observed.

2.4. Discussion

Our current study tested the force-balance model in maintaining the steady-state metaphase spindle length in live cells and using a microfluidic temperature-control device to tune on/off temperature-sensitive mutants during mitosis. Although not exhaustive, we chose the key motors and MAPs that individually showed the most drastic changes to spindle length upon their deletion or inactivation. We have defined four categories in relation to force that exemplify the function of the proteins: (1) active outward-force producer (kinesin-5 cut7p), (2) active inward-force transducer (kinesin-8 klp5/6p heterodimer), (3) passive inward-force transducer (kinetochore protein dam1p), and (4) passive inward-force resistor (MT bundler ase1p). The force balance, or tug-of war, would be cut7p and ase1p against klp5/6p and dam1p. Clearly, our study is not exhaustive of all spindle proteins. There are hundreds of proteins that contribute to spindle length control (Goshima et al., 2005), and thus our approach of studying simultaneous double deletion or inactivation can be applied systematically to all proteins implicated in metaphase spindle length control to define their individual relative contribution to chromosome segregation defects.

2.5 Methods and Materials

Strains and growth conditions

Yeast strains used in this study are listed in Table S1. Standard fission yeast media and techniques were used as described (Moreno et al., 1991). For some experiments, yeasts were grown in YE5S OD_{600} of 0.8. Deletions were constructed by an established homologous recombination technique (Bahler et al., 1998).

Microscopy

Yeast cells were imaged with a Yokogawa spinning-disc confocal microscope equipped with Nikon PlanApo 100X/1.45 NA objective lens and a Hamamatsu cooled back-thinned CCD-camera or EM-CCD camera as previously described (Tran et al., 2004). Images were acquired

and processed with MetaMorph 7.7 (www.MolecularDevices.com). For experiments involving cut7.24^{ts} temperature shift, cells were first imaged at room temperature of 23°C then shifted to the non-permissive temperature of 35°C by either the fast microfluidic temperature device (Velve Casquillas et al., 2011), or 37°C by a home-built fast temperature box. To precisely identify the transition from metaphase to anaphase, cdc13p-GFP signal disappearance from the spindle was used (Fu et al., 2009).

Imaging Conditions

The precise live-cell imaging conditions are stated below for each figure.

Figures 2.1A, 2.S1A, 2.3A, 2.4A, 2.S4A: 3D timelapse stacks consisting of 11 optical sections of 0.5 µm spacing were collected every 1 min with 600-ms exposure for GFP and 800-ms exposure for mCherry.

Figure 2.1C, 2.2A, 2.2B, 2.2C: Images were acquired every 1 min with 1000-ms exposure for both GFP and mCherry. Cell chambers were switched from 23°C (blue) to 35°C (red) with a microfluidic temperature control device.

Figure 2.S2B: Images were acquired every 40 sec with 1000-ms exposure for both GFP and mCherry. Cell chambers were switched from 23°C (blue) to 37°C (red) with a temperature control device.

Figure 2.4C, 2.S4C: 3D timelapse stacks consisting of 11 optical sections of 0.5 µm spacing were collected every 40 sec with 600-ms exposure for GFP and 800-ms exposure for mCherry.

Data Analysis

Spindle lengths were measured by calculating pole-to-pole distances, whose x-y positions were automatically tracked by MTtrackJ plugin in ImageJ (www.imagej.gov) for Figures 2.1D-F and 2.2D-E. Data were plotted as box plots generated with Kaleidagraph 4.0 (www.synergy.com). Each box encloses 50% of the data with the median value displayed as a line. The top and bottom of each box mark the minimum and maximum values within the data set that fall within an

acceptable range. Any value outside of this range, called an outlier, is displayed as an individual point. Statistical analyses of data were performed using the Student's t-test for comparison between means, or Chi-squared test for comparison between frequencies in Microsoft Excel 2010.

Minichromosome loss assay

The assay was performed as previously described (Niwa et al., 1989). Briefly, cells (600 cells based on OD measurements) containing the artificial mini-chromosome were plated onto selection plates YE4S and incubated at 30°C for 3 days. Total colonies and pink colonies were counted to provide cell survival frequencies and percentage of chromosome loss.

Spot assay

For all strains, initial cell concentrations were normalized to OD=0.5. For each strain, successive dilutions of 1, 10-1, 10-2, 10-3, 10-4, 10-5 were spotted at 3 µL onto YE5S plates. Plates were incubated for 3 days at 30°C (control, permissive temperature) or at 37°C (test, non-permissive temperature).

2.6 Supplemental Information

Table 2.S1: List of *S. pombe* strains used in Chapter 2

Strain	Genotype
PT.2133	cdc13-GFP::NatMX mCherry-atb2::HydR leu1-32 ura4-D18 h-
CF.346	klp2Δ::Ura4 cdc13-GFP::KanMX mCherry-atb2::HydR ade6-m210? leu1-32 ura4.D18 his3.D1 h-
CF.348	klp3Δ::KanR cdc13-GFP::NatMX mCherry-atb2::HydR ade6-m210? leu1-32 ura4-D18 h?
CF.349	tea2Δ::KanMX cdc13-GFP::KanMX mCherry-atb2::HydR ade6-m210? leu1-32 ura4-D18 h+
CF.350	klp5Δ::Ura4 cdc13-GFP::KanMX mCherry-atb2::HydR ade6-m210? leu1-32 ura4-D18 his3.D1 h-
CF.352	klp6Δ::Ura4 cdc13-GFP::KanMX mCherry-atb2::HydR ade6-m210? leu1-32 ura4-D18 his3.D1 h+
PT.3318	klp8Δ::NatMX cdc13-GFP::KanMX mCherry-atb2::HydR ade6-m210? leu1-32 ura4-D18 h+

CF.354	klp9Δ::KanMX cdc13-GFP::KanMX mCherry-atb2::HydR ade6-m210? leu1-32 ura4-D18 h?
CF.355	dhc1Δ::KanMX cdc13-GFP::KanMX mCherry-atb2::HydR ade6-m210? leu1-32 ura4-D18 h?
CF.356	ase1Δ::KanMX cdc13-GFP::KanMX mCherry-atb2::HydR ade6-m210? leu1-32? ura4-D18 h-
PT.2441	dam1Δ::KanMX cdc13-GFP::NatMX mCherry-atb2::HydR ade6-m210? leu1-32 ura4-D18 h-
CF.391	cut7.24 cdc13-GFP::NatMX mCherry-atb2::HydR ade6-m210? leu1-32 ura4-D18 h+
CF.408	klp6Δ::Ura4 cut7.24 cdc13-GFP::NatMX mCherry-atb2::HydR ade6-m210? leu1-32 ura4-D18 h-
PT.2443	dam1Δ::KanMX cut7.24 cdc13-GFP::NatMX mCherry-atb2::HydR ade6-m210? leu1-32 ura4-D18 h-
PT.2210	ase1Δ::KanMX klp5Δ::Ura4 cdc13-GFP::NatMX mCherry-atb2::HydR ade6-m210? leu1-32 h+
PT.2509	ase1Δ::KanMX dam1Δ::KanMX cdc13-GFP::NatMX mCherry-atb2::HydR ade6-m210? leu1-32 ura4-D18 h-
CF.441	his7+::LacI-GFP lys1+LacO mCherry-atb2::HydR ade6-m210? leu1-32 ura4-D18 h+
PT.2887	klp5Δ::Ura4 his7+::LacI-GFP lys1+LacO mCherry-atb2::HydR ade6-m210? leu1-32 ura4-D18 h+
CF.443	klp6Δ::Ura4 his7+::LacI-GFP lys1+LacO mCherry-atb2::HydR ade6-m210? leu1-32 ura4-D18 h+
CF.445	dam1Δ::KanMX his7+::LacI-GFP lys1+LacO mCherry-atb2::HydR ade6-m210? leu1-32 ura4-D18 h+
PT.2550	ase1Δ::KanMX klp5Δ::Ura4 his7+::LacI-GFP lys1+LacO mCherry-atb2::HydR ade6-m210? leu1-32 h?
PT.2698	ase1Δ::KanMX dam1Δ::NatMX his7+::LacI-GFP lys1+LacO mCherry-atb2::HydR ade6-m210? leu1-32 ura4-D18 h?
CF.474	klp6Δ::Ura4 cut7.24 his7+::LacI-GFP lys1+LacO mCherry-atb2::HydR ade6-m210? leu1-32 ura4-D18 h+
PT.2815	dam1Δ::KanMX cut7.24 his7+::LacI-GFP lys1+LacO mCherry-atb2::HydR ade6-m210? leu1-32 ura4-D18 h+
CF.658	mini chromosome:: ade ch16 ade6-210 his2 h+
PT.2626	ase1Δ::KanMX mini chromosome:: ade ch16 ade6-210 his2 h?
PT.2639	klp5Δ::NatMX mini chromosome:: ade ch16 ade6-210 his2 h?
PT.2637	dam1Δ::NatMX mini chromosome:: ade ch16 ade6-210 his2 h?
PT.2552	klp5Δ::Ura4 ase1Δ::KanMX mini chromosome:: ade ch16 ade6-210 his2 h?
PT.2638	dam1Δ::NatMX ase1Δ::KanMX mini chromosome:: ade ch16 ade6-210 his2 h+
PT.3100	mad2Δ::KanMX cdc13-GFP::NatMX mCherry-atb2::HydR ade6-m210? leu1-32 ura4-D18 h+
PT.3102	klp5Δ::Ura4 mad2Δ::KanMX cdc13-GFP::NatMX mCherry-atb2::HydR ade6-m210? leu1-32 ura4-D18 h+
PT.3122	dam1Δ::KanMX mad2Δ::KanMX cdc13-GFP:NatMX mCherry-atb2::HydR ade6-m210? leu1-32 ura4-D18 h+
PT.3219	sid4-GFP::KanMX/mCherry-atb2::hph::HydR leu1-32 ura4-D18 h-
PT.3280	pkl1Δ::NatMX sid4-GFP::KanMX mCherry-atb2::HydR ade6-m210? leu1-32 ura4-D18 h+
PT.1939	mCherry-atb2::HydR leu1-32 ura4-D18 h-
PT.2973	Cut7-3xGFP mCherry-atb2::HydR ade6-m210? leu1-32 ura4-D18 h-
CF.340	cut7.24 mCherry-atb2::HydR ade6-m210? leu1-32 ura4-D18 h-
PT.3315	cut7.24-3xGFP mCherry-atb2::HydR ade6-m210? leu1-32 ura4-D18 h+
PT.3316	cut7.24-3xGFP mCherry-atb2::HydR ade6-m210? leu1-32 ura4-D18 h+
CF.124	Mis12-GFP::leu2 mCherry-atb2::HydR leu1-32 h-

PT.2441	dam1Δ::NatMX Mis12-GFP::leu2 mCherry-atb2::HydR leu1-32 h+
PT.3407	klp5Δ::Ura4 Mis12-GFP::leu2 mCherry-atb2::HydR leu1-32 h+
PT.3328	dam1-A8-GFP::NatMX klp5Δ::Ura4 Mis12-GFP::leu2 mCherry-atb2::HydR leu1-32 h+

CHAPTER 3: LOSS OF KINESIN-14 RESULTS IN ANEUPLODIY VIA KINEISN-5-DEPENDANT MICROTUBULE PROTUSIONS LEADIN TO CHROMOSOME CUT[3][4]

3.1 Summary

Aneuploidy – an incorrect chromosome number in dividing cells – can arise from defects in centrosome duplication, bipolar spindle formation, kinetochore-microtubule attachment, chromatid cohesion, mitotic checkpoint monitoring, or cytokinesis (Almonacid and Paoletti, 2010; Fang and Zhang, 2011; Tanenbaum and Medema, 2010; Thompson et al., 2010; Walczak et al., 2010). As most tumors show some degree of aneuploidy, mechanistic understanding of these pathways has been an intense area of research to provide potential therapeutics. We present here a mechanism for aneuploidy in fission yeast based on spindle pole microtubule defocusing by loss of kinesin-14, leading to kinesin-5-dependent aberrant long spindle microtubule minus end protrusions that push the properly segregated chromosomes to the site of cell division, resulting in chromosome cut at cytokinesis. Pkl1p localization and function at the spindle pole mutually dependent on spindle pole-associated protein msd1p. This mechanism of aneuploidy bypasses the known checkpoint that monitors chromosome segregation.

[3] A version of this chapter has been submitted to Nature Communications as a manuscript titled:
Syrovatkina V and Tran PT
Loss of kinesin-14 results in aneuploidy via kinesin-5-dependent microtubule protrusions leading to chromosome cut

[4] V.S. performed experiments and analyzed the data. V.S. and P.T.T. wrote the paper

3.2 Introduction

Aneuploidy is a hallmark of cancer. Defects in spindle formation and dynamics are known to result in chromosome segregation error resulting in aneuploidy (Almonacid and Paoletti, 2010; Fang and Zhang, 2011; Tanenbaum and Medema, 2010; Walczak et al., 2010). The spindle is a machine composed of microtubules (MT), motors, MT-associated proteins (MAP), and other regulatory proteins. Kinesin-14 is an important motor organizing the spindle. Kinesin-14, which includes *human* HSET, *Xenopus* XCTK2, *Drosophila* NCD, *S. cerevisiae* Kar3, and *S. pombe* pkl1p, is a microtubule (MT) minus end-directed motor localized to the spindle poles, able to crosslink parallel MTs to focus the spindle pole during mitosis and meiosis, and to antagonize kinesin-5, a MT plus end-directed motor localized at the spindle midzone, in a force-balance equilibrium to maintain proper spindle length architecture and function (Goshima and Scholey, 2010; Wordeman, 2010). Loss of kinesin-14 generally results in chromosome segregation defects (Cai et al., 2010; Endow et al., 1990; Gordon et al., 2001; Kim and Song, 2013; McDonald and Goldstein, 1990; Walczak et al., 1997). However, how the loss of kinesin-14 leads to aneuploidy has not been determined.

We show in fission yeast that loss of kinesin-14 Pkl1 leads to aberrant spindle pole MT protrusions, resulting from kinesin-5 Cut7 sliding the unfocused pole MTs. Long MT protrusions can subsequently push the post-anaphase segregated chromosomes to the site of cell division, resulting in chromosome cut at cytokinesis, thus producing aneuploid cells.

3.3 Results

pkl1+ Deletion Results in MT Protrusions from the Spindle Pole Bodies

Fission yeast *S. pombe* pkl1p acts similarly to the metazoan kinesin-14. It is a diffusive MT minus end-directed motor (Furuta et al., 2008), localizing at the spindle pole body (SPB) during mitosis (Paluh et al., 2000; Pidoux et al., 1996; Troxell et al., 2001). Deletion of *pkl1+* (pkl1Δ) results in

unfocused mitotic SPB (Grishchuk et al., 2007), metaphase spindle length defects (Syrovatkina et al., 2013; Troxell et al., 2001), and chromosome segregation defects (Pidoux et al., 1996; Troxell et al., 2001). We recently reported that pkl1Δ cells exhibited aberrant spindle MT protrusions (Syrovatkina et al., 2013) . To understand the nature of these protrusions, we performed live-cell imaging of wild-type and pkl1Δ cells expressing mCherry-atb2p (tubulin) and sid4p-GFP (spindle pole body (SPB) marker (Chang and Gould, 2000). We observed spindle MT protrusions in 79% of pkl1Δ cells, compared to none in the wild-type cells (Figure 3.1A and 3.1C). The protrusions were often parallel to the spindle long-axis, appeared during prophase-metaphase, emanated from either one or both spindle poles, and in most cases were maintained throughout anaphase (Figure 3.1A and 3.1C). Importantly, protrusions came from inside the nucleus. Using cut11p-GFP (nuclear membrane marker (West et al., 1998)), we observed protrusions pushing out the nuclear envelope, and puncturing the envelope when the protrusions were long (Figure 3.1B and 3.S3B), indicating force exertion from the protrusions.

We next determined the polarity of these protrusions. Using mal3p-GFP (MT plus end-tracker EB1 (Busch and Brunner, 2004)), we imaged MT dynamics at 10 sec intervals, and observed that protrusions showed varied final lengths between 1μm up to 7μm long (Figure 3.1D and 1E). About 62% of all protrusions were shorter than 3μm, with three out of four of them showing mal3p-GFP signal at their ends, indicating plus end protrusions (Figure 3.1D and 3.1E). The remaining 38% of protrusions were longer than 3μm and never showed mal3p-GFP signal at their ends, suggestive of minus end protrusions (Figure 3.1D and 3.1E). We repeatedly failed to observe *bona fide* MT minus end protrusions (Toya et al., 2007) and mto1p-GFP (Samejima et al., 2010) (γ-tubulin complex and associated proteins) in these long protrusions. Nevertheless, differential MT dynamics between the short and long protrusions, and cut7p-GFP localization at MT minus ends, indicated that long MT protrusions are minus-ended. Short MT protrusions showed mal3p-GFP at their ends, grew at rate of $V_{extension}$= 1.7 μm/min, persisted growing for $T_{catastrophe}$= 0.8min, then exhibited frequent catastrophe F_{cat}=0.7/min (Figure 3.1D and 3.1F, also

Figure 3.1

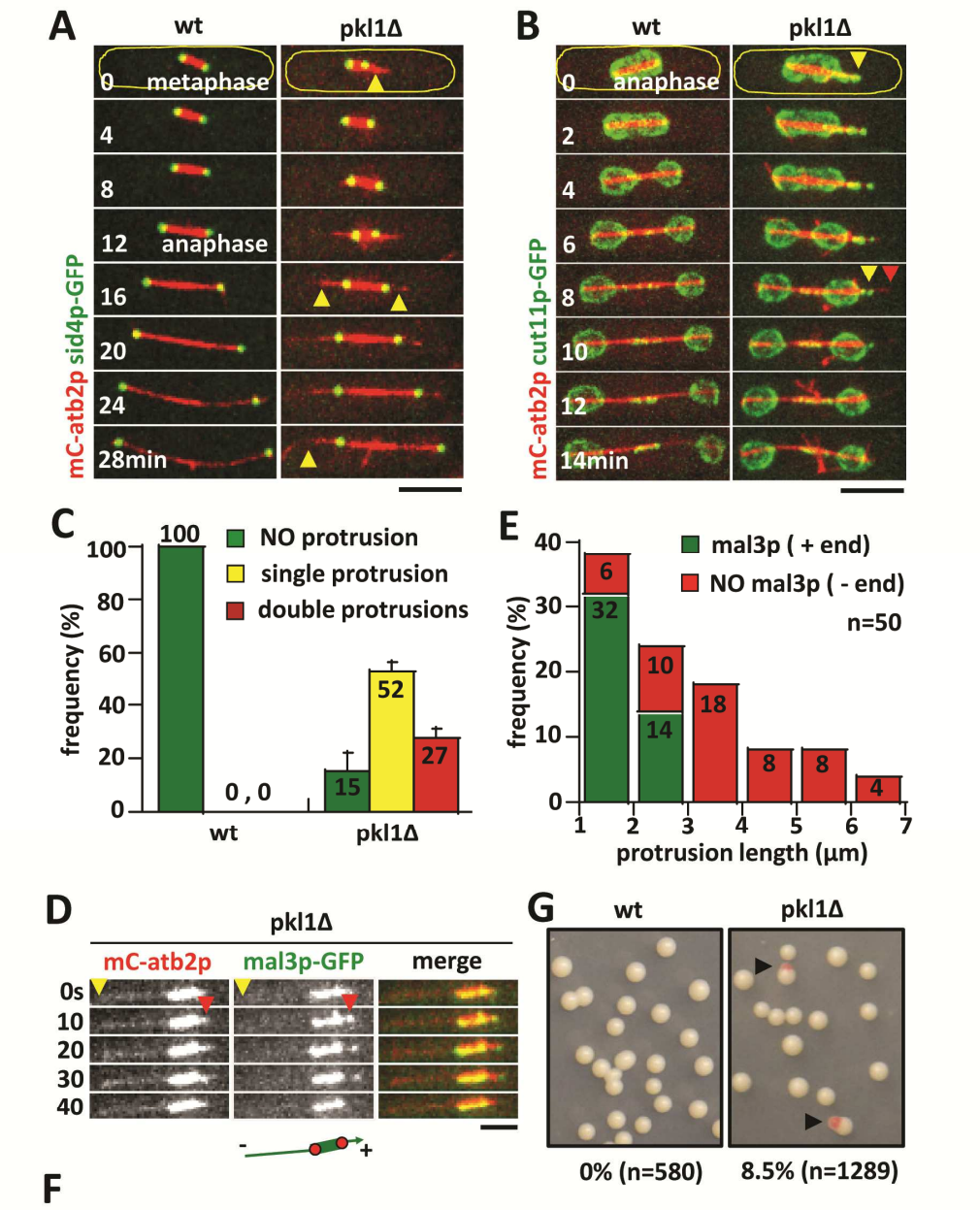

F

MT protrusions pkl1Δ	Extension Rate (µm/min)	Catastrophe (events/min)	Catastrophe time (min)	n
mal3-GFP (+ end)	1.7±0.5	0.70±0.4	0.8±0.3	35
No mal3-GFP (- end)	0.2±0.1	0.03±0.04	12±5	23

Figure 3.1. Kinesin-14 Pkl1p Maintains Spindle Pole Body Integrity.

A) Time-lapse images of wild-type (wt) and pkl1Δ cell expressing mCherry-atb2p (tubulin) and sid4p-GFP (SPB marker) through metaphase and anaphase. The wt cell has no MT protrusions emanating from the SPB. In contrast, the pkl1Δ cell has MT protrusions, which are parallel to the spindle long-axis, emanating from one or both SPB (yellow arrow head). The MT protrusion can be long, reaching the cell tip cortex and buckle (time 28min). Scale bar, 5μm.

B) Time-lapse images of wt and pkl1Δ cell expressing mCherry-atb2p and cut11p-GFP (nuclear membrane marker) through anaphase. The pkl1Δ cell has a MT protrusion from inside the nucleus pushing out the nuclear membrane (yellow arrow head, time 0min). When the MT protrusion reaches a relatively long length, it punctures through the nuclear membrane (red arrow head, time 8min). Scale bar, 5μm.

C) Comparative plot of frequency of different MT protrusions in wt (n=20) and pkl1Δ (n=30) cells. wt cells have no aberrant MT protrusions. In contrast, 79% of pkl1Δ cells have MT protrusions (52% at one SPB, and 27% at both SPB).

D) High-temporal resolution (10s interval) time-lapse images of a mitotic spindle of a pkl1Δ cell expressing mCherry-atb2p and mal3p-GFP (MT plus end tracking protein EB1). mal3p-GFP is present all along the spindle. Distinct dot of mal3p-GFP tracks the short growing MT (red arrow head, time 10-30s), and disappears when the MT depolymerizes (time 40s). This short MT represents MT plus end protrusion. In contrast, the long MT has no mal3p-GFP at its tip (yellow arrow head). This long MT is stable and does not depolymerize, representing MT minus end protrusion. Scale bar, 2μm.

E) Plot of MT protrusion length distribution frequency and MT polarity frequency in pkl1Δ cells. Plus ends are distinguished by mal3p-GFP signal (green). Minus ends are distinguished by no mal3p-GFP signal (red). MT protrusions extend from 1μm (the defined minimum length for reliable measurement) up to 7μm, and distributes as an exponential decay. 62% of protrusions are shorter than 3μm, and 38% of protrusions are longer than 3μm. All plus end protrusions, 46%

of total protrusions, are shorter than 3μm. Minus end protrusions, 54% of total protrusions, can be short or long.

F) Comparison of MT dynamic parameters between MT protrusions with and without mal3p-GFP localization at their ends in pkl1Δ cells. Based on the relative stability of the MT ends without mal3p-GFP, these ends can be classified as minus ends. (See also Figure 3.S1). **G)** The artificial mini-chromosome loss assay for wt and pkl1Δ cells. Pink colonies represent mini-chromosome loss. No pink colony is present in wt. In contrast, about 8.5% of pkl1Δ colonies are pink.

Figure 3.S1

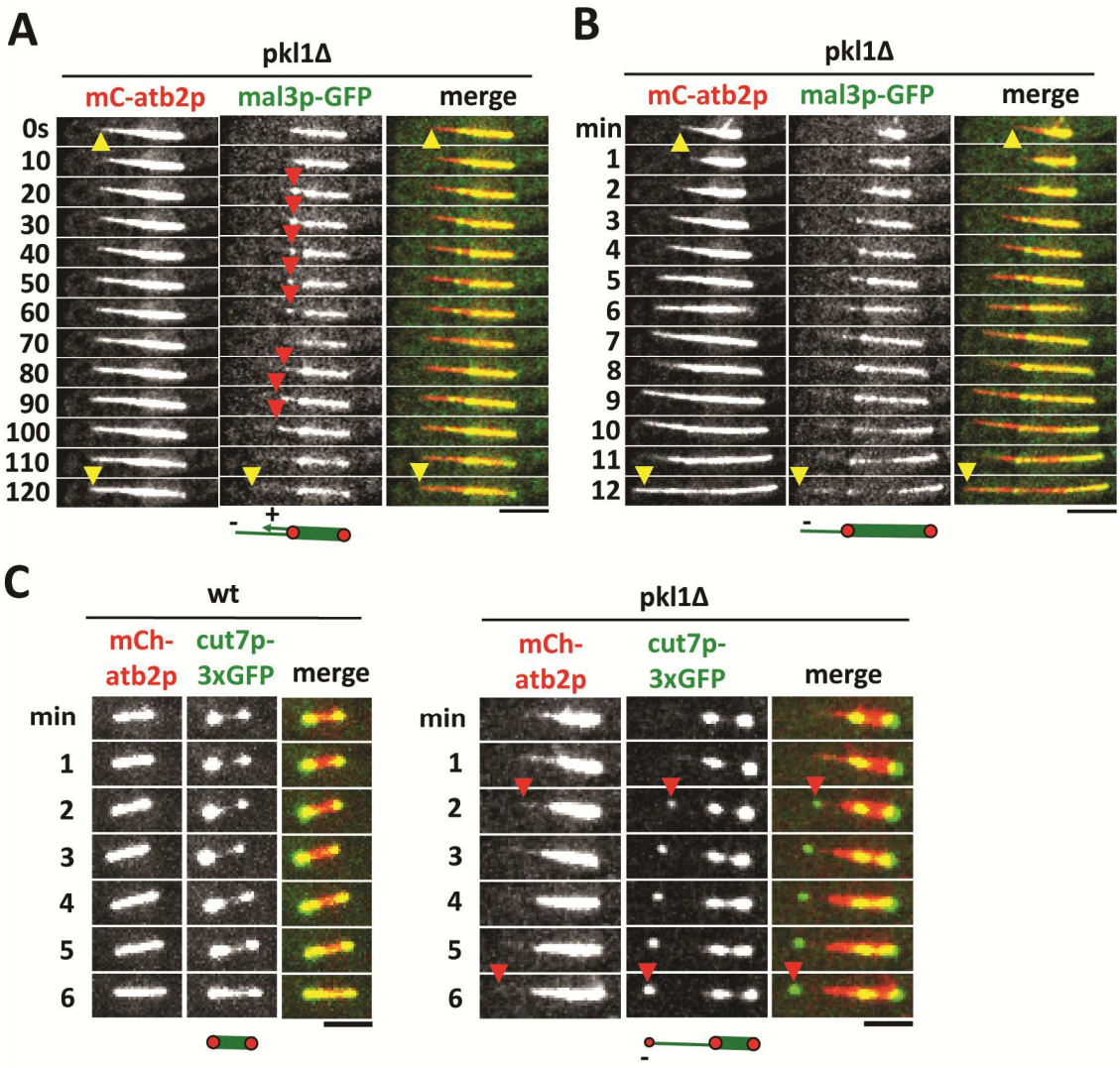

Figure 3.S1. Long MT Protrusions Are Likely Minus-Ended MTs

A) High-temporal resolution (10s interval) time-lapse images of a mitotic spindle of a pkl1Δ cell expressing mCherry-atb2p and mal3p-GFP (MT plus end tracking protein EB1). Mal3p-GFP is present all along the spindle. Distinct dot of mal3p-GFP tracks the short growing MT (red arrow head, time 20-60s), and disappears when the MT depolymerizes (time 70s). This short MT represents MT plus end protrusion. In contrast, the long MT has no mal3p-GFP at its tip (yellow

arrow head). This long MT is stable and does not depolymerize, representing MT minus end protrusion. Note that the MT protrusion can contain more than one individual MT, which can have either plus or minus polarity. Scale bar, 5μm.

B) Low-temporal resolution (1min interval) time-lapse images of a mitotic spindle of a pkl1Δ cell expressing mCherry-atb2p and mal3p-GFP. The long MT protrusion (yellow arrow head) persisted for 12min. This relatively stability is indicative of MT minus ends. Scale bar, 5μm. **C)** Time-lapse images of wt and pkl1Δ mitotic cells expressing mCherry-atb2p and cut7p- 3xGFP (kinesin-5 cut7 can move toward to MT minus end (Edamatsu, 2014)). In the wt cell, cut7p-3xGFP localizes to the spindle, and prominently at the spindle poles. In the pkl1Δ cell, where there is a long MT protrusion (red arrow head), in addition to localizing to the spindle and spindle poles, cut7p-3xGFP also accumulates at the end of the MT protrusion. This indicates that the long MT protrusion is minus ended. Scale bar, 3μm.

Figure 3.S1B). In contrast, long MT protrusions showed no Mal3-GFP at their ends, extended at rate of V_{growth}=0.2 μm/min, persisted growing for $T_{catatrophe}$=12min, and exhibited very infrequent catastrophe F_{cat}=0.03/min (Fig. 3.1D and 3.1F; also Figure 3.S1B). Further, recent works showed that the kinesin-5 cut7p localized to the spindle poles in addition to the spindle midzone (Fu et al., 2009; Hagan and Yanagida, 1992), and *in vitro* exhibited minus end-directed motility (Edamatsu, 2014). We observed prominent cut7p-3xGFP at the spindle poles of wild-type and pkl1Δ cells (Figure 3.S1C). We also observed progressive cut7p-3GFP accumulation at the ends of the long MT protrusions in pkl1Δ cells (Figure 3.S1C). Thus, our result is consistent with long MT protrusions being minus-ended. However, we cannot rule out the possibility that long protrusions are somehow more stable plus-ended MTs.

We observed that the very long protrusions could reach the cell tip cortex and appeared to push the spindle away from the cell tip (Figure 3.1A, also Figure 3.3C and Figure 3.S3B and 3.S3C). The fact that these protrusions form early in mitosis, from inside the nucleus, and parallel to the spindle long-axis distinguishes them from the cytoplasmic astral MTs which form only at anaphase and are perpendicular to the spindle long-axis (Hagan, 1998). Interestingly, in an artificial mini-chromosome loss assay (Niwa et al., 1989), we observed that pkl1Δ cells exhibited 8.5% mini-chromosome loss, whereas wild-type cells showed <0.2% (Figure 3.1G). In addition, previous report also observed similar percentage of pkl1Δ cells that displayed chromosome segregation defects using fix cells (Grishchuk et al., 2007).

Pkl1p and Msd1p Show Co-dependent Localization to the SPBs

The pkl1Δ phenotype of long minus end spindle MT protrusions and mini-chromosome loss is reminiscent of a similar phenotype reported for deletion of *msd1+* (msd1Δ) (Toya et al., 2007). Msd1p was shown to localize to the spindle poles during mitosis and to interact with the gamma-tubulin complex (γ-TuRC) to anchor the MT minus ends at the SPB (Toya et al., 2007). The initial

report on msd1Δ did not explain how the chromosomes were lost. We examined the relationship between pkl1p and msd1p. We observed that pkl1Δ, msd1Δ, and double-deletion pkl1Δ:msd1Δ all exhibited spindle MT protrusions (Figure 3.2A), and at similar high frequencies (Figure 3.2B), indicating that pkl1p and msd1p act in the same pathway.

Consistently, in contrast to wild-type cells where pkl1p-GFP and msd1p-GFP localized to the spindle poles (Paluh et al., 2000; Toya et al., 2007) (Figure 3.2C), pkl1p-GFP was not present at the spindle poles in msd1Δ cells, and msd1p-GFP was not present at the spindle poles in pkl1Δ cell (Figure 3.2C), revealing that both pkl1p and msd1p depends on each other to localize at the SPB during mitosis. This suggests that pkl1p, which has very poor processivity *in vitro* (Furuta et al., 2008), does not localize to the minus end of MT via its motor activity, but instead by interacting with msd1p and the γTuRC associated with the SPB (Olmsted et al., 2013; Paluh et al., 2000; Toya et al., 2007). There, pkl1p and msd1p could function together to focus the MT minus ends, and with pkl1p motor heads having additional property of binding adjacent parallel MT minus ends to focus them further. To test this, we over-expressed (OE) pkl1p-GFP in the pkl1Δ and pkl1Δ:msd1Δ cells; and over-expressed msd1p-YFP in the msd1Δ and pkl1Δ cells (Figure 3.2D). Pkl1p-GFP OE localized to the spindle and spindle poles in pkl1Δ cells, and completely rescued the protrusion phenotype. In pkl1Δ msd1Δ cells, pkl1p-GFP OE localized to the spindle, but not the spindle poles, and 58% of cells had protrusions (Figure 3.2D and 3.2E). This partial rescue indicates that pkl1p motor can bundle parallel MT minus ends, partially keeping the spindle pole focused. Complementarily, msd1p-YFP OE localized to the spindle poles in msd1Δ cells, and completely rescued the protrusion phenotype (Figure 3.2D). Msd1-YFP OE did not localize to the spindle poles in 94% of pkl1Δ cells, and 78% of cells had protrusions (Figure 3.2D, and 3.2E), similar to msd1Δ alone (Figure 3.2B). This indicates that both pkl1 and msd1 are required to maintain wild-type spindle poles with wild-type MT focusing. Further, we examined the motor dead mutant of pkl1 (pkl1^{md}-GFP), where its ATPase activity has been

Figure 3.2

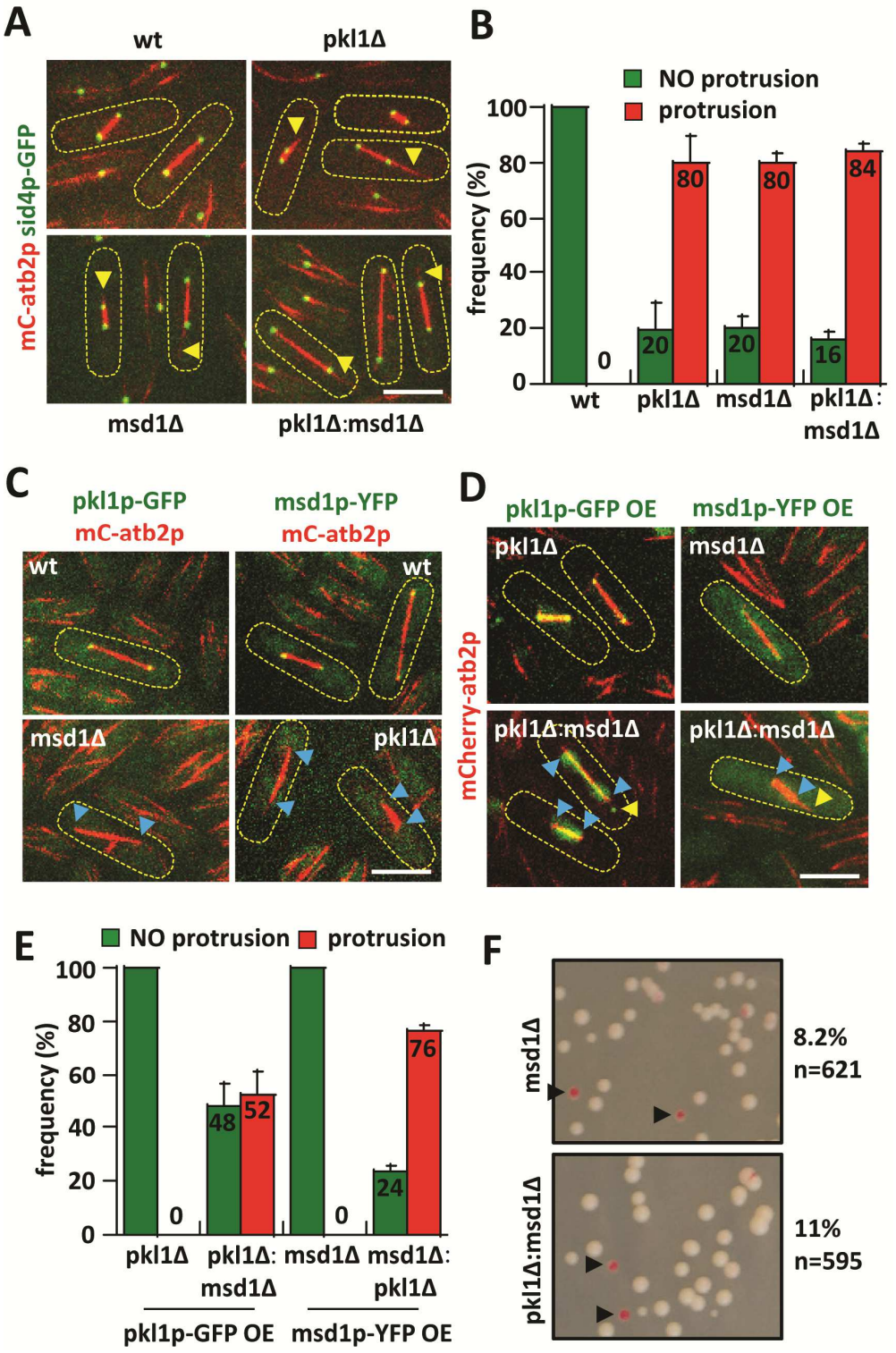
A
wt
pkl1Δ
mC-atb2p sid4p-GFP
msd1Δ
pkl1Δ:msd1Δ
B
NO protrusion
protrusion
frequency (%)
100
80
60
40
20
0
0
20
80
20
80
16
84
wt
pkl1Δ
msd1Δ
pkl1Δ:
msd1Δ
C
pkl1p-GFP
mC-atb2p
msd1p-YFP
mC-atb2p
wt
wt
msd1Δ
pkl1Δ
D
pkl1p-GFP OE
msd1p-YFP OE
mCherry-atb2p
pkl1Δ
msd1Δ
pkl1Δ:msd1Δ
pkl1Δ:msd1Δ
E
NO protrusion
protrusion
frequency (%)
100
80
60
40
20
0
0
48
52
0
24
76
pkl1Δ
pkl1Δ:
msd1Δ
msd1Δ
msd1Δ:
pkl1Δ
pkl1p-GFP OE
msd1p-YFP OE
F
msd1Δ
8.2%
n=621
pkl1Δ:msd1Δ
11%
n=595

Figure 3.2. Pkl1p and Msd1p Show Co-dependent Localization to the Spindle Pole Body

A) Images of mitotic wt, pkl1Δ, msd1Δ, and pkl1Δ:msd1Δ cells expressing mCherry-atb2p and sid4p-GFP. In contrast to wt, which have no aberrant MT protrusions, pkl1Δ, msd1Δ, and pkl1Δ:msd1Δ all have similar short and long MT protrusions (yellow arrow head). The result indicates that pkl1p and msd1p functions in the same pathway. Scale bar, 5μm.

B) Comparative plot of frequency of MT protrusions in wt (n=20), pkl1Δ (n=47), msd1Δ (n=43), and pkl1Δmsd1Δ (n=47) cells. pkl1Δ, msd1Δ, and pkl1Δ:msd1Δ cells have very similar frequencies of MT protrusions.

C) Images of spindle pole localization co-dependency between pkl1p and msd1p. In wt cells, both pkl1p-GFP and msd1p-GFP are at the spindle poles. In msd1Δ cells, pkl1p-GFP is no longer at the spindle pole (blue arrow head). Similarly, in pkl1Δ cells, msd1p-GFP is no longer at the spindle pole (blue arrow head). Scale bar, 5μm.

D) Images pkl1p-GFP over-expression (OE) in pkl1Δ and pkl1Δ:msd1Δ cells; and msd1p-YFP OE in msd1Δ and pkl1Δ cells. Pkl1p-GFP OE localizes to the spindle and the spindle poles in pkl1Δ, but not the spindle poles in pkl1Δ:msd1Δ cells (blue arrow head). Msd1p-YFP OE localizes to the spindle poles in msd1Δ, but not in pkl1Δ cells (blue arrow head). Absence of pkl1p or msd1p results in protrusions (yellow arrow head). Bar, 5 μm.

E) Comparative plot of frequency of MT protrusions in pkl1p-GFP OE and msd1p-YFP OE cells. Pkl1p-GFP OE completely rescue the pkl1Δ (n=45) MT protrusion. Overexpression of pkl1p-GFP in pkl1Δ:msd1Δ (n=66) leads to partial rescue of the pkl1Δ protrusion phenotype, possibly due to pkl1p minus end MT bundling and focusing ability. Msd1p-GFP OE completely rescue the msd1Δ (n=35) MT protrusion. Over-expression of msd1p-YFP in pkl1Δ:msd1Δ (n=43) does not rescue the msd1Δ MT protrusion phenotype. (See also Figure 3.S2).

F) The artificial mini-chromosome loss assay for msd1Δ and msd1Δ:pkl1Δ cells. Pink colonies represent mini-chromosome loss. About 8.2% of msd1Δ colonies are pink. About 11% of msd1Δpkl1Δ colonies are pink. Compared to the 8.5% pink colonies of pkl1Δ cells (Figure 3.1G), there is no statistical difference among pkl1Δ, msd1Δ, and msd1Δ:pkl1Δ cells (p=0.4).

Figure 3.S2

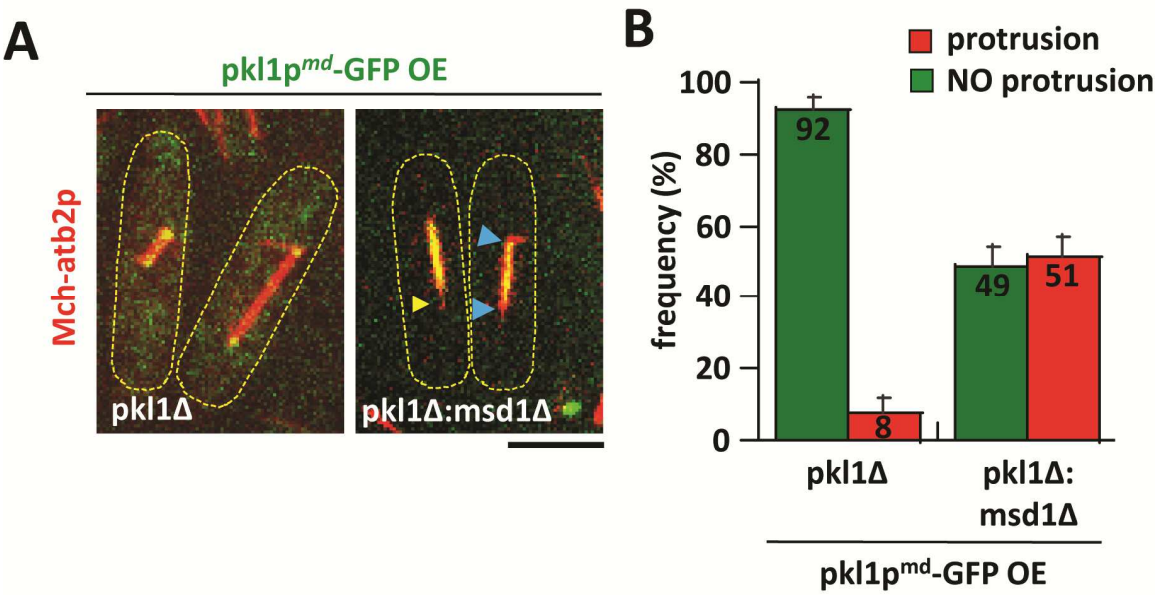

Figure 3.S2. Msd1p Functions in the Same Pathway as Pkl1p

A) Images of pkl1Δ and double-deletion pkl1Δ:msd1Δ cells over-expressing the rigor mutant pkl1p^{md}-GFP. In pkl1Δ cells, pkl1p^{md}-GFP can still localizes to the spindle poles. In contrast, in pkl1Δ:msd11Δ cells, pkl1p^{md}-GFP binds along spindle length, with no clear accumulation at the spindle poles (blue arrow head). Note that MT protrusion (yellow arrow head) can be seen in the pkl1Δ:msd11Δ cells expression pkl1p^{md}-GFP. Scale bar, 5μm.

B) Comparative plot of frequency of MT protrusions in pkl1Δ (n=38) and pkl1Δ:msd1Δ (n=39) cells expressing pkl1p^{md}-GFP. The pkl1Δ cells have 8% MT protrusion, indicating that the rigor pkl1p can mostly (but not completely) rescue the pkl1Δ MT protrusion phenotype (see Figure 3.2E for comparison). The pkl1Δ:msd1Δ cells have 51% MT protrusion, indicating that in the absence of msd1p, the rigor pkl1p can partially rescue the msd1Δ MT protrusion phenotype (see Figure 3.2E for comparison).

rendered inactive resulting in rigor-binding to MTs (Rodriguez et al., 2008). We over-expressed pkl1^{md}-GFP in pkl1Δ and pkl1Δ:msd1Δ cells. In pkl1Δ cells, pkl1^{md}-GFP localized primarily to the spindle poles, and almost completely rescued the protrusion phenotype (MT protrusions seen in 8% of cells) (Figure 3.S2). In contrast, in pkl1Δ:msd1Δ cells, pkl1^{md}-GFP localized primarily to the spindle, and only partially rescued the protrusion phenotype (MT protrusions seen in 51% of cells) (Figure 3.S2). All together, the result confirms that pkl1p and msd1p need each other to properly localize to the spindle poles. This tethering at the poles may be a key to focus MT minus ends at the poles. Further, msd1Δ and double-deletion pkl1Δ:msd1Δ both showed similar rates of mini-chromosome loss compared to pkl1Δ (Figure 3.1F), with msd1Δ at 8.2%, and pkl1Δ:msd1Δ at 11% (Figure 3.2F), consistent with pkl1p and msd1p acting in the same pathway. What is the connection between spindle MT protrusions and chromosome loss?

pkl1Δ minus end MT protrusions lead to chromosome cut at cytokinesis

During mitosis, kinetochore-MT attachment is established at metaphase, and monitored by the spindle assembly checkpoint (SAC); sister chromatid cohesion is severed and the sister chromatids move to the opposite spindle poles during anaphase A; and finally the spindle elongates to separate the segregated chromatids further during anaphase B. Surprisingly, using mis12p-GFP (kinetochore marker (Goshima et al., 1999)), we observed no kinetochore segregation defects, such as kinetochore lagging indicative of kinetochore-MT attachment defects (Syrovatkina et al., 2013), throughout the different phases of mitosis in pkl1Δ cells (Figure 3.3A). Deletion of *mad2+*, the major component of the SAC (Lara-Gonzalez et al., 2012), did not shorten the time pkl1Δ cells spent in prophase-metaphase prior to anaphase (Figure 3.3B). Both pkl1Δ and pkl1Δ:mad2Δ cells spend significantly longer time in prophase-metaphase compared to wild-type (Figure 3.3B), likely because pkl1Δ cells take longer time to organize a bipolar spindle at prophase (Hepperla et al., 2014). All together, these results indicate that the chromosome loss observed in pkl1Δ cells did not arise from defects in the conventional pathways such as SPB

duplication, spindle formation, kinetochore-to-MT attachment, chromosome cohesion, or spindle checkpoint. What then causes chromosome loss in pkl1Δ?

We reasoned that the long spindle MT protrusions seen in pkl1Δ cells may push the spindle poles and associated segregated chromosomes toward the cell division site, leading to chromosome 'cut' at cytokinesis. Accordingly, in wild-type cells the two chromosome masses labeled with hht2p-GFP (histone marker (Cui et al., 2006)) were well separated to the opposite cell tips at the start of cytokinesis (Figure 3.3C) – indicated by the formation of the medial post-anaphase array of MTs (Hagan, 1998) – and no chromosome segregation defects were observed. In contrast, in pkl1Δ cells we observed long MT protrusions which appeared to push – as evident by MT buckling during prolonged contact with the cell tip cortex – its associated chromosome mass to the medial cell division site (Figure 3.3C). Subsequent cytokinesis appeared to 'cut' through the chromosome mass, resulting in aneuploidy in 12% of mitotic cells (Figure 3.3D). We further confirmed the chromosome "cut" phenotype using Cut11-GFP (nuclear membrane maker (West et al., 1998)). In contrast to wild-type cells which showed equal segregation of nuclei, pkl1Δ cells with long MT protursions showed varied combinations of daughter cells with two nuclei and no nucleus, and daughter cells with partial nucleus and one nucleus plus micro-nucleus (Figure 3.S3A and 3.S3B).

We next monitored the long-term fate of the aneuploid cells, specifically where one daughter cell received more than its normal three chromosomes. We observed that 67% of aneuploid cells died, either by failure to septate or failure to grow (Figure 3.3E and 3.3F). Interestingly, 33% of aneuploid cells continued growing. Thus, a very small percentage of pkl1Δ cells (4%) will develop into aneuploid cells which can proliferate.

Concurrent with MT protrusions, we observed shorter anaphase spindles in pkl1Δ cells. We compared wild-type and pkl1Δ anaphase B spindle elongation velocity (Figure 3.3G). Wild-type cells anaphase spindles consistently and typically elongated at 0.51±0.04 μm/min. In contrast, we observed varied spindle velocity in pkl1Δ cells. The majority showed identical velocity as wild-type

Figure 3.3

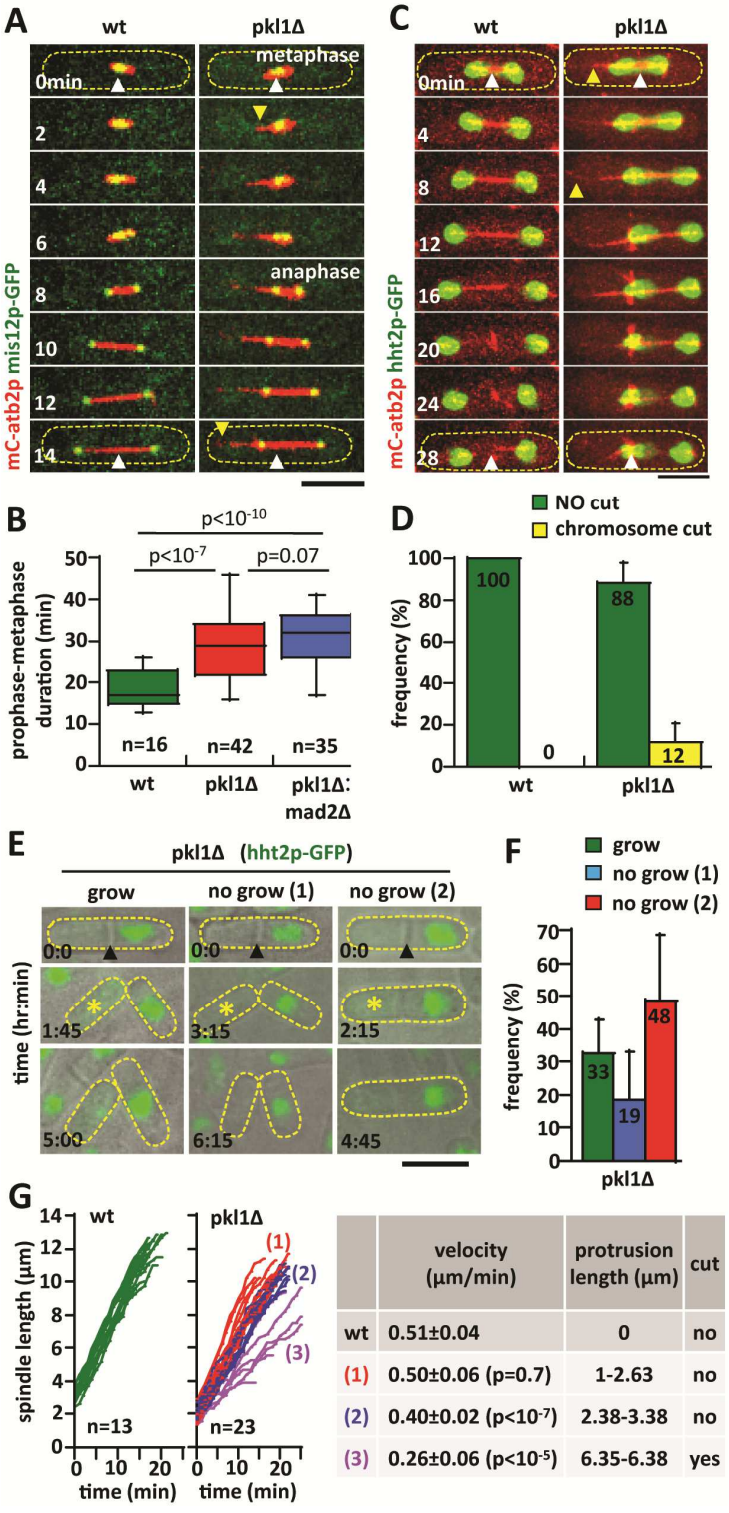

	velocity (µm/min)	protrusion length (µm)	cut
wt	0.51±0.04	0	no
(1)	0.50±0.06 (p=0.7)	1-2.63	no
(2)	0.40±0.02 ($p<10^{-7}$)	2.38-3.38	no
(3)	0.26±0.06 ($p<10^{-5}$)	6.35-6.38	yes

Figure 3.3. pkl1Δ Minus End MT Protrusions Lead to Chromosome Cut at Cytokinesis.

A) Time-lapse images of wt and pkl1Δ cell expressing mCherry-atb2p and mis12p-GFP (kinetochore marker) through metaphase and anaphase. The kinetochores separate properly to the opposite spindle poles at anaphase for both wt (n=50) and pkl1Δ (n=50) mitotic cells. Note the appearance of a pkl1Δ long MT protrusion (yellow arrow head, time 2min) which eventually pushes (time 14min) the associated spindle pole away from the cell tip and toward the medial cell division site (white arrow head). Scale bar, 5μm.

B) Box plot comparing prophase-metaphase duration time of wt, pkl1Δ, and pkl1Δ:mad2Δ mitotic cells. Mad2p is the spindle assembly checkpoint (SAC) protein. There is no statistical difference (p=0.07) between pkl1Δ (28±8 min) and pkl1Δ:mad2Δ (31±6 min) in terms of time to enter anaphase, indicating that pkl1Δ cells have no kinetochore-to-MT attachment problems and thus can bypass the mad2p checkpoint. The relatively shorter wt prophase-metaphase duration time (19±5 min) is possibly due to wt having focused spindle poles and MT minus ends, which can form a proper bipolar spindle more quickly (Hepperla et al., 2014)

C) Time-lapse images of wt and pkl1Δ cell expressing mCherry-atb2p and hht2p-GFP (histone marker) through anaphase and cytokinesis. In wt, the spindle separates the segregated chromosome mass to the opposite cell tips, far from the medial cell division site (white arrow head). In pkl1Δ, the long MT protrusion pushes (yellow arrow head, time 8min) its associated chromosome mass toward the medial cell division site (white arrow head). Cytokinesis subsequently 'cut' the misplaced chromosome mass (time 24-28 min), resulting in aneuploidy. Scale bar, 5μm. (See also Figure 3.S3)

D) Comparative plot of frequency of chromosome 'cut' in wt (n=20) and pkl1Δ (n=69) cells. No chromosome cut is observed in wt. In contrast, 12% of pkl1Δ cells have chromosome cut, or aneuploidy, at cytokinesis.

E) Long-term time-lapse images of pkl1Δ aneuploidy cells. Bright-field image shows the cell, hht2-GFP marks the chromosomes. Three types of aneuploidy cell behavior are observed. After cell division, the two daughter cells undergo septation and physically separate. The daughter cell

receiving none or less (yellow asterisk) than the typical three chromosomes dies. The daughter cell receiving more than the typical three chromosomes continues to grow. Alternatively, daughter cells undergo septation, but both do not grow (1); or daughter cells never septate, and cells do not grow (2). Scale bar, 5μm.

F) Comparative plot of frequency of pkl1Δ (n=46) aneuploidy cell behaviors. Continued growth occurs in 33% of aneuploid cells. 19% of cells septate, but do not grow. 48% of cells do not septate and do not grow.

G) Spindle length versus time plots comparing anaphase B spindle dynamics of wild-type and pkl1Δ cells. Spindle elongation dynamics in wild-type cells are typical and consistent. In contrast, spindle dynamics in pkl1Δ cells are varied, approximately falling into three groups. Group (1) has similar dynamics as wild-type. Group (2) has slower elongation dynamics compared to wild-type, but exhibits no chromosome loss. Group (3) is markedly different than wild-type, and has aneuploidy. There is a negative correlation between spindle velocity and protrusion length. There is a positive correlation between protrusion length and aneuploidy.

Figure 3.S3

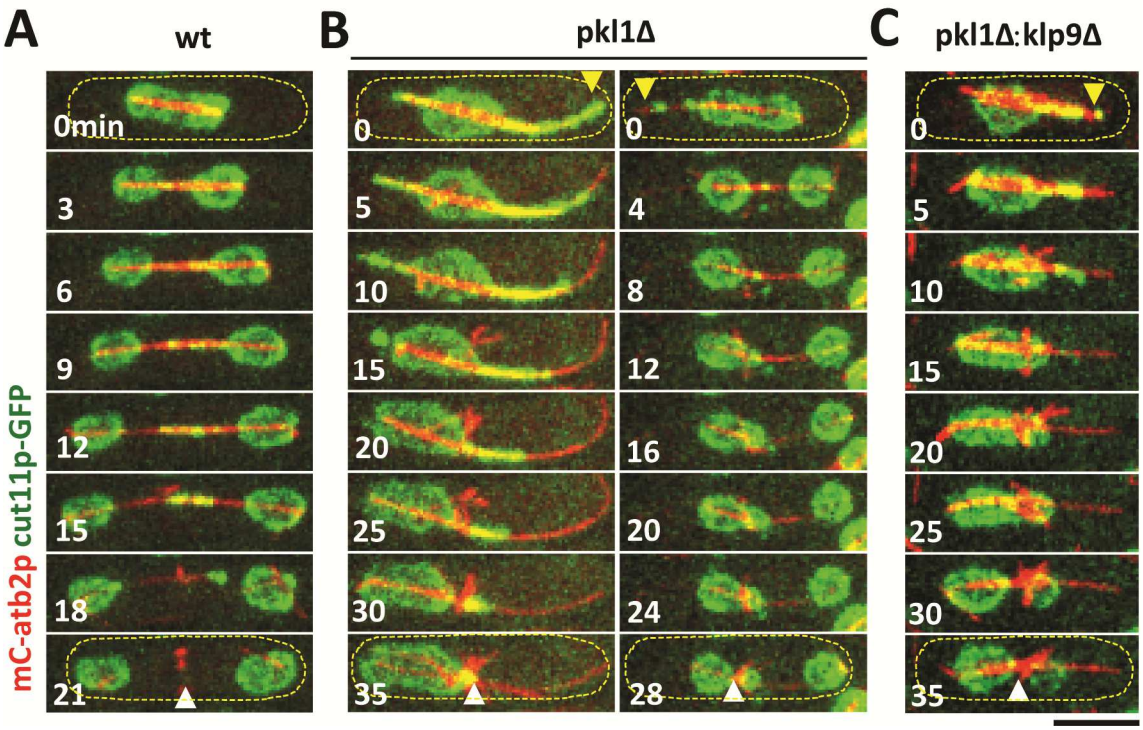

Figure 3.S3. Long MT Protrusions Lead to Chromosome Mis-segregation

Time-lapse images of wt and pkl1Δ cells expressing mCherry-atb2p and cut11p- GFP (nuclear membrane marker). **A)** The wild-type cell shows symmetric and equal segregation of the daughter nuclei into daughter cells at cytokinesis (white arrow head). **B)** In contrast, pkl1Δ cells can have unequal distribution of daughter nuclei. The first panel shows one daughter cell with 2 nuclei and its sister with no nucleus. The second panel shows one daughter cell with 1 nucleus and a micro-nucleus, with its sister having less than 1N chromosome. **C)** The double-deletion pkl1Δ:klp9Δ cell shows one daughter cell with 1 large nucleus and, with its sister having a small nucleus. Scale bar, 5μm.

at 0.50±0.06 μm/min. These had relatively short protrusions between 1-2.63μm which did not make contact with the cortex. The second type showed slower velocity at 0.40±0.02 μm/min. These had protrusions between 2.38-3.38μm which contacted the cortex but had no chromosome segregation defects. Finally, the third type showed very slow velocity at 0.26±0.06 μm/min. These had protrusions greater than 6μm, which contacted the cortex and exhibited chromosome 'cut'. Thus, there appears to be a negative correlation between spindle length (Figure 3.3G and 3.3H); and there appears to be a positive correlation between protrusion length and chromosome loss (Figure 3.3G and 3.3H).

Kinesin-5 cut7p generates long minus end MT protrusions in pkl1Δ cells

The result thus far points to a model of how loss of pkl1p can lead to aneuploidy (Figure 3.4A). In wild-type cells, minus ends of parallel MTs are bundled, focused, and anchored at the spindle poles by pkl1p and msd1p. Spindle sliding forces contributed by plus end-directed motors at the spindle midzone can push the spindle poles apart. In the absence of pkl1p (or msd1p), minus ends of parallel MTs are no longer focused and anchored to the spindle poles (Grishchuk et al., 2007; Toya et al., 2007). An unfocused pole would lead to frequent plus end MT protrusions emanating from the opposite pole. In addition, the pushing forces from the spindle midzone, without a focused pole, would lead to infrequent long MT minus end protrusions. The very long protrusions would reach the cortex and push on already segregated chromosome mass at the pole, bringing the chromosomes to the medial cell division site, where upon cytokinesis the chromosome mass is 'cut' by the contractile ring. Based on the wild-type fission yeast cell size of 14μm at mitosis (Mitchison and Nurse, 1985), the MT protrusions would need to be longer than 5μm to potentially produce chromosome cut (Figure 3.4A). This model may explain why very similar percentages of defects were measured in diverse experiments performed on pkl1Δ (or msd1Δ), e.g., 8% of cells exhibited mini-chromosome loss (Figure 3.1F and 3.2F), 12% of MT

protrusions were longer than 5μm (Figure 3.1E), to push the chromosome mass to the cut site, and 12% of cells exhibited the chromosome 'cut' phenotype (Figure 3.3D).

One prediction from our model is that kinesin-5 cut7p and/or kinesin-6 klp9p, which localize at the spindle midzone (Fu et al., 2009; Hagan and Yanagida, 1992), provide the pushing forces necessary for protrusion. Compared to pkl1Δ cells (Figure 3.2A and 3.2B), double-deletion klp9Δ:pkl1Δ showed similar short metaphase and long anaphase protrusions (Figure 3.4B), with similar protrusion frequency 80-84% of cells (Figure 3.4C), and similar distribution of protrusion lengths between 1-7 μm (Figure 3.4D). Further, the double-deletion pkl1Δ:klp9Δ cells also exhibited long MT protrusion leading to chromosome cut (Figure 3.S3C), similar to pkl1Δ cells (Figure 3.S3B). In contrast, only 30% of double-deletion cut7Δ:pkl1Δ cells exhibited protrusions (Figure 3.4C), and only short protrusions less than 3μm long throughout metaphase and anaphase (Figure 3.4D). These short MT protrusions are plus ended, based on mal3p-GFP localization at the ends (Figure 3.S4A), and their relatively fast MT dynamics parameters (Figure 3.S4B). We observed only one short MT protrusion in the cut7Δ:pkl1Δ which was likely minus ended, based on the absence of mal3p-GFP at its end (Figure 3.S4A), and its relatively slow MT dynamic parameters (Figure 3.S4B). Thus, kinesin-5 cut7p, not kinesin-6 klp9p, produces plus end-directed sliding forces from the spindle midzone to push MT minus ends away from the fragmented poles in the absence of pkl1p.

In complementary experiments, we showed that the double-deletion cut7Δmsd1Δ behaved similarly to cut7Δ:pkl1Δ. In cut7Δmsd1Δ cells, there were less protrusions compared to msd1Δ (Figure 3.S4C and 3.S4D), similar frequency of protrusion at 27% of cells compared to cut7Δ:pkl1Δ (Figure 3.S4D and 3.S4E), and only short protrusions less than 3μm long (Figure 3.4D and 3.S4E). This further confirms that pkl1p and msd1p function in the same pathway at the spindle pole to focus the minus ended MTs.

Figure 3.4

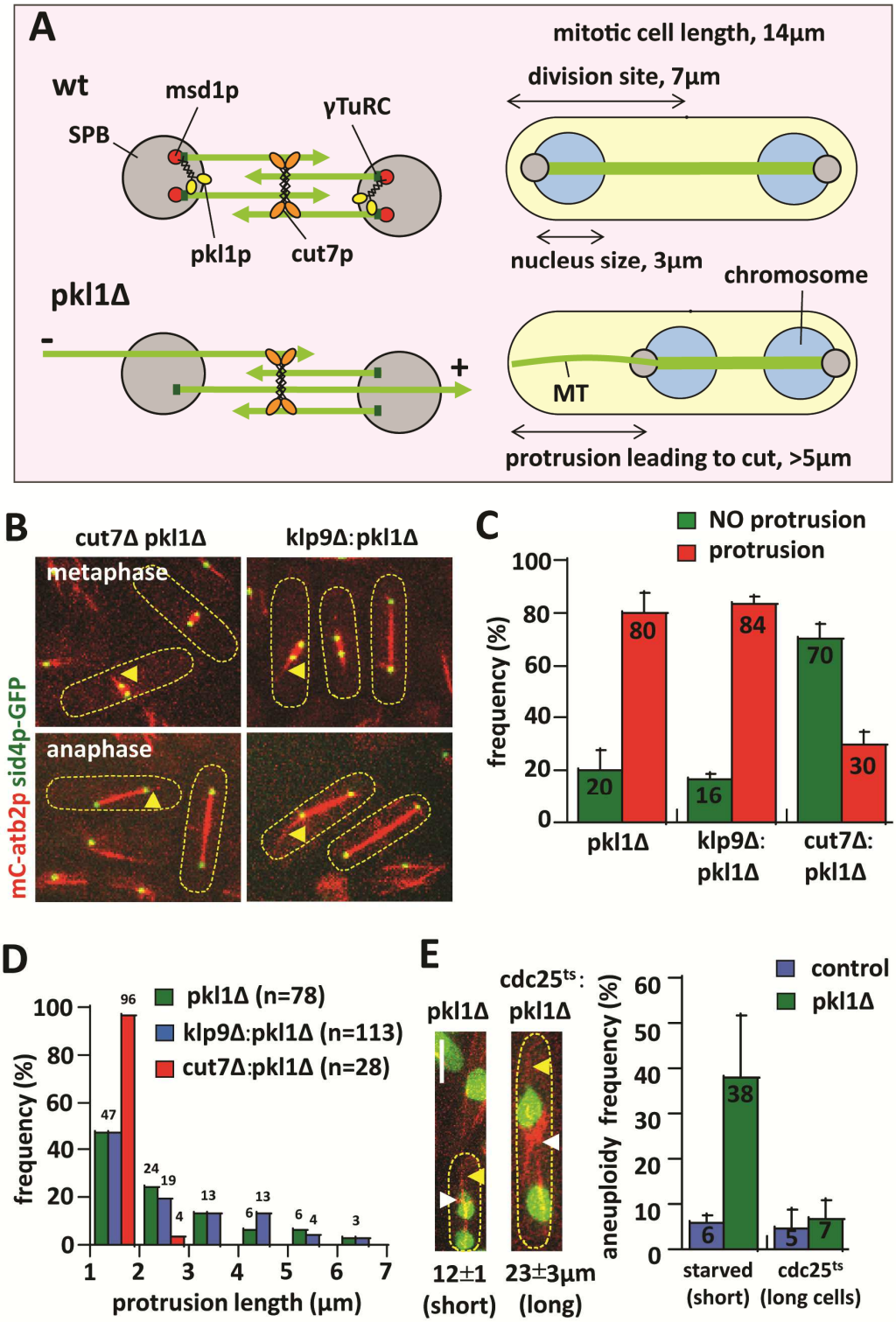
A
mitotic cell length, 14µm
division site, 7µm
wt
msd1p
γTuRC
SPB
pkl1p
cut7p
nucleus size, 3µm
chromosome
pkl1Δ
-
+
MT
protrusion leading to cut, >5µm
B
cut7Δ pkl1Δ
klp9Δ:pkl1Δ
metaphase
anaphase
mC-atb2p sid4p-GFP
C
NO protrusion
protrusion
frequency (%)
100
80
60
40
20
0
80
84
70
20
16
30
pkl1Δ
klp9Δ: pkl1Δ
cut7Δ: pkl1Δ
D
pkl1Δ (n=78)
klp9Δ:pkl1Δ (n=113)
cut7Δ:pkl1Δ (n=28)
frequency (%)
96
47
24
19
4
13
13
6
6
4
3
1 2 3 4 5 6 7
protrusion length (µm)
E
pkl1Δ
cdc25ts: pkl1Δ
12±1 (short)
23±3µm (long)
control
pkl1Δ
aneuploidy frequency (%)
60
50
40
30
20
10
0
38
6
5
7
starved (short)
cdc25ts (long cells)

Figure 3.4. Kinesin-5 Cut7p Generates Long Minus-Ended MT Protrusions in pkl1Δ Cells

A) Mechanism of spindle organization and chromosome segregation. Kinesin-14 pkl1p and msd1p localize to the SPB, where they can bind to the γ-tubulin complex (Olmsted et al., 2013; Toya et al., 2007). Pkl1p can also crosslink parallel minus end MTs similarly to kinesin-14 klp2p (Braun et al., 2009). Together, they focus the spindle poles during mitosis. In the absence of pkl1p (or msd1p), the spindle poles are defocused. Spindle pushing forces from mitotic kinesin-5 cut7p can then slide minus end MTs outward away from the unfocused poles. The long MT protrusions can then push the otherwise properly segregated chromosome to the medial cell division site, resulting in chromosome cut and aneuploidy. Defocused pole can also lead to short plus end MT protrusions (coming from the opposite pole), which have no aneuploidy consequences.

B) Images of cut7Δ:pkl1Δ and klp9Δ:pkl1Δ cells expressing mCherry-atb2p and sid4p- GFP in metaphase and anaphase. Only a few short MT protrusions (yellow arrow head) are present in cut7Δ:kl1Δ cells. In contrast, both short and long MT protrusions (yellow arrow head) are seen in klp9Δ:pkl1Δ cells. Scale bar, 5μm. (See also Figure 3.S4)

C) Comparative plot of frequency of MT protrusions in pkl1Δ, klp9Δ:pkl1Δ, and cut7Δ:pkl1Δ cells. Compared to pkl1Δ (n=50) cells, klp9Δ:pkl1Δ (n=65) cells show an equally high frequency of MT protrusions ($p=0.7$). In contrast, cut7Δ:pkl1Δ (n=50) cells show a significantly lower frequency of MT protrusions ($p<10\text{-}25$), indicating that kinesin-5 cut7p is required to generate the MT protrusions in the absence of pkl1p.

D) Plot of MT protrusion length distribution frequency in pkl1Δ, klp9Δ:pkl1Δ, and cut7Δ:pkl1Δ cells. All MT protrusions cut7Δ:pkl1Δ cells are shorter than 3μm. They likely represent MT plus ends which emanate from the fragmented spindle poles. In contrast, both pkl1Δ and klp9Δ:pkl1Δ cells have similar distributions of short and long MT protrusions. This indicates that cut7p, but not klp9p, produces the sliding forces for minus end MT protrusions in pkl1Δ cells.

E) Comparative plot of frequency of aneuploid cells in short and long mitotic cells. Wild-type (control) and pkl1Δ cells are made short by starvation. The average length of short control mitotic

cells is 12±1 μm (n=72). cdc25^{ts} (control) and cdc25^{ts}:pkl1Δ cells are made long by overnight growth at 25°C. The average length of control long mitotic cells is 24±4 μm (n=89). Note that wild-type and pkl1Δ cells in non-starved growth condition reaches length of 14±1 μm (n>100). Control cells have inherent background aneuploidy of 5-6%. Short pkl1Δ cells have 38% aneuploidy, and long cdc25^{ts}:pkl1Δ cells have 7% aneuploidy, compared to normal pkl1Δ cells which have 12% aneuploidy (Figure 3.3D).

Figure 3.S4

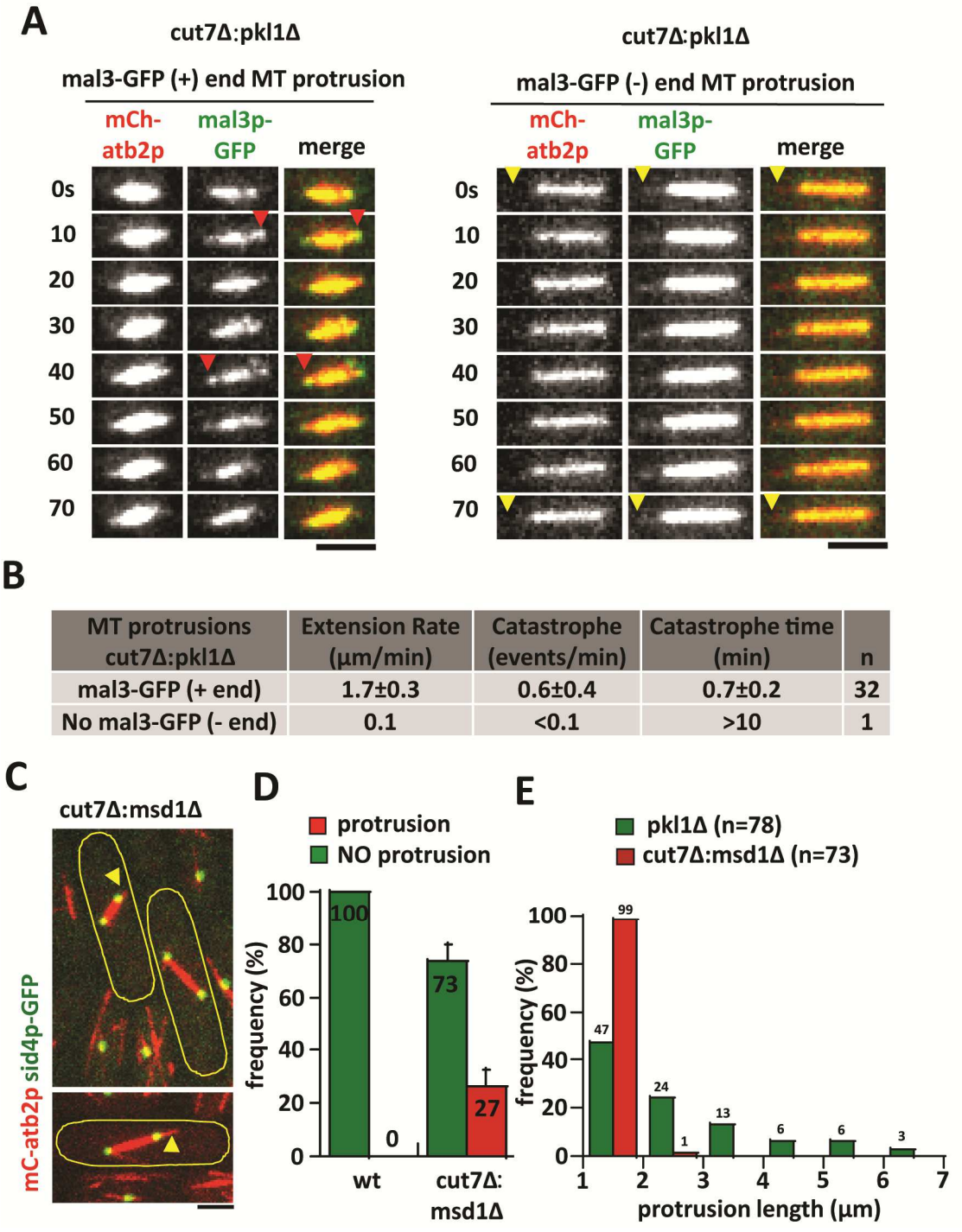

MT protrusions cut7Δ:pkl1Δ	Extension Rate (μm/min)	Catastrophe (events/min)	Catastrophe time (min)	n
mal3-GFP (+ end)	1.7±0.3	0.6±0.4	0.7±0.2	32
No mal3-GFP (- end)	0.1	<0.1	>10	1

Figure 3.S4. Cut7p Functions to Slide Long Minus-Ended MTs into Long Protrusions

A) High-temporal resolution (10s interval) time-lapse images of mitotic spindles of cut7Δ:pkl1Δ cells expressing mCherry-atb2p and mal3p-GFP. We observed only short MT protrusions (23 mitotic cells, 33 independent MT protrusions). The short MT protrusions have mal3p-GFP at their ends (red arrow head), indicating plus end (first panel). We observed only 1 MT protrusion without mal3p-GFP at its end (in 23 mitotic cells), indicating minus end (second panel). Scale bar, 3μm.

B) Comparison of MT dynamic parameters between MT protrusions with and without mal3p-GFP localization at their ends in cut7Δ:pkl1Δ cells. Based on the relative stability of the one MT end without mal3p-GFP, this end can be classified as minus end.

C) Images of double-deletion cut7Δmsd1Δ cells expressing mCherry-atb2p and sid4-GFP (SPB marker). The cut7Δmsd1Δ cells formed bipolar spindles, and showed only short MT protrusions (yellow arrow head), similar to cut7Δ:pkl1Δ cells (see Figure 3.4B). This indicates that msd1p and pkl1p function in the same pathway. Scale bar, 3μm.

D) Comparative plot of frequency of MT protrusions in msd1Δ (n=48) and cut7Δmsd1Δ n=47). The msd1Δ cells have 80% MT protrusion. In contrast, cut7Δmsd1Δ cells have 27% MT protrusion, indicating that cut7p functions to slide the unfocused MT minus ends in msd1Δ cells producing the aberrant MT protrusions.

E) Plot of MT protrusion length distribution frequency in pkl1Δ and cut7Δmsd1Δ cells. For pkl1Δ cells, MT protrusions extend from 1μm (the defined minimum length for reliable measurement) up to 7μm, and distributes as an exponential decay. 71% of protrusions are shorter than 3μm, and 29% of protrusions are longer than 3μm. In contrast, all MT protrusions are shorter than 3μm in the cut7Δmsd1Δ cells. This suggests that msd1p and pkl1p are in the same pathway (compare with Figure 3.1E and 3.4D), and that cut7p functions to produce minus end MT protrusions in msd1Δ (or pkl1Δ) cells.

A second prediction from our model is that cell length negatively correlates with protrusion-dependent chromosome loss. A microtubule can produce pushing forces inversely proportional to the square of its length (Dogterom et al., 2005). Thus, protrusions are expected to push more efficiently in short cells compared to long cells. We starved wild-type (control) and pkl1∆ cells to create short mitotic cells of 12±1 µm, and used $cdc25^{ts}$ and $cdc25^{ts}$pkl1∆ to create long mitotic cells of 23±3 µm ($cdc25^{ts}$ is a cell division cycle temperature sensitive mutant which blocks cells at the G2/M transition, creating long cells (Russell and Nurse, 1986)), compared to the typical 14±1 µm length of unstarved log-phase growth wild-type and pkl1Δ cells. Both the short starved wild-type and the long $cdc25^{ts}$ control cells showed inherent 5-6% background aneuploidy (Figure 3.4E). Both had spindles and protrusions which scaled with the cell length (Figure 3.4E). Nevertheless, the short starved pkl1∆ cells exhibited 36% aneuploidy, and the long $cdc25^{ts}$pkl1∆ exhibited 7% aneuploidy (Figure 3.4E). Thus, the pkl1Δ MT protrusion-dependent mechanism for aneuploidy is more effective in shorter cell and less effective in longer cells.

3.4 Discussion

We identified a potential new mechanism for aneuploidy in fission yeast. Kinesin-14 pkl1p and msd1p localize to the spindle poles and focus the MT minus ends. Their absence leads to pole and MT defocusing, resulting in spindle midzone kinesin-5 cut7p dependent sliding forces pushing the unfocused MT minus ends away from the spindle poles. Infrequent long MT minus end protrusions can push the already separated chromosome mass back to the cell center, where cytokinesis will 'cut' the chromosome mass, creating aneuploidy. This mechanism is particularly dangerous because it bypasses the spindle assembly checkpoint. Further, this mechanism may affect small cells more severely than large cells (Figure 3.4A).

In seeming contrast to our findings, an initial EM sectioning through 2 or 3 pkl1Δ cell did not observe MT protrusions (but did observe spindle pole and MT minus end defocusing) (Grishchuk et al., 2007). We interpret this to mean that as MT protrusions occurred dynamically in ~80% of

pkl1Δ cells, it may require EM sectioning through many cells to catch a protrusion. Consistent with this, EM sectioning through an msd1Δ cell did observe both spindle pole and MT minus end defocusing, and MT protrusions pushing out the nuclear envelope (Toya et al., 2007).

Our work is in slight contrast to a recent report on pkl1p and cut7p (Olmsted et al., 2014). Both works are in agreement with the qualitative findings, e.g., pkl1Δ cells have spindle MT protrusions, pkl1Δ cells have chromosome segregation defects, and the double-deletion pkl1Δ:cut7Δ alleviates the protrusions. However, we are in disagreement concerning the detailed mechanism of function of pkl1p and cut7p. Olmstead et al. concluded that pkl1p interacts with the γ-tubulin complex at the spindle poles to inhibit MT nucleation, then cut7p interacts with pkl1p to remove this inhibition of MT nucleation (Olmsted et al., 2014). This interpretation cannot explain the key observation that in the presence of pkl1p, spindle MT nucleation still robustly occurred (but no bipolar spindle can form) when cut7p is deactivated (Hagan and Yanagida, 1992). Our findings favor the more straight forward conclusion, that pkl1p and cut7p, as motors, bind MTs and organize the dynamic spindle structure.

In human cells, loss of kinesin-14 HSET (Cai et al., 2010; Kim and Song, 2013) or the MT-associated proteins CLASP1/2 (Logarinho et al., 2012), result in spindle pole fragmentation and aneuploidy. It was proposed that spindle sliding forces, particularly by kinesin-5 Eg5, could enhance defects in spindle pole integrity, resulting in chromosome segregation defects (Maiato and Logarinho, 2014). Our current work in fission yeast sheds light on these results and reveals a novel and potentially conserved mechanism for aneuploidy, as all studied proteins are conserved from yeast to human. Aneuploidy can occur due to kinesin-14 pkl1p-dependent (or msd1p-dependent) spindle pole defocusing causing unfocused force distribution from kinesin-5 cut7p, resulting in spindle minus end MT protrusions which push the chromosome mass to the site of cell division, causing chromosome 'cut' at cytokinesis (Figure 3.4A). This pathway may be particularly dangerous as it bypasses checkpoints which ensure chromosome segregation fidelity.

A fraction of the resulting aneuploidy cells can proliferate (Torres et al., 2007), and may thus define cancer.

Interestingly, cancer cells require kinesin-14 HSET to focus the supernumerary centrosomes into a 'bipolar' spindle (Kwon et al., 2008), as the absence of HSET results in multipolar spindles and subsequent daughter cells die. This suggests that our finding in yeast may not be generalized to human cells. Nevertheless, not enough long-term studies have been done in human cells with inactive HSET to determine if a small percentage of daughter cells survive and proliferate, as suggested from our current study in fission yeast. Inhibition of kinesin-14 will not be beneficial in the context of cancer therapeutics if some cells survive and proliferate.

3.5 Methods and Materials

Strains and media

Standard fission yeast media and techniques were used as described (Moreno et al., 1991). Gene deletionand fluorescent protein tagging were carried out using a PCR-based protocol (Bahler et al., 1998). The strains pkl1p-GFP OE and msd1p-YFP OE were under the thiamine-suppressible nmt1- promoter (Rodriguez et al., 2008). In the absence of thiamine, cells moderately over-express pkl1p-GFP and msd1p-YFP after 9 to 24hrs induction. Starved short cells were obtained by growing cells to OD of 1.5-2.0. cdc25-22ts strains were grown at the permissive temperature 25ºC overnight and imaged at OD of 0.2-0.6. At the permissive temperature, cdc25-22ts is inherently longer than wildtype. The rigor pkl1pmd-GFP strain was a kind gift from Dr. Janet Paluh (Rodriguez et al., 2008). Strains used in this study are listed in Table S1.

Microscopy

Yeast cells were imaged with a Yokogawa spinning-disc confocal microscope equipped with Nikon PlanApo 100X/1.45NA or ApoTIRF 60X/1.49NA objective lens and a Hamamatsu cooled

back-thinned CCD-camera or EM-CCD camera as previously described (Tran et al., 2004). Images were acquired at ~20ºC and processed with MetaMorph 7.7 (www.MolecularDevices.com). Precise details of imaging conditions are provided for each figure below.

Imaging

Figures 3.1a, 3.1b, 3.2a, 3.3a, 3.3c, 3.4b, 3.4e and Figures 3.S1c, 3.S3a, 3.S3b, 3.S4c: 3D time-lapse stacks consisting of 11 optical sections of 0.5 µm spacing were collected every 1 min with 500-ms exposure for mCherry and GFP.

Figures 3.3.1D and Figure 3.S1a, 3.S1b, 3.S4a: 3D time-lapse stacks consisting of 3 optical sections of 0.2 µm spacing were collected every 10 sec with 500-ms exposure for mCherry and GFP.

Figures 3.2C: 3D time-lapse stacks consisting of 11 optical sections of 0.5 µm spacing were collected every 1 min with 500-ms exposure for mCherry and 1500-ms exposure for GFP.

Figure 3.2D and Figure 3.S2A: 3D time-lapse stacks consisting of 11 optical sections of 0.5 µm spacing were collected every 1 min with 700-ms exposure for mCherry and GFP.

Figure 3.3E: 3D time-lapse stacks consisting of 11 optical sections of 0.5 µm spacing were collected every 15 min with 300-ms exposure for mCherry and GFP, plus one snapshot in bright-field.

Data Analysis

We defined MT protrusion as MTs parallel to the spindle long-axis that extend beyond the SPB for more than 1 µm in length. Experiments were performed at least 3 times. Data were plotted as Bar ± s.d. (n), or as Box plots, generated with Kaleidagraph 4.0 (www.Synergy.com). Each box encloses 50% of the data with the median value displayed as a line. The top and bottom of each box mark the minimum and maximum values within the data set. Anaphase B spindle lengths were measured by calculating pole-to-pole distances, whose x-y positions were automatically

tracked by MTtrackJ plugin in ImageJ (www.imagej.gov).Statistical analyses of data were performed in Microsoft Excel 2010 using the Student t-test for comparison between means, or Chi-squared test for comparison between frequencies.

Mini-chromosome loss assay

The assay was performed as previously described (Niwa et al., 1989). Briefly, cells (600 cells based on OD measurements) containing the artificial mini-chromosome were plated onto selection plates YE4S and incubated at 30°C for 3 days. Total white colonies and pink colonies were counted to provide the percentage of mini-chromosome loss.

3.6 Supplemental Information

Table 3.S1: List of *S. pombe* strains used in Chapter 3

Strain	Genotype
PT.3380	pkl1Δ::NatR cut7-3xGFP:KanR mCherry-atb2: HphR ade6-m210? leu1-32 ura4-D18 h+
PT.3765	msd1Δ::KanR sid4-GFP:KanR mCherry-atb2:HphR ade6-m210 leu1-32 ura4-D18 h-
PT.3767	pkl1Δ::NatR msd1Δ::KanR sid4-GFP:KanR mCherry-atb2:HphR ade6-m210 leu1-32 ura4-D18 h-
PT.2753	pkl1-3xGFP:KanR mCherry-atb2:HphR ade6-m210? leu1-32 ura4-D18 h+
PT.3559	msd1Δ::NatR pkl1-3xGFP:KanR mCherry-atb2:HphR ade6-m210 leu1-32 ura4-D18 h+
PT.3477	msd1-GFP:KanR mCherry-atb2:HphR ade6-m210? leu1-32 ura4-D18 h-
PT.3480	pkl1Δ::NatR msd1-GFP:KanR mCherry-atb2:HphR ade6-m210? leu1-32 ura4-D18 h-
PT.3808	nmt-pkl1-GFP:LEU1+ pkl1Δ::KanR mCherry-atb2:HphR ade6-m210? leu1-32 h-
PT.3937	nmt-pkl1-GFP:LEU1+ pkl1Δ::KanR msd1Δ::NatR mCherry-atb2:HphR ade6-m210? leu1-32 ura4-D18 h-
PT.3981	msd1Δ::KanR mCherry-atb2:HphR ade6-m210? leu1-32 ura4-D18 h+ [pPT.419 nmt1-msd1-YFP:URA4+]
PT.3985	msd1Δ::KanR pkl1Δ::NatR mCherry-atb2:HphR ade6-m210? leu1-32 ura4-D18 h- [pPT.419 nmt1-msd1-YFP:URA4+]
PT.3775	msd1Δ::NatR miniChromosome ch16::ade6-m216 leu1-32 his2 h?
PT.3777	pkl1Δ::KanR msd1Δ::NatR miniChromosome ch16::ade6-m216 leu1-32 his2 h?
PT.3811	nmt1-rigor-pkl1-GFP:LEU1+ pkl1Δ::KanR mCherry-atb2:HphR ade6-m210? leu1-32 h-

PT.3939	nmt1-rigor-pkl1-GFP:LEU1+ pkl1Δ::KanR msd1Δ::NatR mCherry-atb2:HphR ade6-m210? leu1-32 h+
CF.124	mis12-GFP:LEU1+ mCherry-atb2:HphR ade6-m210 leu1-32 ura4-D18 h-
PT.3235	pkl1Δ::KanR mis12-GFP:LEU1+ mCherry-atb2:HphR ade6-m210? leu1-32 ura4-D18 h?
PT.3251	hht2-GFP::URA4+ mCherry-atb2:HphR ade6-m210? leu1-32 ura4-D18 h-
PT.3382	pkl1Δ::NatR hht2-GFP::URA4+ mcherry-atb2:hph ade6-m210? leu1-32 ura4-D18 h+
PT.3681	pkl1Δ::KanR hht2-GFP::URA4+ mcherry-atb2:hph ade6-m210? leu1-32 ura4-D18 h-
PT.3818	pkl1Δ::NatR mad2Δ:: KanR mis12-GFP:LEU1+ mCherry-atb2:HphR ade6-m210? leu1-32 ura4-D18 leu1-32 ura4-D18 h
PT.4043	klp9Δ::URA4+ pkl1Δ::KanR cut11-GFP:NatR mCherry-atb2:HphR ade6-m210? leu1-32 ura4-D18 h-
PT.3763	pkl1Δ::NatR klp9Δ::URA4+ sid4-GFP:KanR mCherry-atb2:HphR ade6-m210? leu1-32 ura4-D18 h?
PT.3729	pkl1Δ::KanR cut7Δ::NatR+ sid4-GFP:KanR mCherry-atb2:HphR ade6-m210? leu1-32 ura4-D18 h-
PT.3942	hht2-GFP:URA4+ mCherry-atb2:HphR cdc25-22 ade6-m210? leu1-32 ura4-D18 h-
PT.3944	pkl1Δ::NatR hht2-GFP:URA4+ mCherry-atb2:HphR cdc25-22 ade6-m210? leu1-32 ura4-D18 h-
PT.4030	msd1Δ::NatR mal3-linker-GFP:KanR mcherry-atb2:HphR ade6-m210? leu1-32 ura4-D18 h+
PT.4060	msd1Δ::KanR cut7Δ::NatR sid4-GFP:KanR mCherry-atb2:HphR ade6-m210? leu1-32 ura4-D18 h+

CHAPTER 4: DISCUSSION

4.1 Summary

Chromosomes must be faithfully segregated to maintain genome integrity during mitosis. The dynamic mitotic spindle, a macromolecular machine, drives this process. However, little is known about how defects in spindle mechanics affect chromosome segregation. For example, the metaphase spindle is maintained at relatively constant length (Dumont & Mitchison, 2009; Goshima & Scholey, 2010) by antagonistic force-balance, yet how the regulation of metaphase spindle length contribute to subsequent chromosome segregation remain unexplored. It is proposed that a balance of antagonistic forces produced by motors and MAPs located at the spindle midzone, the kinetochore, and/or aster MTs is required to maintain the constant metaphase spindle length (Dumont and Mitchison, 2009; Goshima and Scholey, 2010; Mogilner and Craig). It is also suggested that the deviation from the characteristic spindle length may cause cellular defects during or after cell division (Goshima and Scholey, 2010). For example, shorter or longer metaphase spindle, due to deletion of inhibition of a single motor or MAPs, displays chromosome segregation defect (Goshima et al., 1999; Loiodice et al., 2005; West et al., 2001; Yamashita et al., 2005). However, studies to test the force-balance model and its effect on chromosome segregation has not been performed in living cells, due to the technical difficulties of monitoring a dynamic spindle and its chromosomes while simultaneously inhibiting the function of antagonistic motors and MAPs. In addition, the large list of genes involved in spindle length control (Goshima et al, 2005) can obscure system-level understanding of force-balance, spindle length, and chromosome segregation. In the present live-cell study, we used the simple fission yeast *Schizosaccharomyces pombe*, combined with fast microfluidic temperature-control for inactivating thermo-sensitive proteins, effectively tuning protein functions on-off rapidly during mitosis, to directly test the force-balance model and determine its consequences on chromosome segregation. We show that spindle midzone proteins kinesin-5 cut7p and microtubule bundler ase1p contribute to outward pushing force, and spindle kinetochore proteins kinesin-8 klp5/6p

and dam1p contribute to inward pulling force. Removing these proteins individually led to aberrant metaphase spindle length and chromosome segregation defects. Removing these proteins in antagonistic combination rescued the defective spindle length and, in some combinations, also partially rescued chromosome segregation defects (Chapter 2).

Bipolar spindle requires properly organized spindle poles that can resist pulling and pushing forces mediated by antagonistic forces acting on MTs to drive spindle pole separation, chromosome alignment and segregation. Subsequently, proteins such as kinesin-14 HSET and the NuMA–dynein–dynactin complex help to focus MTs at the spindle pole body (Gordon et al., 2001). In anaphase, chromosomes segregate to their respective spindle pole and spindle continues to elongate to ensure that chromosomes are far away from division site. However, mechanism governing spindle mechanics such as spindle pole focusing and its effect on chromosome segregation remains largely unknown. Fission yeast kinesin-14 pkl1p plays a key role in the SPB organization and/or maintenance. In pkl1p-deleted (pkl1 Δ) cells, the SPBs are fragmented (Grishchuk et al., 2007) and display frequent MT protrusions (Syrovatkina et al., 2013). In addition, frequent chromosome mis-segregation is observed in pkl1Δ cells (Grishchuk et al., 2007). We investigated herein mechanism of unfocused SPBs and its effect on spindle dynamics and chromosome segregation. We identified a potential new mechanism that leads to unequal chromosome segregation in fission yeast. Kinesin-14 pkl1p and MAP msd1p localize to the spindle poles and focus the MT minus ends. Their absence leads to pole and MT defocusing, resulting in spindle midzone kinesin-5 cut7p dependent sliding forces pushing the unfocused MT minus ends away from the spindle poles. Infrequent long MT minus end protrusions can push the already separated chromosome mass back to the cell center, where cytokinesis will ‘cut’ the chromosome mass, creating two daughter cells with unequal chromosome content or aneuploidy (Figure 3.4).

The above results cumulatively emphasize the importance of proper spindle mechanics for chromosome segregation fidelity. In addition, powerful model system such as fission yeast can be

successfully utilized to address fundamental questions regarding spindle dynamics that are challenging to dissect in more complex systems such as mammalian. This chapter focuses on the significance of these findings and provides insights into future directions for research.

4.2 Regulation of Metaphase Spindle Length

Eduard Strasburger was the first to characterize in detail, and to name, the first three phases of mitosis as prophase, metaphase and anaphase in 1884 (Baluska et al., 2012). In 1953, by using centrifuged oocytes from the annelid parchment worm *Chaetopterus pergamentaceous*, Shinya Inoue was able to visualize metaphase spindle at a constant length which lasted for more than an hour (Inoue, 2008). We now know that the metaphase spindle is a highly dynamic structure which is composed of MTs that oscillate between growing and shortening phases (Desai and Mitchison, 1997), motors that move along the surface of, or destabilize, microtubules (Verhey and Hammond, 2009) and MAPs that regulate MTs in various ways (Maiato et al., 2004), yet metaphase spindle maintains steady-state constant length. The stability of this steady-state is evident from the remarkable ability of metaphase spindles to recover from transient physical and chemical perturbations (Dumont and Mitchison, 2009). This steady-state constant length is maintained by force-balance model between antagonistic pushing outward and pulling inward forces (Figure 1.5). Remarkably, removal of any single or combination of force contributors results in a new steady-state length. The stability of a new spindle length can be stable or unstable, depending on the state of antagonism between force contributors. We have defined four categories of force contributors based on the function of these proteins: **(1)** cut7p as an active outward-force producer, **(2)** klp5/6p as an active inward-force transducer, **(3)** dam1p as a passive inward-force transducer, and **(4)** ase1p a passive inward-force resistor. Active-active antagonism, such as found in dam1Δ:ase1Δ, where antagonism is set between cut7p, an active outward pushing force producer and klp5/6p, an active inward pulling force transducer leads to new and stable steady-state length. In contrast, an active-passive antagonism, such as found in

klp5Δ:ase1Δ, where antagonism is set between cut7p, an active outward pushing force producer and dam1p, a passive inward pulling force transducer, leads to a new and unstable steady-state length with transient length fluctuations. Interestingly, both of these new stable and unstable steady-state spindles display similar spindle length at metaphase to anaphase A transition as wild-type spindles, suggesting that removal of antagonistic force contributors leads to an apparent rescue of the spindle length at anaphase onset.

The steady-state constant length of the metaphase spindle is proposed to be important for chromosome segregation fidelity (Goshima and Scholey, 2010). This hypothesis, however, has been challenging to address because any modification to proteins that play role in kinetochore-to-MT attachments results in both spindle length and chromosome segregation defects. For example, both klp5/6p heterodimer and dam1p localize to the kinetochores (Liu et al., 2005; West et al., 2001) and single deletion of heterodimer klp5/6p or dam1p results in longer spindle lengths and chromosome segregation defects (Garcia et al., 2002; West et al., 2002). Removal of either klp5p or dam1p with opposing antagonistic force contributor such as ase1p or cut7p results in a new steady state spindle length that is similar to wild-type length. The apparent spindle length rescue correlates with rescue of chromosome segregation only in combinations that involve klp5/6p but not dam1p. This suggests that the major role of klp5/6p at the kinetochores is to regulate MT dynamics to control spindle length and the minor role is to attach MTs to the kinetochores. In contrast, dam1p plays an essential role in kinetochore-to-MT attachments (Franco et al., 2007; Grishchuk et al., 2008a; Sanchez-Perez et al., 2005) because its absence could not improve chromosome segregation defects even when the metaphase spindle length appeared rescued. Overall, our observations highlight the importance of proper kinetochore-to-MT attachment over proper metaphase spindle length in relation to chromosome segregation. However, spindle length regulation still may have positive effect on proper chromosome segregation in conditions where kinetochore-to-MT attachments are not severely compromised as found in klp5Δ or klp6Δ. For example, in absence of klp5/6p when spindle length is rescued to

apparent wild-type length, chromosome segregation defects, e.g. mis-attached or lagging chromosome, are reduced. It is possible that transient spindle length decrease in the double-deletions klp5Δ:ase1Δ and klp6Δ:cut7.24^{ts} maybe a serendipitous mechanism. By shortening the spindle length, the distances between microtubule plus ends and kinetochores are also shortened, thus enabling more efficient proper kinetochore-to-MT attachments. Alternatively, improper kinetochore-to-MT attachments such as merotelic attachments that lead to chromosome segregation defect may be actively corrected through Aurora kinase -depended mechanism when spindle length is corrected (Choi and McCollum, 2012). Aurora kinase plays an essential role at centromeres in destabilizing erroneous attachment and thereby aid in the establishment of correct bipolar attachment (Hochegger et al., 2013). It is proposed that merotelic attachments are pulled away from Aurora correction zone due to outward pushing forces (Choi and McCollum, 2012). However, when spindle length is corrected, it might reduce tension at the kinetochores to allow the merotelic attachment to be destabilized by Aurora kinase. More experiments are needed to be performed to distinguish between these two passive and active mechanisms.

Although not exhaustive, our study allowed us to define four categories in relation to forces that exemplify the function of the proteins. However, many more proteins contribute to spindle length control (Figure 1.5 and Goshima et al. 2005) and I envision that our approach of studying simultaneous double-deletion or inactivation can be applied systematically to all proteins implicated in metaphase spindle length control to define their individual relative contribution to chromosome segregation defects. For example, mis4p which is the cohesin that binds sister chromatids together (Goshima et al., 1999), can act as **(5)** a passive outward force resistor (or a spring) (Gay et al., 2012). I imagine that removing both mis4p and ase1p would establish active-active antagonism and lead to a new and stable steady-stable spindle length whereas removing mis4p and cut7p would establish passive-active antagonism and lead to a new and unstable steady-stable spindle length. Potentially, the same analogy of force balance model can be applied to any other kinetochore proteins such as ncd80p or mis12p to define their relative contribution to

spindle length regulation and chromosome segregation. I imagine that ndc80p could act as active inward-force transducer similarly to klp5/6p **(2)**. Ndc80p is essential for the formation of kinetochore-to-MT attachments (Wigge and Kilmartin, 2001) and crucial for recruitment of dis1p that can influence MT dynamics at the kinetochores (Hsu and Toda, 2011). This suggests that the ndc80p complex may act as an active inward-force transducer that converts MT dynamics to cargo movement. In contrast, mis12p complex acts as the major platform for outer kinetochores assembly (Yamagishi et al., 2014) suggesting that mis12p complex may function as a passive inward-force transducer **(3)**.

Metaphase spindle length is also regulated by motor proteins such as dynein or kinesin-14 klp2p which localize to the kinetochores and can act as active inward force producers **(6)**. Dynein is a large minus end-directed motor complex that localizes to kinetochores through multiple adaptors proteins (Raaijmakers et al., 2013) to generate force to regulate metaphase spindle length in mammalian cells. In fission yeast, however, dynein has been proposed to aid in anchoring MTs at the pole (Grishchuk et al., 2007). Our screen for motors that regulate metaphase spindle length indicates that in the absence of dhc1p (*dhc1Δ),* the dynein heavy chain, metaphase spindle does not vary dramatically from wild-type (Figure 2.1), suggesting that dhc1p does not play a major role in regulating metaphase spindle length. On the other hand, in the absence of klp2p, a minus end-directed kinesin, the metaphase spindle is significantly longer compared to wild-type cells (Figure 2.1; Troxell et al., 2001) suggesting that klp2p might contribute to inward pulling force at the kinetochores in fission yeast instead of dynein. Interestingly, another member of kinesin-14, pkl1p, localizes to the SPBs and contributes to inward pulling forces to antagonize cut7p. Deactivation of cut7p through temperature-sensitive mutations in the wild-type background leads to monopolar spindles and subsequent cell death. However, deletion of the *pkl1+* gene is able to suppress the temperature-sensitivity of growth in cut7^{ts} cells at 37ºC (Pidoux et al., 1996; Troxell et al., 2001). It is thought that pkl1p, like other kinesin-14 members including *human* HSET, *Xenopus* XCTK2, *Drosophila* NCD, is able to crosslink parallel MTs at the SPBs and thus oppose

forces generated by cut7p (Fink et al., 2009; Mountain et al., 1999; Pidoux et al., 1996; Troxell et al., 2001; Walczak et al., 1997). In addition, a motor dead mutant of pkl1p is able to suppress the temperature-sensitivity growth in cut7^{ts} cells at 37ºC similarly to pkl1Δ, suggesting that pkl1p needs its motor activity to generate inward pulling forces to oppose outward pushing force by cut7p (Rodriguez et al., 2008).

Importantly, Olmstead et al. recently reported that deletion of the essential *cut7+* in the background of pkl1Δ cells results in viable cells (Olmsted et al., 2014). This work might have been inspired by the original observation of pkl1Δ:cut7^{ts} cells survival at 37 ºC using cell growth assays (Pidoux et al., 1996; Troxell et al., 2001). This significant finding illustrates that the bipolar spindle can be established through kinesin-5 independent mechanism in fission yeast. Another motor, kinesin-6 klp9p is able to elongate the spindle by sliding antiparallel MTs apart (Fu et al, 2009) and thus could substitute for the function of cut7p. However, this is unlikely because klp9p is inactive in early mitosis due to phosphorylation by cdc2p, the cyclin-dependent kinase Cdk1 (Fu et al, 2009). At the onset of anaphase, phosphatase clp1p, homolog of Cdc14 dephosphorylates klp9p allowing klp9p to initiate rapid spindle elongation (Fu et al, 2009). I imagine that the absence of both cut7p and pkl1p results in a passive-passive antagonism where major active outward pushing and inward pulling force producers are missing, which leads to a new and stable steady-state length. In this condition, MT pushing forces may contribute to SPBs separation. Initially, MTs may be stabilized between duplicated SPBs through csi1p mechanism proposed by Zheng et al. Csi1p recruits alp7p and its adaptor protein alp14p to the SPBs. Once at the SPB, alp7p-alp14p complex may facilitate the lateral binding of adjacent microtubules for promoting bipolar spindle formation (Zheng et al., 2014). Subsequently, ase1p that preferentially binds to antiparallel MTs (Janson et al., 2007) can potentially stabilize the bipolar spindle while MTs exert pushing forces to elongate the spindle. Perhaps, clustering of centromeres at the SPBs may serendipitously aid in the survival of the double-deletion pkl1Δ:cut7Δ mutant. When the

Figure 4.1

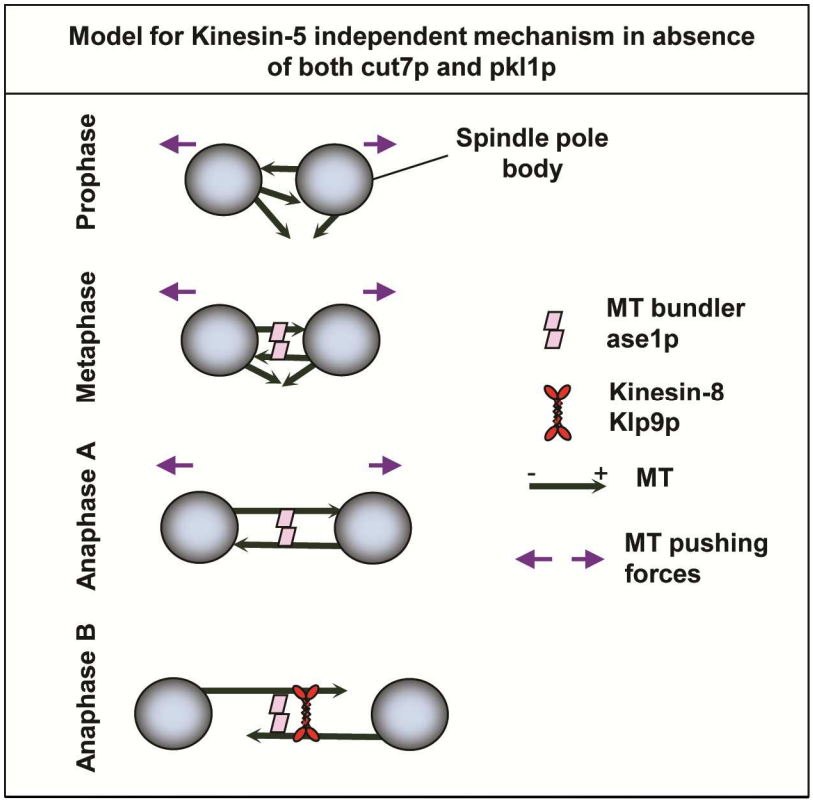

Figure 4.1. Simplified Model for Kinesin-5 Independent Mechanism of SPB Separation and Bipolar Spindle Assembly.

MTs are growing from each SPB in all directions. In prophase, when SPBs are positioned close together, many short MTs will collide with the opposing SPB, generating a pushing force that pushes SPB apart. Ase1p preferentially binds to antiparallel MTs (Janson et al., 2007) and stabilizes the bipolar spindle while MTs continue to exert pushing forces to elongate the spindle in metaphase and anaphase A. In anaphase B, klp9p is activated to elongate the spindle (Fu et al, 2009).

bipolar spindle is formed, kinetochores are conveniently located close to SPBs possibly allowing for efficient capture of chromosomes by spindle MTs. Upon chromosomes capture, the cells can transition into anaphase B where klp9p is activated to elongate the spindle (Figure 4.1). I predict that chromosome segregation defects in the double-deletion pkl1Δ:cut7Δ mutant could dramatically increase in combination with csi1Δ or csi2Δ. In absence of csi1p, cells exhibit declustered centromere and defects with the formation of bipolar spindle, while in absence of csi2p, cells display only defects with the formation of bipolar spindle (Costa et al., 2014; Zheng et al., 2014). Investigating spindle formation and chromosome segregation in the triple-deletion mutants, pkl1Δ:cut7Δ:csi1Δ and pkl1Δ:cut7Δ:csi2Δ may be particularly useful because these studies may illuminate the relative contribution of centromere declustering and the formation of spindle bipolarity to the survival of the double-deletion pkl1Δ:cut7Δ mutant.

The contribution of factors other than the six discussed above to spindle length control in fission yeast is also possible. For example, because yeast undergoes “closed” mitosis where the nuclear envelope does not breakdown, it is possible that forces produce by the intact nuclear membrane may regulate metaphase spindle length. However, in the single pkl1Δ mutant, the nuclear envelope deforms and sometimes is punctured due to MT protrusions pushing without obvious buckling of those MTs, suggesting that the membrane’s resistive forces might not be very strong. Disruption of the spindle midzone in anaphase B by laser cut leads to rapid spindle collapse (Khodjakov et al., 2004), which also suggests that nuclear envelope may exert resistive forces on the spindle but these forces only apparent when motors, major force generators, are perturbed.

4.3 Focusing of Microtubule Minus Ends at the Spindle Pole

Centrosomes nucleate MTs efficiently *in vitro*, therefore it has been generally accepted that centrosomal microtubule organizing centers are essential features of spindle assembly and organization (Merdes and Cleveland, 1997). However, numerous experiments have shown that focusing of microtubule minus ends at spindle poles also involves non-centrosomal factors such

as molecular motors. For example, cytoplasmic dynein is necessary to efficiently focus microtubule minus ends at spindle poles in a variety of animal systems (Gaglio et al., 1997; Merdes et al., 1996). The multiprotein activator of cytoplasmic dynein, dynactin, is also required for spindle pole organization in these systems. Cytoplasmic dynein and dynactin appear to act together to both focus microtubule minus ends and to transport the structural protein NuMA (nuclear mitotic apparatus protein) to the site of the developing spindle pole (Merdes et al., 2000). In addition, the plus end-directed kinesin-5, Eg5, has been shown to contribute to spindle pole organization. In the absence of Eg5 activity, microtubule minus ends are inefficiently focused, leading to broad spindle poles, and it is proposed that Eg5 contributes to spindle organization by cross-linking constituent microtubules (Sharp et al., 1999). Recent experiments also show that Eg5 appears to directly interact with NuMa *in vitro*, and in Eg5-depleded cells, NuMA is reduced from the spindle poles in HeLa cells (Iwakiri et al., 2013), suggesting that Eg5 might also regulate NuMA localization. In addition, HSET and its homologues (XCTK2, NCD, Kar3 and pkl1p) contribute to both the overall structural integrity of the spindle and the efficiency of spindle formation by focusing microtubule minus ends (Fink et al., 2009; Mountain et al., 1999; Pidoux et al., 1996; Troxell et al., 2001; Walczak et al., 1997). HSET is essential to establish cohesive poles in mouse meiotic spindles and to generate microtubule asters *in vitro*, but its role is masked by centrosomes in somatic cells (Mountain et al., 1999). Nevertheless, simultaneous perturbation of both HSET and NuMA severely suppresses chromosome movement in mitosis (Gordon et al., 2001), suggesting that MTs minus end anchorage at spindle poles is essential for chromosome segregation fidelity.

A plethora of motor proteins is important for focusing of MT minus ends at the spindle poles in mammalian cells. In fission yeast however, the major motor protein that plays a role in focusing of SPBs is kinesin-14 pkl1p. During mitosis, pkl1p localizes to SPBs by interacting with the γ-tubulin complex (Rodriguez et al., 2008). We also show that pkl1p and MAP msd1p are co-dependent to localize to the SPBs. The absence of pkl1p and msd1p leads to spindle pole and MT defocusing.

A recent report identified *human* Msd1/SSX2IP as an orthologue of msd1p based on three internal coiled-coil domains that exhibit the highest homology (Hori et al., 2014). hMsd1/SSX2IP depletion leads to misoriented mitotic spindles with reduced length and intensity. Mitotic regrowth assay has not identified any defect with initial MT nucleation around the centrosome in hMsd1-depleted cells, suggesting that MT nucleation is not effected in these cells. However, the formation of tilted spindle MTs with compromised aster MTs suggest that there might be a defect with aster MTs anchorage at the centrosome, which subsequently results in mitotic spindle misorientation (Hori et al., 2014). These observations suggest that pkl1p and msd1p dependent pole focusing mechanism maybe be conserved in other eukaryotes beyond fungi.

Localization dependency between msd1p and pkl1p is shown by live-cell imaging (Figure 3.2C). However, it is still unclear whether these two proteins interact directly at the SPBs. It is clear however that our study highlights the difference between pkl1p and msd1p in their contribution to spindle pole focusing. Over-expression of msd1p-YFP in absence of pkl1p does not localize msd1-YFP to the poles or mitotic spindle and consequently does not rescue MT protrusions. In contrast, over-expression pkl1p-GFP in absence of msd1p localizes pkl1p-GFP to the spindle, but not to the spindle pole body and partially rescues MT protrusions. These observations suggest that pkl1p motor can bundle parallel MT minus ends, partially keeping the spindle pole focused while msd1p cannot be recruited to the SPBs without pkl1p.

We show that the absence of pkl1p and msd1p leads to pole and MT defocusing, resulting in cut7p dependent sliding forces pushing the unfocused MT minus ends away from the spindle poles (Figure 3.4). Removal of cut7p in pkl1Δ or msd1Δ cells can rescue minus ends MT protrusions but not plus ends protrusions, suggesting that by focusing the minus end of MTs at the spindle pole, pkl1p and msd1p help to organize the spindle so that the plus end of MTs from one pole do not grow past the other pole. Possible role of pkl1p or msd1p in regulating plus end dynamics has not been reported therefore I speculate that pkl1p and msd1p play indirect role in MT dynamics at the plus ends.

It has been challenging to study MT dynamics by live-cell imaging during the early stages of mitosis in fission yeast because individual microtubules that emanate from each pole are relatively short and numerous. Recently, however, Costa et al. develop a novel method to image short fission yeast mitotic spindle MTs through the use of the thermo-sensitive cut7.24^{ts} to create monopolar spindles and subsequently image and measure individual MT dynamics in mitosis (Costa et al., 2013). This exact method might not be extremely useful for MT dynamics analysis in the double-deletion pkl1Δ:cut7Δ mutant. However, in combination with csi1Δ that alone displays transient monopolar spindle, the triple-deletion pkl1Δ:cut7Δ:csi1Δ may display enhanced monopolar spindle thus providing a condition where it might be possible to ask whether MT plus end dynamics is altered in absent of pkl1p or msd1p.

Recent report suggests that both pkl1p and cut7p interacts with the γ-tubulin complex at the spindle poles (Olmsted et al., 2014). It is proposed that pkl1p inhibits MT nucleation and cut7p counteracts its function at the SPBs. This report has a number of inconsistencies and shortcomings which make it challenging to interpret the results. First, it is unclear how pkl1p could inhibit MT nucleation without changing the number of MTs observed at the SPB. Second, *in vivo* nucleation assay is performed only using the double-deletion pkl1Δ:cut7Δ mutant and not wild-type or pkl1Δ mutant. If pkl1p inhibits MT nucleation, removing pkl1p should increase MT nucleation which could potentially be observed using nucleation assay. Third, the conclusion that cut7p regulates pkl1p lacks direct evidences and only based on genetic evidence that over-expression of pkl1p in the deletion or inactivation of cut7p background results in unformed spindle.

Our and Olmsted et al. works are in agreement with the qualitative findings that pkl1Δ cells have spindle MT protrusions, pkl1Δ cells have chromosome segregation defects, and the double-deletion pkl1Δ:cut7Δ alleviates the protrusions. However, a few discrepancies exist between our manuscript and the Olmsted et al. paper. First, we are in disagreement on the increase of spindle thickness in pkl1Δ. We have not observed any differences in intensity of the mCherry-tagged

atb2p (tubulin) between wild-type and pkl1Δ. In support of our observation, previous study using electron tomography to examine pkl1Δ cells reported no obvious defects in number of MTs growing from the pole in pkl1Δ (Grishchuk et al., 2007). Second, Olmstead et al. reported normal mitotic progression in pkl1Δ as evident by similar to wild-type spindle length changes from prophase to anaphase. We, however, observed that pkl1Δ cells display significant delay in the prophase to metaphase duration as comparted to that in wild-type. Third, Olmsted et al. showed that the nuclear envelope did not deform in the pkl1Δ cells. Olmsted et al. did not simultaneously imaged MTs and nuclear envelope dynamics in the pkl1Δ strain. Meanwhile, we imaged MTs and nuclear envelope the same time, and showed that nuclear envelope deformation is transient, as long MTs can puncture nuclear envelope (Figure 3.1B). Olmsted et al. might have missed this transient process by not having MT and nuclear envelope markers together in the pkl1Δ strain.

It is possible that some of these discrepancies exist due to differences in utilized yeast strains and techniques. Primarily, we use antibiotic marker cassettes such as *kanMX6* or *natMX6* for gene disruption while the Olmstead et al. paper utilized auxotrophic marker cassettes such as ura4+ and his3+ genes. The presence of antibiotic markers gives rise to strong, selectable resistance to the antibiotic geneticin (for *kanMX6*) and nourseothricin (for *natMX6*). In contrast, the limitations of auxotrophic markers are reported to include unwanted phenotypic effects, such as growth defects (Hentges et al., 2005). Furthermore, for most of our live-cell imaging experiments, we used endogenously tagged proteins such as mCherry-atb2p (tubulin). The Olmstead et al. paper however performed their live-cell experiments using tagged proteins expressed on the plasmid under control of thiamine promoter (*nmt1* promoter). The main drawback with the *nmt1* promoter is that it is leaky, even in the present of thiamine (Boe et al., 2008). This makes it challenging to control the expression of the tagged protein in the cell. Lastly but perhaps most importantly, imaging parameters differed greatly. During our imaging we acquired 11-imaged with 0.5 μm Z-stacks, which were all used to make each image for all time points. Those settings allowed us to visualize the whole cell in Z-plane which is about ~4 μm in

depth (Piel and Tran, 2009). Instead, the Olmstead et al. paper acquired 20-images with 0.1 μm Z-stacks and only 10 of those frames were used to make an image for each time point. Subsequently, these settings might not allow Olmstead et al. to properly visualize the whole yeast cell, and possibly underestimating their signals.

Overall, Olmstead et al. concluded that pkl1p inhibits MT nucleation at the spindle poles while cut7p counteracts its activity at the SPBs through direct interact with γ-tubulin, and this counteracting activity of both proteins somehow contributes to the formation of proper bipolar spindle (Olmsted et al., 2014). On the other hand, our findings favor the more straight forward conclusion, that pkl1p and cut7p, as motors, bind MTs and organize the dynamic spindle structure. Therefore, we are in disagreement concerning the detailed mechanism of function of pkl1p and cut7p.

Loss of kinesin-14 HSET in human cells results in spindle pole fragmentation and aneuploidy (Cai et al., 2010; Kim and Song, 2013) yet the precise mechanism of how unfocused poles contribute to aneuploidy remains unknown. Our current work in fission yeast reveals a novel and potentially conserved mechanism for aneuploidy, as all studied proteins are conserved from yeast to human. Importantly, we show that a small percentage of aneuploidy cells (4%) survive and proliferate. Aneuploidy cells in absence of pkl1p have variable chromosome defects e.g. whole-chromosome and partial chromosome gain or loss. How does this type of aneuploidy affect the proliferation and physiology of these cells? It is reported that whole-chromosome aneuploidy causes a proliferative disadvantage to normal yeast cells (Niwa et al., 2006; Torres et al., 2007). Additional long-term imaging experiments are needed to investigate whether the aneuploid cells generated in absence of pkl1p or msd1p results in impaired proliferation. It is proposed that aneuploidy contributes to tumorigenesis by promoting a mechanism by which oncogenes are gained or tumors suppressor genes are lost (Lengauer et al., 1998). Investigating how partial chromosome aneuploidy affects pkl1Δ cells could potentially offer new insights into tumor pathogenesis.

4.4 Future Direction

How the directionality of cut7p is regulated during mitosis?

Kinesin-5 separates the spindle pole bodies via the plus-end-directed sliding motility between antiparallel MTs; thus its ability to move towards the plus end of MTs is essential to its function in mitosis. Eg5 (mammalian kinesin-5) has been shown to be a tetramer that cross-links MTs and walks toward their plus ends, and thus slides them apart (Kapitein et al., 2008; Kapitein et al., 2005). Fission yeast, kinesin-5 cut7p is required for the formation of bipolar spindle (Hagan and Yanagida, 1990; Hagan and Yanagida, 1992). The $cut7^{ts}$ mutants displays monopolar spindles at the restrictive temperature, suggesting that cut7p generates the outward forces on the spindle poles. However, no *in vitro* cut7p assays have been performed to test whether cut7p can slide antiparallel MTs. Recent *in vitro* gliding experiments show that the glass bound full length cut7p displays the minus-end-directed motility whereas the glass bound cut7p motor domain exhibits the plus-end-directed motility (Edamatsu, 2014). It would be important to perform *in vitro* assays similar to the ones previously described by Surrey lab (Kapitein et al., 2005) where MTs can be observed to slide pass one another in the presence of the motor. It is possible that cut7p might function similarly to budding yeast kinesin-5 Cin8. Single Cin8 motors are minis-end-directed motors whereas they switch to the plus-end-directionality when working in a team of motors sliding antiparallel MTs apart (Roostalu et al., 2011).

In addition to the spindle midzone, cut7p localizes to the SPBs during mitosis (Hagan and Yanagida, 1992) but its function near the SPBs remains unexplored. Recent report shows that cut7p interacts with the γ-tubulin complex at the spindle poles to presumably counteract pkl1p activity (Olmsted et al., 2014). However, how this function of cut7p contributes to spindle dynamics or chromosome segregation is not known. It might be possible to investigate the role of cut7p at the poles using the double-deletion pkl1Δ:cut7Δ mutant. For example, one could make different truncation version of cut7p and then express them in the double-deletion pkl1Δ:cut7Δ

mutant to observe how they affects spindle dynamics and chromosome segregation. These experiments might provide some insights into function of cut7p at the SPBs and the spindle midzone.

How does kinesin-14 klp2p contribute to metaphase spindle length control and chromosome segregation?

Metaphase spindle length is significantly longer in klp2Δ cells compared to wild-type cells (Figure 2.1B; Troxell et al., 2001), suggesting that klp2p contributes to inward pulling forces at the kinetochores. To define whether klp2p is an active inward force producer, one could inactive cut7.24^{ts} or delete ase1p in the klp2Δ background then monitor metaphase spindle length as shown in Figure 2.2. Klp2p localizes to kinetochores during mitosis (Troxell et al., 2001) however whether it controbutes to chromsome segregation is not known. First, one could characterize chromosome behavior in the single klp2Δ mutant as shown in Figure 2.3. If chromosome segregation defects are observed in the single klp2Δ mutant, one could further quantify similar defects in klp2Δ:ase1Δ and klp2Δ:cut7.24^{ts} mutants. These experiments will clarify klp2p contribution to metaphase spindle length control and chromosome segregation.

How does kinesin-14 pkl1p contribute to metaphase spindle length control and spindle pole organization?

Pkl1p is thought to produce the inward pulling force on the spindle pole to antagonize cut7p which produces the outward pushing force (Pidoux et al., 1996; Troxell et al., 2001). However precise function of pkl1p in force production is not clear. Over-expression of pkl1p results a monopolar spindles suggesting that pkl1p produces inward pulling force on the spindle pole. A motor dead mutant of pkl1p is able to suppress the temperature-sensitivity growth in cut7^{ts} cells at the restrictive temperature similarly to pkl1Δ, suggesting that pkl1p needs its motor activity to generate inward pulling force to oppose outward pushing force by cut7p (Rodriguez et al., 2008). On the other hand, motor dead mutant is able to rescue pole focusing in pkl1 Δ (Figure 3.2S).

These observations suggest that pkl1p has two functions within the spindle: to 1) regulate metaphase spindle length which requires motor activity, and 2) organize minus-end of MTs at the poles which might not require motor activity. It is proposed that kinesin-14 motors form stable contacts between parallel-oriented microtubules near the spindle poles but cause sliding between anti-parallel microtubules in the midzone (Endow et al., 1994; Mountain et al., 1999; Walczak et al., 1997). It would be important to perform *in vitro* single molecule assays as described previously by Diez lab (Fink et al., 2009) to elucidate precise interaction between pkl1p and MTs. *Drosophila melanogaster* kinesin-14 (Ncd) motors slide antiparallel MTs and statically crosslink parallel MTs *in vitro* (Fink et al., 2009). It is possible that pkl1p might interact with MTs similarly to Ncd while localized to the spindle pole bodies (Syrovatkina et al., 2013). Pkl1p may have additional properties that might allow it to produce inward pulling force on parallel MTs.

Do pkl1p and msd1p physically interact?

Pkl1p and msd1p are co-dependented on each other to localize to SPBs (Figure 3.2C). It has been shown that pkl1p and msd1p interact with gamma tubulin at the minus ends (Paluh et al., 2000; Toya et al., 2007). Therefore, it is important to address whether pkl1p and msd1p interact directly or indirectly by utilizing molecular biochemical experiments. For example, direct interaction can be tested by standard GST pull-down assays *in vitro* (Fu et al., 2009) using full-length recombinant GST-pkl1p and HA-msd1p. It also will be interesting to investigate which domains in pkl1p and msd1p are important for their co-dependent localization to the SPBs. To this aim, standard molecular cloning techniques can be utilized to obtain truncated versions of msd1p, for example. Then, using live-cell imaging it is possible to observed whether those truncated versions of msd1p are able to recruit pkl1p to the spindle pole *in vivo*. This approach will be useful for mapping pkl1p and msd1p interactions *in vivo*.

4.5 Significance for Human Diseases

Since the pioneer discovery of monastrol, the first small-molecule inhibitor of kinesin-5 Eg5 (Mayer et al., 1999), mitotic kinesins have been considered as a potential target for cancer therapeutics in addition to anti-mitotic drugs such as taxanes and vinca alkaloids, which target MT dynamics (Jordan and Wilson, 2004). MTs play an important role in many other functions of the cell beside mitosis, therefore patients treated with anti-mitotic drugs develop numerous undesirable side-effects (Manchado et al., 2012). On the other hand, mitotic kinesins perform specialized function in mitosis such as bipolar spindle assembly and maintenance or spindle pole organization. This specificity of kinesins offer potentially ideal target to be utilized for more rapidly dividing tumours such as lymphomas and leukemias (Rath and Kozielski, 2012). In fact, deactivation of kinesin-5 by drug monastrol leads to monopolar spindles and subsequent cell death, therefore many clinical trials involving Eg5-targeting agents have been attempted. Although side effects are moderate, the clinical efficacy of Eg5 inhibitors has been limited, with only a few studies demonstrating a partial response (Manchado et al., 2012). There could be a number of potential reasons for the observed lack of efficacy of these inhibitors, one of which is mechanistic redundancy in the formation and maintenance of the mitotic spindle. It is reported that Eg5 is not essential for maintenance of metaphase spindle in mammalian somatic cells (Blangy et al. 1995; Kapoor et al., 2000). It is thought that highly dynamic interpolar MTs may compensate for the absence of Eg5 (Kollu et al., 2009) or another motor such as Kif15 may substitute for Eg5 function in bipolar spindle assembly (Tanenbaum et al., 2009). Importantly, simultaneous inhibition of kinesin-5 and a minus-end-directed motor (dynein or kinesin-14 HSET) results in bipolar spindle formation (Ferenz et al., 2009; Mountain et al., 1999; O'Connell et al., 1993; Sharp et al., 1999; Tanenbaum et al., 2008). These studies suggest that additional kinsine-5 independent mechanism must exist to promote spindle bipolarity. Fission yeast might provide an excellent tool to investigate this hypothesis since simultaneous inhibition of kinesin-5 cut7p and kinesin-14 pkl1p results in viable cells (Olmstead et al., 2014). Understanding how the

double-deletion cut7Δ:pkl1Δ mutant is able to build the bipolar spindle without cut7p might provide important insights into kinsin-5- independent mechanism and possibly uncover conserved mechanism, as many proteins are conserved from yeast to human.

Early experiments using the injection of antibodies again HSET revealed that it is a non-essential kinesin that is involved in promoting spindle bipolarity in cultured cells (Mountain et al., 1999). Recently Kwon and colleague showed that in cancer cells, HSET focuses supernumerary centrosomes into a pseudo-bipolar spindle to avoid triggering apoptosis as the absence of HSET results in multipolar spindles and subsequent daughter cells die (Kwon et al., 2008). These findings make HSET a particularly attractive anticancer target because it is essential for tumors cells to survive, but it is not essential in normal cells. However, these studies are relatively short-term, and not enough long-term studies have been completed in human cells with inactive HSET to determine if a small percentage of daughter cells survive and proliferate as suggested from our current study for pkl1Δ (Figure 3.3). Even though our finding using fission yeast kinesin-14 pkl1p may not be generalized to human cells, nevertheless it suggests that if some cells survive and proliferate, inhibition of kinesin-14 might not be very effective as anticancer therapeutic.

REFERENCES

Adams, I.R., and J.V. Kilmartin. 2000. Spindle pole body duplication: a model for centrosome duplication? *Trends in cell biology*. 10:329-335.

Akhmanova, A., and M.O. Steinmetz. 2008. Tracking the ends: a dynamic protein network controls the fate of microtubule tips. *Nature reviews. Molecular cell biology*. 9:309-322.

Al-Bassam, J., H. Kim, G. Brouhard, A. van Oijen, S.C. Harrison, and F. Chang. 2010. CLASP promotes microtubule rescue by recruiting tubulin dimers to the microtubule. *Developmental cell*. 19:245-258.

Al-Bassam, J., H. Kim, I. Flor-Parra, N. Lal, H. Velji, and F. Chang. 2012. Fission yeast Alp14 is a dose-dependent plus end-tracking microtubule polymerase. *Molecular biology of the cell*. 23:2878-2890.

Almonacid, M., and A. Paoletti. 2010. Mechanisms controlling division-plane positioning. *Seminars in cell & developmental biology*. 21:874-880.

Anders, A., P.C. Lourenco, and K.E. Sawin. 2006. Noncore components of the fission yeast gamma-tubulin complex. *Molecular biology of the cell*. 17:5075-5093.

Anders, A., and K.E. Sawin. 2011. Microtubule stabilization in vivo by nucleation-incompetent gamma-tubulin complex. *Journal of cell science*. 124:1207-1213.

Appelgren, H., B. Kniola, and K. Ekwall. 2003. Distinct centromere domain structures with separate functions demonstrated in live fission yeast cells. *Journal of cell science*. 116:4035-4042.

Asakawa, H., A. Hayashi, T. Haraguchi, and Y. Hiraoka. 2005. Dissociation of the Nuf2-Ndc80 complex releases centromeres from the spindle-pole body during meiotic prophase in fission yeast. *Molecular biology of the cell*. 16:2325-2338.

Asbury, C.L., D.R. Gestaut, A.F. Powers, A.D. Franck, and T.N. Davis. 2006. The Dam1 kinetochore complex harnesses microtubule dynamics to produce force and movement. *Proceedings of the National Academy of Sciences of the United States of America*. 103:9873-9878.

Bahler, J., J.Q. Wu, M.S. Longtine, N.G. Shah, A. McKenzie, 3rd, A.B. Steever, A. Wach, P. Philippsen, and J.R. Pringle. 1998. Heterologous modules for efficient and versatile PCR-based gene targeting in Schizosaccharomyces pombe. *Yeast*. 14:943-951.

Baluska, F., D. Volkmann, D. Menzel, and P. Barlow. 2012. Strasburger's legacy to mitosis and cytokinesis and its relevance for the Cell Theory. *Protoplasma*. 249:1151-1162.

Blangy, A., H.A. Lane, P. d'Herin, M. Harper, M. Kress, and E.A. Nigg. 1995. Phosphorylation by p34cdc2 regulates spindle association of human Eg5, a kinesin-related motor essential for bipolar spindle formation in vivo. *Cell*. 83:1159-1169.

Boe, C.A., I. Garcia, C.C. Pai, J.R. Sharom, H.C. Skjolberg, E. Boye, S. Kearsey, S.A. Macneill, M.D. Tyers, and B. Grallert. 2008. Rapid regulation of protein activity in fission yeast. *BMC cell biology*. 9:23.

Bouck, D.C., and K. Bloom. 2007. Pericentric chromatin is an elastic component of the mitotic spindle. *Current biology : CB*. 17:741-748.

Bouhlel, I.B., M. Ohta, A. Mayeux, N. Bordes, F. Dingli, J. Boulanger, G. Velve Casquillas, D. Loew, P.T. Tran, M. Sato, and A. Paoletti. 2015. Cell cycle control of spindle pole body duplication and splitting by Sfi1 and Cdc31 in fission yeast. *Journal of cell science*.

Bouissou, A., C. Verollet, A. Sousa, P. Sampaio, M. Wright, C.E. Sunkel, A. Merdes, and B. Raynaud-Messina. 2009. {gamma}-Tubulin ring complexes regulate microtubule plus end dynamics. *The Journal of cell biology*. 187:327-334.

Bratman, S.V., and F. Chang. 2007. Stabilization of overlapping microtubules by fission yeast CLASP. *Developmental cell*. 13:812-827.

Braun, M., D.R. Drummond, R.A. Cross, and A.D. McAinsh. 2009. The kinesin-14 Klp2 organizes microtubules into parallel bundles by an ATP-dependent sorting mechanism. *Nature cell biology*. 11:724-730.

Bridge, A.J., M. Morphew, R. Bartlett, and I.M. Hagan. 1998. The fission yeast SPB component Cut12 links bipolar spindle formation to mitotic control. *Genes & development*. 12:927-942.

Busch, K.E., and D. Brunner. 2004. The microtubule plus end-tracking proteins mal3p and tip1p cooperate for cell-end targeting of interphase microtubules. *Current biology : CB*. 14:548-559.

Buttrick, G.J., and J.B. Millar. 2011. Ringing the changes: emerging roles for DASH at the kinetochore-microtubule Interface. *Chromosome research : an international journal on the molecular, supramolecular and evolutionary aspects of chromosome biology*. 19:393-407.

Cai, S., L.N. Weaver, S.C. Ems-McClung, and C.E. Walczak. 2010. Proper organization of microtubule minus ends is needed for midzone stability and cytokinesis. *Curr Biol*. 20:880-885.

Chang, L., and K.L. Gould. 2000. Sid4p is required to localize components of the septation initiation pathway to the spindle pole body in fission yeast. *Proc Natl Acad Sci U S A*. 97:5249-5254.

Cheeseman, I.M., and A. Desai. 2008. Molecular architecture of the kinetochore-microtubule interface. *Nature reviews. Molecular cell biology*. 9:33-46.

Choi, S.H., and D. McCollum. 2012. A role for metaphase spindle elongation forces in correction of merotelic kinetochore attachments. *Current biology : CB*. 22:225-230.

Cimini, D. 2007. Detection and correction of merotelic kinetochore orientation by Aurora B and its partners. *Cell cycle*. 6:1558-1564.

Costa, J., C. Fu, V.M. Khare, and P.T. Tran. 2014. csi2p modulates microtubule dynamics and organizes the bipolar spindle for chromosome segregation. *Molecular biology of the cell*. 25:3900-3908.

Costa, J., C. Fu, V. Syrovatkina, and P.T. Tran. 2013. Imaging individual spindle microtubule dynamics in fission yeast. *Methods in cell biology*. 115:385-394.

Cui, B., Y. Liu, and M.A. Gorovsky. 2006. Deposition and function of histone H3 variants in Tetrahymena thermophila. *Mol Cell Biol*. 26:7719-7730.

Cytrynbaum, E.N., J.M. Scholey, and A. Mogilner. 2003. A force balance model of early spindle pole separation in Drosophila embryos. *Biophysical journal*. 84:757-769.

Decottignies, A., P. Zarzov, and P. Nurse. 2001. In vivo localisation of fission yeast cyclin-dependent kinase cdc2p and cyclin B cdc13p during mitosis and meiosis. *Journal of cell science*. 114:2627-2640.

Dell, K.R., and R.D. Vale. 2004. A tribute to Shinya Inoue and innovation in light microscopy. *The Journal of cell biology*. 165:21-25.

Desai, A., and T.J. Mitchison. 1997. Microtubule polymerization dynamics. *Annual review of cell and developmental biology*. 13:83-117.

Ding, R., R.R. West, D.M. Morphew, B.R. Oakley, and J.R. McIntosh. 1997. The spindle pole body of Schizosaccharomyces pombe enters and leaves the nuclear envelope as the cell cycle proceeds. *Molecular biology of the cell*. 8:1461-1479.

Dogterom, M., J.W. Kerssemakers, G. Romet-Lemonne, and M.E. Janson. 2005. Force generation by dynamic microtubules. *Current opinion in cell biology*. 17:67-74.

Dumont, S., and T.J. Mitchison. 2009. Force and length in the mitotic spindle. *Current biology : CB*. 19:R749-761.

Edamatsu, M. 2014. Bidirectional motility of the fission yeast kinesin-5, Cut7. *Biochemical and biophysical research communications*. 446:231-234.

Endow, S.A., R. Chandra, D.J. Komma, A.H. Yamamoto, and E.D. Salmon. 1994. Mutants of the Drosophila ncd microtubule motor protein cause centrosomal and spindle pole defects in mitosis. *Journal of cell science*. 107 (Pt 4):859-867.

Endow, S.A., S. Henikoff, and L. Soler-Niedziela. 1990. Mediation of meiotic and early mitotic chromosome segregation in Drosophila by a protein related to kinesin. *Nature*. 345:81-83.

Erent, M., D.R. Drummond, and R.A. Cross. 2012. S. pombe kinesins-8 promote both nucleation and catastrophe of microtubules. *PloS one*. 7:e30738.

Fang, X., and P. Zhang. 2011. Aneuploidy and tumorigenesis. *Seminars in cell & developmental biology*. 22:595-601.

Ferenz, N.P., R. Paul, C. Fagerstrom, A. Mogilner, and P. Wadsworth. 2009. Dynein antagonizes eg5 by crosslinking and sliding antiparallel microtubules. *Current biology : CB*. 19:1833-1838.

Fink, G., L. Hajdo, K.J. Skowronek, C. Reuther, A.A. Kasprzak, and S. Diez. 2009. The mitotic kinesin-14 Ncd drives directional microtubule-microtubule sliding. *Nature cell biology*. 11:717-723.

Fink, G., I. Schuchardt, J. Colombelli, E. Stelzer, and G. Steinberg. 2006. Dynein-mediated pulling forces drive rapid mitotic spindle elongation in Ustilago maydis. *The EMBO journal*. 25:4897-4908.

Fong, C.S., M. Sato, and T. Toda. 2010. Fission yeast Pcp1 links polo kinase-mediated mitotic entry to gamma-tubulin-dependent spindle formation. *The EMBO journal*. 29:120-130.

Franck, A.D., A.F. Powers, D.R. Gestaut, T. Gonen, T.N. Davis, and C.L. Asbury. 2007. Tension applied through the Dam1 complex promotes microtubule elongation providing a direct mechanism for length control in mitosis. *Nature cell biology*. 9:832-837.

Franco, A., J.C. Meadows, and J.B. Millar. 2007. The Dam1/DASH complex is required for the retrieval of unclustered kinetochores in fission yeast. *Journal of cell science*. 120:3345-3351.

Fu, C., J.J. Ward, I. Loiodice, G. Velve-Casquillas, F.J. Nedelec, and P.T. Tran. 2009. Phospho-regulated interaction between kinesin-6 Klp9p and microtubule bundler Ase1p promotes spindle elongation. *Developmental cell*. 17:257-267.

Fujita, A., L. Vardy, M.A. Garcia, and T. Toda. 2002. A fourth component of the fission yeast gamma-tubulin complex, Alp16, is required for cytoplasmic microtubule integrity and becomes indispensable when gamma-tubulin function is compromised. *Molecular biology of the cell*. 13:2360-2373.

Funabiki, H., I. Hagan, S. Uzawa, and M. Yanagida. 1993. Cell cycle-dependent specific positioning and clustering of centromeres and telomeres in fission yeast. *The Journal of cell biology*. 121:961-976.

Furuta, K., M. Edamatsu, Y. Maeda, and Y.Y. Toyoshima. 2008. Diffusion and directed movement: in vitro motile properties of fission yeast kinesin-14 Pkl1. *J Biol Chem*. 283:36465-36473.

Gachet, Y., C. Reyes, T. Courtheoux, S. Goldstone, G. Gay, C. Serrurier, and S. Tournier. 2008. Sister kinetochore recapture in fission yeast occurs by two distinct mechanisms, both requiring Dam1 and Klp2. *Molecular biology of the cell*. 19:1646-1662.

Gaglio, T., M.A. Dionne, and D.A. Compton. 1997. Mitotic spindle poles are organized by structural and motor proteins in addition to centrosomes. *The Journal of cell biology*. 138:1055-1066.

Gao, Q., T. Courtheoux, Y. Gachet, S. Tournier, and X. He. 2010. A non-ring-like form of the Dam1 complex modulates microtubule dynamics in fission yeast. *Proceedings of the National Academy of Sciences of the United States of America*. 107:13330-13335.

Garcia, M.A., N. Koonrugsa, and T. Toda. 2002. Two kinesin-like Kin I family proteins in fission yeast regulate the establishment of metaphase and the onset of anaphase A. *Current biology : CB*. 12:610-621.

Garcia, M.A., L. Vardy, N. Koonrugsa, and T. Toda. 2001. Fission yeast ch-TOG/XMAP215 homologue Alp14 connects mitotic spindles with the kinetochore and is a component of the Mad2-dependent spindle checkpoint. *The EMBO journal*. 20:3389-3401.

Gay, G., T. Courtheoux, C. Reyes, S. Tournier, and Y. Gachet. 2012. A stochastic model of kinetochore-microtubule attachment accurately describes fission yeast chromosome segregation. *The Journal of cell biology*. 196:757-774.

Gordon, M.B., L. Howard, and D.A. Compton. 2001. Chromosome movement in mitosis requires microtubule anchorage at spindle poles. *The Journal of cell biology*. 152:425-434.

Goshima, G., S. Saitoh, and M. Yanagida. 1999. Proper metaphase spindle length is determined by centromere proteins Mis12 and Mis6 required for faithful chromosome segregation. *Genes & development*. 13:1664-1677.

Goshima, G., and J.M. Scholey. 2010. Control of mitotic spindle length. *Annual review of cell and developmental biology*. 26:21-57.

Goshima, G., R. Wollman, N. Stuurman, J.M. Scholey, and R.D. Vale. 2005. Length control of the metaphase spindle. *Current biology : CB*. 15:1979-1988.

Griffiths, K., H. Masuda, S. Dhut, and T. Toda. 2008. Fission yeast dam1-A8 mutant is resistant to and rescued by an anti-microtubule agent. *Biochemical and biophysical research communications*. 368:670-676.

Grishchuk, E.L., A.K. Efremov, V.A. Volkov, I.S. Spiridonov, N. Gudimchuk, S. Westermann, D. Drubin, G. Barnes, J.R. McIntosh, and F.I. Ataullakhanov. 2008a. The Dam1 ring binds microtubules strongly enough to be a processive as well as energy-efficient coupler for chromosome motion. *Proceedings of the National Academy of Sciences of the United States of America*. 105:15423-15428.

Grishchuk, E.L., and J.R. McIntosh. 2006. Microtubule depolymerization can drive poleward chromosome motion in fission yeast. *The EMBO journal*. 25:4888-4896.

Grishchuk, E.L., M.I. Molodtsov, F.I. Ataullakhanov, and J.R. McIntosh. 2005. Force production by disassembling microtubules. *Nature*. 438:384-388.

Grishchuk, E.L., I.S. Spiridonov, and J.R. McIntosh. 2007. Mitotic chromosome biorientation in fission yeast is enhanced by dynein and a minus-end-directed, kinesin-like protein. *Molecular biology of the cell*. 18:2216-2225.

Grishchuk, E.L., I.S. Spiridonov, V.A. Volkov, A. Efremov, S. Westermann, D. Drubin, G. Barnes, F.I. Ataullakhanov, and J.R. McIntosh. 2008b. Different assemblies of the DAM1 complex follow shortening microtubules by distinct mechanisms. *Proceedings of the National Academy of Sciences of the United States of America*. 105:6918-6923.

Grissom, P.M., T. Fiedler, E.L. Grishchuk, D. Nicastro, R.R. West, and J.R. McIntosh. 2009. Kinesin-8 from fission yeast: a heterodimeric, plus-end-directed motor that can couple microtubule depolymerization to cargo movement. *Molecular biology of the cell*. 20:963-972.

Hagan, I., and M. Yanagida. 1990. Novel potential mitotic motor protein encoded by the fission yeast cut7+ gene. *Nature*. 347:563-566.

Hagan, I., and M. Yanagida. 1992. Kinesin-related cut7 protein associates with mitotic and meiotic spindles in fission yeast. *Nature*. 356:74-76.

Hagan, I.M. 1998. The fission yeast microtubule cytoskeleton. *Journal of cell science*. 111 (Pt 12):1603-1612.

Hagan, I.M. 2008. The spindle pole body plays a key role in controlling mitotic commitment in the fission yeast Schizosaccharomyces pombe. *Biochemical Society transactions*. 36:1097-1101.

Hentges, P., B. Van Driessche, L. Tafforeau, J. Vandenhaute, and A.M. Carr. 2005. Three novel antibiotic marker cassettes for gene disruption and marker switching in Schizosaccharomyces pombe. *Yeast*. 22:1013-1019.

Hepperla, A.J., P.T. Willey, C.E. Coombes, B.M. Schuster, M. Gerami-Nejad, M. McClellan, S. Mukherjee, J. Fox, M. Winey, D.J. Odde, E. O'Toole, and M.K. Gardner. 2014. Minus-end-directed Kinesin-14 motors align antiparallel microtubules to control metaphase spindle length. *Developmental cell*. 31:61-72.

Hirano, T., S. Funahashi, T. Uemura, and M. Yanagida. 1986. Isolation and characterization of Schizosaccharomyces pombe cutmutants that block nuclear division but not cytokinesis. *The EMBO journal*. 5:2973-2979.

Hiraoka, Y., H. Maekawa, H. Asakawa, Y. Chikashige, T. Kojidani, H. Osakada, A. Matsuda, and T. Haraguchi. 2011. Inner nuclear membrane protein Ima1 is dispensable for intranuclear positioning of centromeres. *Genes to cells : devoted to molecular & cellular mechanisms*. 16:1000-1011.

Hiraoka, Y., T. Toda, and M. Yanagida. 1984. The NDA3 gene of fission yeast encodes beta-tubulin: a cold-sensitive nda3 mutation reversibly blocks spindle formation and chromosome movement in mitosis. *Cell*. 39:349-358.

Hochegger, H., N. Hegarat, and J.B. Pereira-Leal. 2013. Aurora at the pole and equator: overlapping functions of Aurora kinases in the mitotic spindle. *Open biology*. 3:120185.

Hoog, J.L., S.M. Huisman, D. Brunner, and C. Antony. 2013. Electron tomography reveals novel microtubule lattice and microtubule organizing centre defects in +TIP mutants. *PloS one*. 8:e61698.

Hori, A., C. Ikebe, M. Tada, and T. Toda. 2014. Msd1/SSX2IP-dependent microtubule anchorage ensures spindle orientation and primary cilia formation. *EMBO reports*. 15:175-184.

Horio, T., S. Uzawa, M.K. Jung, B.R. Oakley, K. Tanaka, and M. Yanagida. 1991. The fission yeast gamma-tubulin is essential for mitosis and is localized at microtubule organizing centers. *Journal of cell science*. 99 (Pt 4):693-700.

Hou, H., S.P. Kallgren, and S. Jia. 2013. Csi1 illuminates the mechanism and function of Rabl configuration. *Nucleus*. 4:176-181.

Hsu, K.S., and T. Toda. 2011. Ndc80 internal loop interacts with Dis1/TOG to ensure proper kinetochore-spindle attachment in fission yeast. *Current biology : CB*. 21:214-220.

Inoue, S. 2008. Microtubule dynamics in cell division: exploring living cells with polarized light microscopy. *Annual review of cell and developmental biology*. 24:1-28.

Inoue, S., and E.D. Salmon. 1995. Force generation by microtubule assembly/disassembly in mitosis and related movements. *Molecular biology of the cell*. 6:1619-1640.

Inoue, S., and H. Sato. 1967. Cell motility by labile association of molecules. The nature of mitotic spindle fibers and their role in chromosome movement. *The Journal of general physiology*. 50:Suppl:259-292.

Iwakiri, Y., S. Kamakura, J. Hayase, and H. Sumimoto. 2013. Interaction of NuMA protein with the kinesin Eg5: its possible role in bipolar spindle assembly and chromosome alignment. *The Biochemical journal*. 451:195-204.

Janson, M.E., R. Loughlin, I. Loiodice, C. Fu, D. Brunner, F.J. Nedelec, and P.T. Tran. 2007. Crosslinkers and motors organize dynamic microtubules to form stable bipolar arrays in fission yeast. *Cell*. 128:357-368.

Jiang, K., and A. Akhmanova. 2011. Microtubule tip-interacting proteins: a view from both ends. *Current opinion in cell biology*. 23:94-101.

Jordan, M.A., and L. Wilson. 2004. Microtubules as a target for anticancer drugs. *Nature reviews. Cancer*. 4:253-265.

Kanbe, T., Y. Hiraoka, K. Tanaka, and M. Yanagida. 1990. The transition of cells of the fission yeast beta-tubulin mutant nda3-311 as seen by freeze-substitution electron microscopy. Requirement of functional tubulin for spindle pole body duplication. *Journal of cell science*. 96 (Pt 2):275-282.

Kapitein, L.C., E.J. Peterman, B.H. Kwok, J.H. Kim, T.M. Kapoor, and C.F. Schmidt. 2005. The bipolar mitotic kinesin Eg5 moves on both microtubules that it crosslinks. *Nature*. 435:114-118.

Kapoor, T.M., T.U. Mayer, M.L. Coughlin, and T.J. Mitchison. 2000. Probing spindle assembly mechanisms with monastrol, a small molecule inhibitor of the mitotic kinesin, Eg5. *The Journal of cell biology*. 150:975-988.

Karsenti, E., and I. Vernos. 2001. The mitotic spindle: a self-made machine. *Science*. 294:543-547.

Kerres, A., V. Jakopec, and U. Fleig. 2007. The conserved Spc7 protein is required for spindle integrity and links kinetochore complexes in fission yeast. *Molecular biology of the cell*. 18:2441-2454.

Khodjakov, A., S. La Terra, and F. Chang. 2004. Laser microsurgery in fission yeast; role of the mitotic spindle midzone in anaphase B. *Current biology : CB*. 14:1330-1340.

Kim, N., and K. Song. 2013. KIFC1 is essential for bipolar spindle formation and genomic stability in the primary human fibroblast IMR-90 cell. *Cell Struct Funct*. 38:21-30.

King, M.C., T.G. Drivas, and G. Blobel. 2008. A network of nuclear envelope membrane proteins linking centromeres to microtubules. *Cell*. 134:427-438.

Kirschner, M.W., and T. Mitchison. 1986. Microtubule dynamics. *Nature*. 324:621.
Kniola, B., E. O'Toole, J.R. McIntosh, B. Mellone, R. Allshire, S. Mengarelli, K. Hultenby, and K. Ekwall. 2001. The domain structure of centromeres is conserved from fission yeast to humans. *Molecular biology of the cell*. 12:2767-2775.
Kollu, S., S.F. Bakhoum, and D.A. Compton. 2009. Interplay of microtubule dynamics and sliding during bipolar spindle formation in mammalian cells. *Current biology : CB*. 19:2108-2113.
Koshland, D.E., T.J. Mitchison, and M.W. Kirschner. 1988. Polewards chromosome movement driven by microtubule depolymerization in vitro. *Nature*. 331:499-504.
Kwon, M., S.A. Godinho, N.S. Chandhok, N.J. Ganem, A. Azioune, M. Thery, and D. Pellman. 2008. Mechanisms to suppress multipolar divisions in cancer cells with extra centrosomes. *Genes Dev*. 22:2189-2203.
Lara-Gonzalez, P., F.G. Westhorpe, and S.S. Taylor. 2012. The spindle assembly checkpoint. *Curr Biol*. 22:R966-980.
Lee, I.J., N. Wang, W. Hu, K. Schott, J. Bahler, T.H. Giddings, Jr., J.R. Pringle, L.L. Du, and J.Q. Wu. 2014. Regulation of spindle pole body assembly and cytokinesis by the centrin-binding protein Sfi1 in fission yeast. *Molecular biology of the cell*. 25:2735-2749.
Lengauer, C., K.W. Kinzler, and B. Vogelstein. 1998. Genetic instabilities in human cancers. *Nature*. 396:643-649.
Liu, X., I. McLeod, S. Anderson, J.R. Yates, 3rd, and X. He. 2005. Molecular analysis of kinetochore architecture in fission yeast. *The EMBO journal*. 24:2919-2930.
Logarinho, E., S. Maffini, M. Barisic, A. Marques, A. Toso, P. Meraldi, and H. Maiato. 2012. CLASPs prevent irreversible multipolarity by ensuring spindle-pole resistance to traction forces during chromosome alignment. *Nat Cell Biol*. 14:295-303.
Loiodice, I., J. Staub, T.G. Setty, N.P. Nguyen, A. Paoletti, and P.T. Tran. 2005. Ase1p organizes antiparallel microtubule arrays during interphase and mitosis in fission yeast. *Molecular biology of the cell*. 16:1756-1768.
Luders, J., and T. Stearns. 2007. Microtubule-organizing centres: a re-evaluation. *Nature reviews. Molecular cell biology*. 8:161-167.
Maiato, H., and E. Logarinho. 2014. Mitotic spindle multipolarity without centrosome amplification. *Nat Cell Biol*. 16:386-394.
Maiato, H., P. Sampaio, and C.E. Sunkel. 2004. Microtubule-associated proteins and their essential roles during mitosis. *International review of cytology*. 241:53-153.
Mallavarapu, A., K. Sawin, and T. Mitchison. 1999. A switch in microtubule dynamics at the onset of anaphase B in the mitotic spindle of Schizosaccharomyces pombe. *Current biology : CB*. 9:1423-1426.
Manchado, E., M. Guillamot, and M. Malumbres. 2012. Killing cells by targeting mitosis. *Cell death and differentiation*. 19:369-377.
Masuda, H., R. Mori, M. Yukawa, and T. Toda. 2013. Fission yeast MOZART1/Mzt1 is an essential gamma-tubulin complex component required for complex recruitment to the microtubule organizing center, but not its assembly. *Molecular biology of the cell*. 24:2894-2906.
Masuda, H., M. Sevik, and W.Z. Cande. 1992. In vitro microtubule-nucleating activity of spindle pole bodies in fission yeast Schizosaccharomyces pombe: cell cycle-dependent activation in xenopus cell-free extracts. *The Journal of cell biology*. 117:1055-1066.

Masuda, H., and T. Shibata. 1996. Role of gamma-tubulin in mitosis-specific microtubule nucleation from the Schizosaccharomyces pombe spindle pole body. *Journal of cell science*. 109 (Pt 1):165-177.

Mayer, T.U., T.M. Kapoor, S.J. Haggarty, R.W. King, S.L. Schreiber, and T.J. Mitchison. 1999. Small molecule inhibitor of mitotic spindle bipolarity identified in a phenotype-based screen. *Science*. 286:971-974.

McDonald, H.B., and L.S. Goldstein. 1990. Identification and characterization of a gene encoding a kinesin-like protein in Drosophila. *Cell*. 61:991-1000.

McIntosh, J.R., M.I. Molodtsov, and F.I. Ataullakhanov. 2012. Biophysics of mitosis. *Quarterly reviews of biophysics*. 45:147-207.

McIntosh, J.R., E. O'Toole, K. Zhudenkov, M. Morphew, C. Schwartz, F.I. Ataullakhanov, and E.L. Grishchuk. 2013. Conserved and divergent features of kinetochores and spindle microtubule ends from five species. *The Journal of cell biology*. 200:459-474.

McIntosh, J.R., V. Volkov, F.I. Ataullakhanov, and E.L. Grishchuk. 2010. Tubulin depolymerization may be an ancient biological motor. *Journal of cell science*. 123:3425-3434.

Mekhail, K., and D. Moazed. 2010. The nuclear envelope in genome organization, expression and stability. *Nature reviews. Molecular cell biology*. 11:317-328.

Merdes, A., and D.W. Cleveland. 1997. Pathways of spindle pole formation: different mechanisms; conserved components. *The Journal of cell biology*. 138:953-956.

Merdes, A., R. Heald, K. Samejima, W.C. Earnshaw, and D.W. Cleveland. 2000. Formation of spindle poles by dynein/dynactin-dependent transport of NuMA. *The Journal of cell biology*. 149:851-862.

Merdes, A., K. Ramyar, J.D. Vechio, and D.W. Cleveland. 1996. A complex of NuMA and cytoplasmic dynein is essential for mitotic spindle assembly. *Cell*. 87:447-458.

Mitchison, J.M., and P. Nurse. 1985. Growth in cell length in the fission yeast Schizosaccharomyces pombe. *J Cell Sci*. 75:357-376.

Mogilner, A., and E. Craig. 2009. Towards a quantitative understanding of mitotic spindle assembly and mechanics. *Journal of cell science*. 123:3435-3445.

Moreno, S., A. Klar, and P. Nurse. 1991. Molecular genetic analysis of fission yeast Schizosaccharomyces pombe. *Methods in enzymology*. 194:795-823.

Moseley, J.B., A. Mayeux, A. Paoletti, and P. Nurse. 2009. A spatial gradient coordinates cell size and mitotic entry in fission yeast. *Nature*. 459:857-860.

Mountain, V., C. Simerly, L. Howard, A. Ando, G. Schatten, and D.A. Compton. 1999. The kinesin-related protein, HSET, opposes the activity of Eg5 and cross-links microtubules in the mammalian mitotic spindle. *The Journal of cell biology*. 147:351-366.

Musacchio, A. 2011. Spindle assembly checkpoint: the third decade. *Philosophical transactions of the Royal Society of London*. 366:3595-3604.

Musacchio, A., and E.D. Salmon. 2007. The spindle-assembly checkpoint in space and time. *Nature reviews. Molecular cell biology*. 8:379-393.

Nabeshima, K., H. Kurooka, M. Takeuchi, K. Kinoshita, Y. Nakaseko, and M. Yanagida. 1995. p93dis1, which is required for sister chromatid separation, is a novel microtubule and spindle pole body-associating protein phosphorylated at the Cdc2 target sites. *Genes & development*. 9:1572-1585.

Nabeshima, K., T. Nakagawa, A.F. Straight, A. Murray, Y. Chikashige, Y.M. Yamashita, Y. Hiraoka, and M. Yanagida. 1998. Dynamics of centromeres during metaphase-anaphase

transition in fission yeast: Dis1 is implicated in force balance in metaphase bipolar spindle. *Molecular biology of the cell*. 9:3211-3225.

Nguyen-Ngoc, T., K. Afshar, and P. Gonczy. 2007. Coupling of cortical dynein and G alpha proteins mediates spindle positioning in Caenorhabditis elegans. *Nature cell biology*. 9:1294-1302.

Niwa, O., T. Matsumoto, Y. Chikashige, and M. Yanagida. 1989. Characterization of Schizosaccharomyces pombe minichromosome deletion derivatives and a functional allocation of their centromere. *The EMBO journal*. 8:3045-3052.

Niwa, O., Y. Tange, and A. Kurabayashi. 2006. Growth arrest and chromosome instability in aneuploid yeast. *Yeast*. 23:937-950.

Nogales, E. 2000. Structural insights into microtubule function. *Annual review of biochemistry*. 69:277-302.

Nurse, P., P. Thuriaux, and K. Nasmyth. 1976. Genetic control of the cell division cycle in the fission yeast Schizosaccharomyces pombe. *Molecular & general genetics : MGG*. 146:167-178.

Olmsted, Z.T., A.G. Colliver, T.D. Riehlman, and J.L. Paluh. 2014. Kinesin-14 and kinesin-5 antagonistically regulate microtubule nucleation by gamma-TuRC in yeast and human cells. *Nature communications*. 5:5339.

Olmsted, Z.T., T.D. Riehlman, C.N. Branca, A.G. Colliver, L.O. Cruz, and J.L. Paluh. 2013. Kinesin-14 Pkl1 targets gamma-tubulin for release from the gamma-tubulin ring complex (gamma-TuRC). *Cell Cycle*. 12:842-848.

Paluh, J.L., E. Nogales, B.R. Oakley, K. McDonald, A.L. Pidoux, and W.Z. Cande. 2000. A mutation in gamma-tubulin alters microtubule dynamics and organization and is synthetically lethal with the kinesin-like protein pkl1p. *Molecular biology of the cell*. 11:1225-1239.

Pidoux, A.L., M. LeDizet, and W.Z. Cande. 1996. Fission yeast pkl1 is a kinesin-related protein involved in mitotic spindle function. *Molecular biology of the cell*. 7:1639-1655.

Pidoux, A.L., S. Uzawa, P.E. Perry, W.Z. Cande, and R.C. Allshire. 2000. Live analysis of lagging chromosomes during anaphase and their effect on spindle elongation rate in fission yeast. *Journal of cell science*. 113 Pt 23:4177-4191.

Piel, M., and P.T. Tran. 2009. Cell shape and cell division in fission yeast. *Current biology : CB*. 19:R823-827.

Raaijmakers, J.A., M.E. Tanenbaum, and R.H. Medema. 2013. Systematic dissection of dynein regulators in mitosis. *The Journal of cell biology*. 201:201-215.

Roberts, A.J., T. Kon, P.J. Knight, K. Sutoh, and S.A. Burgess. 2013. Functions and mechanics of dynein motor proteins. *Nature reviews. Molecular cell biology*. 14:713-726.

Rodriguez, A.S., J. Batac, A.N. Killilea, J. Filopei, D.R. Simeonov, I. Lin, and J.L. Paluh. 2008. Protein complexes at the microtubule organizing center regulate bipolar spindle assembly. *Cell cycle*. 7:1246-1253.

Roostalu, J., C. Hentrich, P. Bieling, I.A. Telley, E. Schiebel, and T. Surrey. 2011. Directional switching of the kinesin Cin8 through motor coupling. *Science*. 332:94-99.

Roy, B., N. Varshney, V. Yadav, and K. Sanyal. 2013. The process of kinetochore assembly in yeasts. *FEMS microbiology letters*. 338:107-117.

Russell, P., and P. Nurse. 1986. cdc25+ functions as an inducer in the mitotic control of fission yeast. *Cell*. 45:145-153.

Sagolla, M.J., S. Uzawa, and W.Z. Cande. 2003. Individual microtubule dynamics contribute to the function of mitotic and cytoplasmic arrays in fission yeast. *Journal of cell science*. 116:4891-4903.

Saitoh, S., Y. Kobayashi, Y. Ogiyama, and K. Takahashi. 2008. Dual regulation of Mad2 localization on kinetochores by Bub1 and Dam1/DASH that ensure proper spindle interaction. *Molecular biology of the cell*. 19:3885-3897.

Saitoh, S., K. Takahashi, and M. Yanagida. 1997. Mis6, a fission yeast inner centromere protein, acts during G1/S and forms specialized chromatin required for equal segregation. *Cell*. 90:131-143.

Samejima, I., V.J. Miller, L.M. Groocock, and K.E. Sawin. 2008. Two distinct regions of Mto1 are required for normal microtubule nucleation and efficient association with the gamma-tubulin complex in vivo. *Journal of cell science*. 121:3971-3980.

Samejima, I., V.J. Miller, S.A. Rincon, and K.E. Sawin. 2010. Fission yeast Mto1 regulates diversity of cytoplasmic microtubule organizing centers. *Current biology : CB*. 20:1959-1965.

Sanchez-Perez, I., S.J. Renwick, K. Crawley, I. Karig, V. Buck, J.C. Meadows, A. Franco-Sanchez, U. Fleig, T. Toda, and J.B. Millar. 2005. The DASH complex and Klp5/Klp6 kinesin coordinate bipolar chromosome attachment in fission yeast. *The EMBO journal*. 24:2931-2943.

Sato, M., and T. Toda. 2007. Alp7/TACC is a crucial target in Ran-GTPase-dependent spindle formation in fission yeast. *Nature*. 447:334-337.

Sato, M., L. Vardy, M. Angel Garcia, N. Koonrugsa, and T. Toda. 2004. Interdependency of fission yeast Alp14/TOG and coiled coil protein Alp7 in microtubule localization and bipolar spindle formation. *Molecular biology of the cell*. 15:1609-1622.

Saunders, A.M., J. Powers, S. Strome, and W.M. Saxton. 2007. Kinesin-5 acts as a brake in anaphase spindle elongation. *Current biology : CB*. 17:R453-454.

Saunders, W., V. Lengyel, and M.A. Hoyt. 1997. Mitotic spindle function in Saccharomyces cerevisiae requires a balance between different types of kinesin-related motors. *Molecular biology of the cell*. 8:1025-1033.

Saunders, W.S., and M.A. Hoyt. 1992. Kinesin-related proteins required for structural integrity of the mitotic spindle. *Cell*. 70:451-458.

Sawin, K.E., P.C. Lourenco, and H.A. Snaith. 2004. Microtubule nucleation at non-spindle pole body microtubule-organizing centers requires fission yeast centrosomin-related protein mod20p. *Current biology : CB*. 14:763-775.

Sharp, D.J., K.L. McDonald, H.M. Brown, H.J. Matthies, C. Walczak, R.D. Vale, T.J. Mitchison, and J.M. Scholey. 1999. The bipolar kinesin, KLP61F, cross-links microtubules within interpolar microtubule bundles of Drosophila embryonic mitotic spindles. *The Journal of cell biology*. 144:125-138.

Starr, D.A. 2009. A nuclear-envelope bridge positions nuclei and moves chromosomes. *Journal of cell science*. 122:577-586.

Stearns, T., L. Evans, and M. Kirschner. 1991. Gamma-tubulin is a highly conserved component of the centrosome. *Cell*. 65:825-836.

Subramanian, R., E.M. Wilson-Kubalek, C.P. Arthur, M.J. Bick, E.A. Campbell, S.A. Darst, R.A. Milligan, and T.M. Kapoor. 2010. Insights into antiparallel microtubule crosslinking by PRC1, a conserved nonmotor microtubule binding protein. *Cell*. 142:433-443.

Syrovatkina, V., C. Fu, and P.T. Tran. 2013. Antagonistic spindle motors and MAPs regulate metaphase spindle length and chromosome segregation. *Current biology : CB*. 23:2423-2429.

Tamm, T., A. Grallert, E.P. Grossman, I. Alvarez-Tabares, F.E. Stevens, and I.M. Hagan. 2011. Brr6 drives the Schizosaccharomyces pombe spindle pole body nuclear envelope insertion/extrusion cycle. *The Journal of cell biology*. 195:467-484.

Tanaka, K., H.L. Chang, A. Kagami, and Y. Watanabe. 2009. CENP-C functions as a scaffold for effectors with essential kinetochore functions in mitosis and meiosis. *Developmental cell*. 17:334-343.

Tanaka, K., and T. Kanbe. 1986. Mitosis in the fission yeast Schizosaccharomyces pombe as revealed by freeze-substitution electron microscopy. *Journal of cell science*. 80:253-268.

Tanaka, N., W. Meng, S. Nagae, and M. Takeichi. 2012. Nezha/CAMSAP3 and CAMSAP2 cooperate in epithelial-specific organization of noncentrosomal microtubules. *Proceedings of the National Academy of Sciences of the United States of America*. 109:20029-20034.

Tanenbaum, M.E., L. Macurek, N. Galjart, and R.H. Medema. 2008. Dynein, Lis1 and CLIP-170 counteract Eg5-dependent centrosome separation during bipolar spindle assembly. *The EMBO journal*. 27:3235-3245.

Tanenbaum, M.E., L. Macurek, A. Janssen, E.F. Geers, M. Alvarez-Fernandez, and R.H. Medema. 2009. Kif15 cooperates with eg5 to promote bipolar spindle assembly. *Current biology : CB*. 19:1703-1711.

Tanenbaum, M.E., and R.H. Medema. 2010. Mechanisms of centrosome separation and bipolar spindle assembly. *Developmental cell*. 19:797-806.

Tang, N.H., N. Okada, C.S. Fong, K. Arai, M. Sato, and T. Toda. 2014. Targeting Alp7/TACC to the spindle pole body is essential for mitotic spindle assembly in fission yeast. *FEBS letters*. 588:2814-2821.

Tang, N.H., H. Takada, K.S. Hsu, and T. Toda. 2013. The internal loop of fission yeast Ndc80 binds Alp7/TACC-Alp14/TOG and ensures proper chromosome attachment. *Molecular biology of the cell*. 24:1122-1133.

Tang, N.H., and T. Toda. 2015. Alp7/TACC recruits kinesin-8-PP1 to the Ndc80 kinetochore protein for timely mitotic progression and chromosome movement. *Journal of cell science*. 128:354-363.

Tatebe, H., G. Goshima, K. Takeda, T. Nakagawa, K. Kinoshita, and M. Yanagida. 2001. Fission yeast living mitosis visualized by GFP-tagged gene products. *Micron*. 32:67-74.

Thompson, S.L., S.F. Bakhoum, and D.A. Compton. 2010. Mechanisms of chromosomal instability. *Current biology : CB*. 20:R285-295.

Torres, E.M., T. Sokolsky, C.M. Tucker, L.Y. Chan, M. Boselli, M.J. Dunham, and A. Amon. 2007. Effects of aneuploidy on cellular physiology and cell division in haploid yeast. *Science*. 317:916-924.

Toya, M., M. Sato, U. Haselmann, K. Asakawa, D. Brunner, C. Antony, and T. Toda. 2007. Gamma-tubulin complex-mediated anchoring of spindle microtubules to spindle-pole bodies requires Msd1 in fission yeast. *Nature cell biology*. 9:646-653.

Tran, P.T., L. Marsh, V. Doye, S. Inoue, and F. Chang. 2001. A mechanism for nuclear positioning in fission yeast based on microtubule pushing. *The Journal of cell biology*. 153:397-411.

Tran, P.T., A. Paoletti, and F. Chang. 2004. Imaging green fluorescent protein fusions in living fission yeast cells. *Methods*. 33:220-225.

Troxell, C.L., M.A. Sweezy, R.R. West, K.D. Reed, B.D. Carson, A.L. Pidoux, W.Z. Cande, and J.R. McIntosh. 2001. pkl1(+)and klp2(+): Two kinesins of the Kar3 subfamily in fission yeast perform different functions in both mitosis and meiosis. *Molecular biology of the cell*. 12:3476-3488.

Unsworth, A., H. Masuda, S. Dhut, and T. Toda. 2008. Fission yeast kinesin-8 Klp5 and Klp6 are interdependent for mitotic nuclear retention and required for proper microtubule dynamics. *Molecular biology of the cell*. 19:5104-5115.

Uzawa, S., F. Li, Y. Jin, K.L. McDonald, M.B. Braunfeld, D.A. Agard, and W.Z. Cande. 2004. Spindle pole body duplication in fission yeast occurs at the G1/S boundary but maturation is blocked until exit from S by an event downstream of cdc10+. *Molecular biology of the cell*. 15:5219-5230.

Vardy, L., A. Fujita, and T. Toda. 2002. The gamma-tubulin complex protein Alp4 provides a link between the metaphase checkpoint and cytokinesis in fission yeast. *Genes to cells : devoted to molecular & cellular mechanisms*. 7:365-373.

Vardy, L., and T. Toda. 2000. The fission yeast gamma-tubulin complex is required in G(1) phase and is a component of the spindle assembly checkpoint. *The EMBO journal*. 19:6098-6111.

Velve Casquillas, G., C. Fu, M. Le Berre, J. Cramer, S. Meance, A. Plecis, D. Baigl, J.J. Greffet, Y. Chen, M. Piel, and P.T. Tran. 2011. Fast microfluidic temperature control for high resolution live cell imaging. *Lab on a chip*. 11:484-489.

Venkatram, S., J.J. Tasto, A. Feoktistova, J.L. Jennings, A.J. Link, and K.L. Gould. 2004. Identification and characterization of two novel proteins affecting fission yeast gamma-tubulin complex function. *Molecular biology of the cell*. 15:2287-2301.

Verhey, K.J., and J.W. Hammond. 2009. Traffic control: regulation of kinesin motors. *Nature reviews. Molecular cell biology*. 10:765-777.

Vleugel, M., E. Hoogendoorn, B. Snel, and G.J. Kops. 2012. Evolution and function of the mitotic checkpoint. *Developmental cell*. 23:239-250.

Volkov, V.A., A.V. Zaytsev, N. Gudimchuk, P.M. Grissom, A.L. Gintsburg, F.I. Ataullakhanov, J.R. McIntosh, and E.L. Grishchuk. 2013. Long tethers provide high-force coupling of the Dam1 ring to shortening microtubules. *Proceedings of the National Academy of Sciences of the United States of America*. 110:7708-7713.

Walczak, C.E., S. Cai, and A. Khodjakov. 2010. Mechanisms of chromosome behaviour during mitosis. *Nature reviews. Molecular cell biology*. 11:91-102.

Walczak, C.E., S. Verma, and T.J. Mitchison. 1997. XCTK2: a kinesin-related protein that promotes mitotic spindle assembly in Xenopus laevis egg extracts. *The Journal of cell biology*. 136:859-870.

Walde, S., and M.C. King. 2014. The KASH protein Kms2 coordinates mitotic remodeling of the spindle pole body. *Journal of cell science*. 127:3625-3640.

Wang, H.W., and E. Nogales. 2005. Nucleotide-dependent bending flexibility of tubulin regulates microtubule assembly. *Nature*. 435:911-915.

Weaver, B.A., and D.W. Cleveland. 2006. Does aneuploidy cause cancer? *Current opinion in cell biology*. 18:658-667.

West, R.R., T. Malmstrom, and J.R. McIntosh. 2002. Kinesins klp5(+) and klp6(+) are required for normal chromosome movement in mitosis. *Journal of cell science*. 115:931-940.
West, R.R., T. Malmstrom, C.L. Troxell, and J.R. McIntosh. 2001. Two related kinesins, klp5+ and klp6+, foster microtubule disassembly and are required for meiosis in fission yeast. *Molecular biology of the cell*. 12:3919-3932.
West, R.R., E.V. Vaisberg, R. Ding, P. Nurse, and J.R. McIntosh. 1998. cut11(+): A gene required for cell cycle-dependent spindle pole body anchoring in the nuclear envelope and bipolar spindle formation in Schizosaccharomyces pombe. *Molecular biology of the cell*. 9:2839-2855.
Westermann, S., A. Avila-Sakar, H.W. Wang, H. Niederstrasser, J. Wong, D.G. Drubin, E. Nogales, and G. Barnes. 2005. Formation of a dynamic kinetochore- microtubule interface through assembly of the Dam1 ring complex. *Molecular cell*. 17:277-290.
Westermann, S., and A. Schleiffer. 2013. Family matters: structural and functional conservation of centromere-associated proteins from yeast to humans. *Trends in cell biology*. 23:260-269.
Wickstead, B., and K. Gull. 2007. Dyneins across eukaryotes: a comparative genomic analysis. *Traffic*. 8:1708-1721.
Wigge, P.A., and J.V. Kilmartin. 2001. The Ndc80p complex from Saccharomyces cerevisiae contains conserved centromere components and has a function in chromosome segregation. *The Journal of cell biology*. 152:349-360.
Wordeman, L. 2010. How kinesin motor proteins drive mitotic spindle function: Lessons from molecular assays. *Seminars in cell & developmental biology*. 21:260-268.
Yamagishi, Y., T. Sakuno, Y. Goto, and Y. Watanabe. 2014. Kinetochore composition and its function: lessons from yeasts. *FEMS microbiology reviews*. 38:185-200.
Yamamoto, A., and Y. Hiraoka. 2003. Monopolar spindle attachment of sister chromatids is ensured by two distinct mechanisms at the first meiotic division in fission yeast. *The EMBO journal*. 22:2284-2296.
Yamashita, A., M. Sato, A. Fujita, M. Yamamoto, and T. Toda. 2005. The roles of fission yeast ase1 in mitotic cell division, meiotic nuclear oscillation, and cytokinesis checkpoint signaling. *Molecular biology of the cell*. 16:1378-1395.
Yount, A.L., H. Zong, and C.E. Walczak. 2015. Regulatory mechanisms that control mitotic kinesins. *Experimental cell research*.
Zhang, D., and S. Oliferenko. 2013. Remodeling the nuclear membrane during closed mitosis. *Current opinion in cell biology*. 25:142-148.
Zheng, F., T. Li, D.Y. Jin, V. Syrovatkina, K. Scheffler, P.T. Tran, and C. Fu. 2014. Csi1p recruits alp7p/TACC to the spindle pole bodies for bipolar spindle formation. *Molecular biology of the cell*. 25:2750-2760.
Zimmerman, S., and F. Chang. 2005. Effects of {gamma}-tubulin complex proteins on microtubule nucleation and catastrophe in fission yeast. *Molecular biology of the cell*. 16:2719-2733.